Dynamics of Hair Follicle Morphogenesis and Skin Homeostasis

by

Arlee L. Mesler

A dissertation submitted in partial fulfillment
of the requirements for the degree of
Doctor of Philosophy
(Cellular and Molecular Biology)
in the University of Michigan
2018

Doctoral Committee:

       Assistant Professor Sunny Y. Wong, Chair
       Professor Andrzej A. Dlugosz
       Associate Professor Marina Pasca di Magliano
       Professor Linda C. Samuelson

Arlee L. Mesler

amesler@umich.edu

ORCID iD: 0000-0003-3510-4929

Acknowledgements

The work presented in this dissertation would not have been possible without the help of many talented and dedicated individuals in both my personal and professional life.

First, I would like to acknowledge my mentor Dr. Sunny Wong. The passion you have for science and the precision with which you address scientific questions is inspiring. Thank you for helping me develop as a scientist and pushing me to think critically and always ask questions. I appreciate that you were always around to talk science and even help with experiments. Finally, thank you for supporting my interests outside of lab.

I would also like to thank my committee members, Dr. Andrzej Dlugosz, Dr. Linda Samuelson, and Dr. Marina Pasca Di Magliano. Thanks first to Anj whose thoughtful questions during lab meetings propelled my projects forward. Thank you to Linda and Marina for always providing critical feedback and encouraging me to consider alternative explanations for my data. I walked away from each committee meeting feeling optimistic and excited by the feedback I received. I feel so fortunate to have had the support of such excellent scientists throughout my graduate career.

I am so lucky to have been a member of the CMB graduate program. The diversity in research topics helped keep me up to date on scientific happenings outside of skin and hair biology. Thank you to Dr. Robert Fuller and the CMB support staff

Table of Contents

List of Figures

List of Tables

Abstract

Mammalian skin and hair act as a protective barrier to protect our bodies from external damage while also regulating water loss. Hair follicles form in development and continue to produce new hairs throughout adult life. My thesis examined poorly understood aspects of hair follicle biology, including temporal features of terminal differentiation within the follicle, and the link between hair canal development and the severe human skin disease, harlequin ichthyosis.

During hair growth, matrix progenitor cells housed at the bottom of the follicle undergo terminal differentiation to form the concentric layers of the hair follicle. These differentiation events are believed to require signals from the mesenchymal dermal papilla (DP), although it remains unclear how DP-progenitor cell interactions regulate specific cell fate decisions. I found that the matrix progenitor population can be separated into early and late phases based on distinct temporal, molecular and functional characteristics. Early matrix cells can undergo differentiation in the absence of sonic hedgehog (Shh), bone morphogenetic protein (BMP) signaling, and DP maturation. In contrast, later matrix cell populations require a mature DP and Shh and BMP signaling for differentiation to occur.

The acquisition of epidermal barrier function occurs in conjunction with hair follicle morphogenesis, with the hair shaft extending out of an opening in the epidermis called the hair canal. The mechanisms underlying hair canal formation are poorly understood. Previous findings from our lab identified a novel population of hair follicle-

derived cells marked by the expression of keratin 79 (K79), which may play a role in hair canal formation. I found that K79+ cells stream into the epidermis prior to barrier formation and remain there until late in development, when they are lost to apoptosis concurrent with initial canal specification. The early entry of K79+ cells into the epidermis sets the stage for canal formation and circumvents the complications associated with breaching a complete epidermal barrier.

Epidermal barrier function is compromised in the severe skin disease harlequin ichthyosis (HI), which is caused by loss-of-function mutations in the lipid transporter gene *ABCA12*. HI patients are born with a thick plate-like outer skin layer and frequently die shortly after birth. Interestingly, case studies indicate that the HI phenotype appears in the hair canal, prior to the epidermis. These observations raise the possibility of a link between a barrier disease and hair follicle formation. I found that *Abca12* is expressed in the hair canal, the same site affected in HI patients. The involvement of the hair follicle in HI has not been addressed due to limitations of the available genetic tools. I generated a new mouse model which facilitates spatial and temporal deletion of *Abca12.* Using this model, I can delete *Abca12* in specific cell populations (e.g., hair follicle) at specific times (e.g., development, adult). This model will allow for critical evaluation of HI pathogenesis as well as the role of ABCA12 in normal skin and hair follicle development.

In summary, my findings expand our understanding of key aspects of hair follicle biology, including terminal differentiation, and the mechanisms governing hair canal formation. Further, the conditional *Abca12*-knockout mouse model can be leveraged in

future studies to address critical questions in skin biology and to understand the role of

ABCA12 in diverse organ systems.

Chapter I: Introduction

1.1 Summary

Mammalian skin and hair act together as a protective barrier that shields us from environmental insults while also preventing dehydration. Hair follicles formed in development continue to produce new hairs throughout adult life, in a process that is thought to require extensive signal cross-talk with the underlying mesenchyme. During hair growth, cells termed matrix progenitors at the bottom of the follicle produce the hair shaft and associated supporting cell layers. Despite our understanding of the origins and ultimate positioning of the concentric cellular layers, many questions remain about the temporal and functional aspects governing cell-fate decisions in the hair follicle.

Epidermal barrier function is compromised in several human pathologies, including the severe congenital disease, Harlequin Ichthyosis (HI). HI patients are born with a thick plate-like outer skin layer due to mutations in the lipid transporter gene, *ABCA12,* and frequently die shortly after birth. Interestingly, case studies have suggested that the HI phenotype appears *in utero* before exposure to a dry environment and may be most severe in the hair canal. The involvement of the hair follicle in the pathogenesis of HI has not been addressed as the available genetic tools did not allow ABCA12 deletion within specific cell populations.

In this chapter, I provide an overview of hair follicle biology and the signaling pathways involved in regulating different steps in development and regeneration. Specifically, I focus on the processes of progenitor cell differentiation and hair canal

formation. I also discuss epidermal barrier formation and HI. Finally, I introduce the major questions that I will address in subsequent chapters.

1.2 Hair Follicle Biology

1.21 Introduction

Hair follicles represent the major appendage of the skin, playing key roles in barrier function, thermoregulation, sensation, and camouflage [1-3]. These mini-organs form in development and undergo cyclical phases of growth (anagen), regression (catagen), and rest (telogen) throughout adult life to produce new hairs **(Figure 1.1)**. During each growth phase, undifferentiated matrix progenitor cells located at the epithelial-mesenchymal interface produce the hair shaft and several auxiliary cell layers required for proper hair growth **(Figure 1.2B & 1.2C)**. Like many other organs, hair follicle development and homeostasis require reciprocal interactions between the epithelium and associated mesenchymal cells [4, 5].

Studies using mouse models have driven much of our understanding of mammalian hair follicle biology. The overall structure of human and mouse hair follicles is remarkably similar, and both species undergo the same phases of follicle growth, regression, and rest during homeostasis (reviewed in [6]). There are also notable differences between the two species including synchronization of the hair cycle and length of the growth phase. Murine follicles go through hair cycles that are initially synchronized, with each growth phase lasting 2-3 weeks [7-9]. In contrast, human hair follicles cycle independently from one another and, depending on where on the body they are located, may remain in the growth phase for several years [10, 11]. Because

2

hair shaft elongation occurs only during growth, a long anagen phase is responsible for exceptionally long scalp hairs.

The canonical stem cell niche (bulge) differs in both morphology and marker expression between the two species. In mice, this region is easily distinguished from neighboring domains in the follicle, while human follicles lack a morphologically distinct bulge. Further, established bulge stem cell markers in mice (e.g., CD34) are not expressed by human bulge stem cells [12-14]. Despite these differences, the similar structure and cycling behavior between the two species along with the ability to generate genetic mutants in mouse make mice an ideal model organism to study the mechanisms governing human hair follicle biology.

1.22 Hair Follicle Structure

Mature anagen follicles contain both permanent and transient regions **(Figure 1.2A)**. The upper, permanent portion contains the infundibulum (INF), isthmus and bulge. These regions of the follicle are not subject to the massive apoptosis during hair regression (reviewed in [3]). Hair follicles also contain associated sebaceous glands comprised of lipid-filled sebocytes which contribute to barrier function via extrusion of their lipid content (reviewed in [15]). The INF or hair canal serves as the interface between the follicle and overlying interfollicular epidermis and is affected in numerous human pathologies, including acne, hair loss (alopecia areata, androgenetic alopecia), and the inflammatory disease, hidradenitis suppurativa [16-19] (reviewed in [20]). Often incorrectly depicted as a single layer, the INF contains an inner layer marked by the expression of keratin 79 (K79) [21]. During homeostasis, both layers of the INF are

maintained by LRIG1+ stem cells that reside directly below in the isthmus, but not by bulge stem cells located further down the follicle **(Figure 1.2A)** [21]. Instead, these bulge stem cells contribute to the regeneration of hair lineages during anagen [22-24].

The lower, cycling portion of the hair follicle contains matrix progenitor cells as well as their terminally differentiated progeny **(Figure 1.2B &1.2C)**. Anagen hair follicles contain 7 differentiated layers arranged in a radial pattern. The hair shaft (HS), comprised of three distinct cellular layers (Medulla, Cortex, Cuticle) sits centrally within the follicle, directly above the dermal papilla. Just to the outside of the HS sits the inner root sheath (IRS), also made up of three layers of cells (Cuticle, Huxley, Henle). The IRS acts as a channel to support the upward movement of the growing hair [9]. Sandwiched in between the IRS and outer root sheath is the companion layer (CL) **(Figure 1.2C)**. The CL was once considered to be the outer-most layer of the IRS, rather than a separate cellular entity [25, 26]. Intricate cell-cell junctions link the outer layer of the IRS to the CL [27]. This fact coupled with their shared origins, kinetics and expression of some shared markers [26, 28-31] fueled speculations that the CL was part of the IRS. Functional data does not support this notion, however, as three distinct genetic manipulations (Gata3-knockout, *Bmpr1a*-knockout, *NuMa*-mutant) result in deformed IRS structure, while seemingly sparing the CL [32-35]. The precise function of the CL remains unclear. Mice lacking the desmosome components, desmoglein 1 and 3, display impaired hair anchorage as well as a separation between the CL and outer root sheath [36]. These findings suggest that the CL may be involved in anchoring the HS via desmosomes. Further, they also support a hypothesized role for the CL in acting as a slippage plane during hair growth [30, 36]. In this role, the CL may act as a buffer

between the outer root sheath which is expanding down, and the HS which is growing up. Many of the uncertainties about the CL stem from the paucity of studies about it. Future work should focus on defining the true function of the CL in the hair follicle.

1.23 Hair Follicle Stem Cells

Adult stem cells (SCs) drive homeostasis and response to injury across most tissue types including hair follicles. Hair follicles possess multiple adult SC populations located in different regions of the follicle (reviewed in [37]). The canonical SC niche is the bulge, located at the base of the permanent portion of the follicle **(Figure 1.2A)**. This region was identified based on the slow cycling behavior of its cells, a fundamental property of SCs. Experiments utilizing a short, labeled-nucleotide pulse followed by an extended chase period revealed label-retaining cells within the bulge region of the follicle [23]. Another critical feature of SCs is their capacity to self-renew, which can be evaluated using *in vitro* colony forming assays. When different regions of the hair follicle were isolated and placed in culture, only the bulge was able to form colonies [38, 39]. Tissue reconstitution experiments reveal the multipotency of different cell populations. In these studies, isolated SCs are combined with niche dermal cells and placed in a chamber on the back of a nude mouse for several weeks to test their ability to contribute to different follicular lineages. Bulge SCs can reconstitute all hair lineages in this context [22, 40, 41].

Notable markers of murine bulge SCs include CD34, keratin 15 (K15), and LGR5 [12, 13, 24, 40-43]. CD34 and LGR5 also mark SCs of the hematopoietic and gastrointestinal systems, respectively [44-46]. The expression domains of CD34+ and

K15+ cells strongly overlap with the slow-cycling label-retaining population in the bulge [12, 24, 40, 42, 43]. In contrast, LGR5+ cells are located in the lower bulge and directly below in the secondary hair germ (SHG) **(Figure 1.2A).** This population cycles actively and are rarely label-retaining [41]. Despite these differences, lineage tracing studies show that both K15 and LGR5 bulge SCs contribute to hair lineages during regeneration, demonstrating their multipotency [24, 41, 47]. This observation indicates functional SCs within the bulge are not restricted to the quiescent, label-retaining population.

A recent mouse genetic study utilized a diphtheria toxin-based approach to probe the importance of LGR5+ cells during hair growth [48]. In this system, cells expressing *Lgr5* undergo apoptosis upon administration of diphtheria toxin (DT) to *Lgr5-EGFP-CreERT2;R26-DTR* mice. *Lgr5*+-cell ablation blocked hair regeneration, indicating that this population of cells is required for homeostasis in the hair follicle [48]. Intriguingly, when DT treatment was stopped, and follicles were allowed to recover, the CD34+ SC compartment replenished the lost LGR5+ cells [48]. This finding supports a model wherein slow cycling CD34+ SCs give rise to proliferative and active LGR5+ SCs, which contribute directly to the next growth phase. It also highlights the plasticity of SCs within the hair follicle bulge under stress conditions. Similarly, while bulge SCs do not contribute to the upper hair follicle or interfollicular epidermis during homeostasis [41, 47, 49], they can be mobilized to do so during wound healing [47].

Another critical SC population in the mid-follicle (isthmus) (**Figure 1.2A)** contributes to the upper hair follicle [50, 51]. Marked by the expression of LRIG1, these SCs are responsible for regenerating the differentiated cells of the INF (hair canal) and

sebaceous glands during homeostasis [21, 50]. They also hold the capacity to contribute to the interfollicular epidermis during stress conditions, like wound healing or genetic blockade of the Notch pathway, and can regenerate all hair follicle lineages in tissue reconstitution experiments [21, 50-52].

If these SC populations possess the intrinsic ability to produce all lineages under stress, what stops them from doing so during homeostasis? Local niche-derived signals play a crucial role in governing the behavior and cell-fate decisions of SCs. These signals vary spatially (i.e., bulge vs. isthmus) as well as temporally (i.e., telogen vs. anagen), adding to the complexity of hair follicle biology. An important component of the bulge SC niche is the dermal papilla which is situated directly below the SHG **(Figure 1.2A)**. BMP-inhibition, along with FGF7 and TGFβ2 are key dermal-derived signals that activate SCs within the bulge and SHG to initiate anagen [53-56]. While less well defined, the isthmus SC niche likely contains local niche-derived factors that direct SC behavior towards replenishing the upper hair follicle during homeostasis.

1.24 Hair Follicle Development

Hair follicle development proceeds in three waves to generate the four hair types of mouse fur coat. Guard follicles, which constitute 1-2% of the coat, are specified first at embryonic day (E) 14.5. The second and third waves specify the three other hair types (awl, zig-zag, and auchene), which together comprise over 98% of the fur coat [57] (reviewed in [58]). These hair types require different signaling pathways for their development. Genetic disruption of members of the ectodysplasin (EDA) pathway blocks the initial wave of hair follicle induction, resulting in the complete absence of

guard hairs [59-62]. Conversely, altering the bone morphogenetic protein (BMP)

cascade via knockout of noggin (NOG) sees the initial wave of guard hairs form, but not

the hair types of the second and third waves [63]. The precise role of signaling

pathways across hair development is discussed in depth below (Section 1.3). Despite

differences in timing of induction, reliance on signaling pathways, and morphology, all

four hair types largely undergo the same developmental stages.

These stages are primarily defined by the morphology of the hair follicle, as well

as its association with a population of dermal fibroblasts that sit below the epithelium.

These fibroblasts represent the presumptive dermal papilla, an important signaling

center driving hair follicle development **(Figure 1.3A)** [5, 64]. Follicle development

begins with placode formation (stage 1) or thickened regions of the epidermis with

underlying dermal fibroblasts. As this process continues, the hair bud grows down, and

the dermal condensate congregates under the hair follicle epithelium. Progenitor cells

located at the base of the follicle, called matrix cells, communicate with the forming

dermal papilla and initiate terminal differentiation. Previous reports [9, 64] proposed that

terminal differentiation began after the hair follicle had wrapped around the dermal

papilla (stage 4) with the specification of the IRS. This notion was rooted in the belief

that a mature dermal signaling population was required for initiation of differentiation

events. However, Veniaminova et al. identified differentiated keratin 79+ (K79) CL cells

as early as stage 2, when the dermal population was still developing demonstrating that

cellular differentiation begins much earlier [21]. One open question is whether these CL

cells represent the first differentiated cells in the follicle, or if there are IRS cells

specified at the same time. Detailed analysis of the timing of CL and IRS specification

across development and regeneration is needed to answer this question. In stages 5-8, the hair follicle continues its downgrowth and maturation. Lipid-filled sebocytes are specified at stage 5 and sit in the distal follicle epithelium until the mature sebaceous gland forms in stage 6. The hair canal (opening) also forms at stage 6, allowing the hair shaft to emerge a few days after birth completing hair follicle development **(Figure 1.3A)** [64].

1.25 Hair Canal Formation

The mechanisms governing the generation of the hair pore (canal) are poorly understood. The hair canal is the opening at the top of the follicle that the hair shaft emerges from once development is complete. New hairs grown during adult regeneration exit from the same canal specified in development. Hair canal generation occurs at the same time as epidermal barrier formation **(Figure 1.3A)**. The epidermis develops from a single layer of epidermal cells at embryonic day (E)12.5 to a multi-layered functional barrier by E18.5, a time when the hair pore is forming in the surrounding hair follicles [65]. Synchronizing these processes is significant; if the hair canal formed later, the HS would be tasked with penetrating the strong epidermal barrier.

Descriptive studies from the early 1900's outlined two alternative models for hair canal formation. In one model, the opening is proposed to begin late in development when cells attached to the sebaceous gland are pushed out of the follicle into the epidermis **(Figure 1.4A)** [66, 67]. These follicle-derived cells displace epidermal cells resulting in the creation of a small opening which becomes keratinized, forming the

mature canal [66, 67]. This model was based on descriptive studies in sheep and opossum and supports canal specification late in development. A later report studying mouse skin explants failed to find a link between the sebaceous gland and canal formation [68]. In this system, the canal appeared before the formation of differentiated sebocytes. This finding suggests that, at least in an *in vitro* system, movement of sebocytes is not required for canal specification. Instead, the author proposed that canal formation proceeds from the outside, initiating with keratinization of epidermal cells above the hair bud and progressing down into the follicle **(Figure 1.4B)** [68]. In support of this model, Pinkus et al. reported that murine hair canal specification begins with epidermal cells turning 90 degrees during stage 3 of follicle development (**Figure 1.4B**). Similar mechanisms are reported for human hair canal formation [70].

Both models posit that canal formation occurs at late stages of follicular development when differentiated cell types, such as the IRS and sebocytes, have formed. However, at this time the epidermal barrier is complete and breaking through the barrier to generate the canal would likely prove difficult**.** Our rudimentary understanding of this complicated process did not progress for nearly 80 years until Veniaminova et al. identified a novel population of cells marked by the expression of K79 that may contribute to hair canal formation [21]. Lineage-tracing experiments revealed that K79+ cells extend out of the developing follicle into the epidermis. Importantly, the distal tip of these K79 cell streams was lost concomitant with hair canal generation. These hair follicle-derived K79 cells sit in the epidermis and may act as a placeholder for the future hair canal. Once the distal K79+ cells are lost, a hole forms in the epidermal layers representing the putative hair canal.

1.26 The Hair Cycle

Adult hair follicles undergo cycles of growth (anagen), regression (catagen), and rest (telogen) **(Figure 1.1)**. The first anagen phase responsible for producing hairs initiated in embryonic development completes by the second week of postnatal life [9]. Next, the lower portion of the hair follicle is lost to massive apoptosis during catagen, drawing the dermal papilla upwards near the bulge stem cell compartment **(Figure 1.1)** [9]. Some bulge-derived outer root sheath cells survive catagen, contributing to the secondary hair germ (SHG) that will drive differentiation in the next growth phase [71, 72]. The hair follicle remains in telogen until the appropriate signals (BMP inhibition, WNT activation) initiate the next anagen phase **(Figure 1.5)**. Anagen largely recapitulates embryonic development with the hair follicles proceeding through 6 defined stages [9] **(Figure 1.3B)**, leading to the growth of a new hair shaft (HS) and associated supporting layers, inner root sheath (IRS) and companion layer (CL). The new HS emerges from the same hair canal formed during development. Entry of the nascent HS into the original canal involves K79+ cells extending up the follicle and joining with another population of K79+ cells in the suprabasal INF **(Figure 1.3B)** [21]. The original HS is shed out of the hair canal during exogen. The precise mechanisms controlling exogen remain unclear, but it is proposed to be an active process, likely involving the proteolytic loosening of cellular junctions facilitating release the old HS [73, 74] (reviewed in [75]).

1.27 Matrix Progenitors and Anagen

The transition from telogen to anagen begins with the proliferation of cells in the SHG sitting directly above the dermal papilla [56]. A few days after this event, bulge stem cells are activated and start to produce outer root sheath (ORS) cells, which continue to expand down to support the trajectory of the growing anagen follicle [56, 76-78]. Matrix progenitors located in the SHG produce the suite of differentiated layers in the follicle, including the HS, IRS, and CL **(Figure 1.2B &1.2C)** [25, 79]. Basal matrix cells sometimes referred to as the "germinative layer," are located at the epithelial-mesenchymal interface and divide asymmetrically to generate the suprabasal matrix population **(Figure 1.2B)** [79].

Similar to development, as anagen proceeds, the dermal papilla becomes progressively engulfed by the maturing matrix population. Production of the first terminally differentiated layers, like the IRS, was thought to occur during anagen III [9]. However, recent reports show that the first K79+ CL cells are formed as early as anagen II, suggesting these matrix-driven differentiation events initiate earlier than previously appreciated [21, 80].

The location of a given matrix cell impacts its cell-fate decision. Lineage tracing experiments in late anagen found that matrix cells sitting in the center of the hair bulb produced the HS, whereas matrix cells located more peripherally gave rise to the IRS and CL [25]. One explanation for this observation is the existence of sub-domains within the matrix population, driven by different dermal-derived signals. Yang et al. employed single-cell RNA sequencing to examine this possibility [80]. They found that basal matrix cells are molecularly heterogeneous, separating into distinct clusters indicative of cell

12

lineage [80]. The dermal papilla also exhibited molecular heterogeneity, separating into four distinct clusters along the length of the anagen bulb [80]. These findings suggest that basal matrix cells located at the top of the anagen bulb receive different dermal-derived signals from their counterparts located proximally. Spatially-distinct dermal signals likely contribute to the molecular heterogeneity and cell-lineage choices of the matrix population.

Collectively, these studies demonstrate the inherent complexity of cell-fate decisions during hair regeneration. The matrix population is dynamic throughout anagen, expanding in number as well as changing its relationship with the dermal papilla. As most of these studies were conducted in late anagen, many questions remain about the timing of matrix cell differentiation. Do matrix progenitors produce the terminally differentiated layers at the same time, or in sequential steps? If the layers are specified asynchronously, which layer forms first? Future work is needed to address these outstanding questions.

1.3 Signaling Pathways Driving Hair Follicle Morphogenesis and Homeostasis

1.31 Introduction

Elegant genetic studies using mouse models have demonstrated the role of signaling pathways at distinct stages of hair follicle development and regeneration (reviewed in [4, 81-83]). Key regulators of hair follicle biology include the Wnt/β-catenin, Hedgehog (HH), BMP, and Notch signaling pathways. These cascades play critical roles in both hair follicle (epithelial) as well as dermal papilla (mesenchymal) formation and cycling, and often cross-talk with each other. Disruption of these pathways leads to

13

abnormal hair follicle development and can drive numerous pathologies, including skin cancer [84-88]. Each pathway is briefly summarized below. Given the significant cross-talk that occurs between pathways, their roles in regulating hair follicle biology are discussed together **(Figure 1.5)**.

1.32 Wnt/β-catenin

The first mammalian Wnt gene was discovered in 1982 during studies with oncogenic retroviruses in breast cancer [89]. Later, this gene was traced back to its *Drosophila melanogaster* counterpart wingless (wg) described ten years previously for its role in segment polarity [90, 91]. Subsequent studies established the canonical Wnt/β-catenin pathway as a critical regulator of stem cell biology across several tissues, including the intestine [92-95] and hair follicle [96-98]. Given its importance in stem cell regulation, it is not surprising that activating mutations in this pathway are found in epithelial malignancies (reviewed in [99]). Most notably, loss of function mutations in the tumor suppressor *APC* result in excessive Wnt signaling that drive colorectal adenocarcinoma [100].

The critical mediator of the pathway, β-Catenin, is targeted by a multiprotein degradation complex in the absence of ligand. This complex is comprised of APC, Axin, CK1, and GSK3-β. Sequential phosphorylation events by CK1 and GSK3-β lead to recruitment of the E3 ubiquitin ligase, β-TRCP, and ultimately proteasomal degradation. WNT ligand binding to Frizzled and Lrp5/6 co-receptors results in phosphorylation of the Lrp5/6 cytoplasmic tail by GSK3β and CK1 [101]. This event leads to the recruitment of Dishevelled (DSH) and Axin, resulting in the inactivation of the degradation complex.

With the degradation complex inactive, β-Catenin can accumulate and translocate to the nucleus and bind with co-activators of LEF/TCF family to affect target gene expression [102]. Transcriptional targets of the pathway include *Lgr5* and *Axin2* [98, 103].

1.33 Hedgehog

First identified in a *Drosophila melanogaster* screen [104], the HH pathway is highly conserved from insects to mammals [105] and plays diverse roles during embryogenesis (reviewed in [106-109]). *Drosophila* have a single *Hh* gene, while mammals have three (sonic, indian, desert). Sonic (*Shh)* is expressed broadly throughout a wide range of tissues while Indian (*Ihh)* and Desert (*Dhh)* display restricted expression profiles and are required for bone formation and spermatogenesis, respectively [110, 111]. The importance of the HH cascade for embryonic patterning is easily appreciated by analysis of *Shh*^{-/-} mutant mice which develop cyclopia with an overlying proboscis and exhibit severely impaired forebrain development [112]. These features are characteristic of the human developmental condition, holoprosencephaly, which has been linked to mutations in the HH pathway [113, 114] (reviewed in [115]). *Shh*^{-/-} mice also display profound defects in limb bud development as well as the formation of the heart, lungs, and foregut [112, 116-118]. Interestingly, the epidermis appears relatively normal in *Shh*^{-/-} mice, although hair follicle development halts at an early stage [119].

In addition to developmental conditions (e.g., holoprosencephaly), mutations in HH signaling also drive human cancers (reviewed in [120]). Aberrant HH signaling is

found in sub-types of medulloblastoma [121, 122], as well as the most prevalent cancer, basal cell carcinoma [123-125] (reviewed in [126]).

In mammals, the initiation of HH signaling requires the formation of the primary cilium [127, 128]. In the absence of ligand, the transmembrane protein patched 1 (PTCH1) localizes to the primary cilium and blocks the entry and function of the 7-pass transmembrane protein, smoothened (SMO) [129-132]. Without SMO activation, downstream GLI family transcription factors repress HH target genes. The cascade is activated when HH ligands bind to PTCH1 [133, 134], resulting in its exit from the primary cilia and facilitating SMO entry [135]. These events lead to the processing of GLI transcription factors into their activator and suppression of repressor forms. Two principal target genes are the HH pathway members *Ptch1* and *Gli1.*

There are three GLI proteins in vertebrates, with GLI1 and GLI2 acting primarily as activators and GLI3 functioning as a repressor [136-138]. GLI1 is dispensable for development, while GLI2 and GLI3 are needed to provide their respective activating and repressive roles [136, 138-141]. GLI2 plays critical roles in neural tube development [136, 140]. The specification of neural progenitors within the neural tube involves a ventral-dorsal HH gradient (reviewed in [142]). *Gli2* mutants lack floor plate cells which require high HH pathway activity for their specification [140, 143]. However, cell types which require a lower HH level (e.g., motor neurons) are still specified in GLI2 mutants [140, 143]. These data suggest that GLI2 is required to transduce high-level HH signaling in the forming neural tube. Interestingly, *Gli1/2* double mutants display more severe phenotypes than single mutants in the neural tube as well as the lung [138]. This

observation implies that GLI1 and GLI2 have overlapping roles in the developing neural tube and lung.

In contrast to GLI2, GLI3 acts as a repressor of HH signaling [144-147]. In the developing limb, GLI3 counteracts SHH expression to modulate HH pathway levels and control digit specification [148]. In line with this role, *Gli3*-deficient mice exhibit polydactyly [149]. *Gli1/2* double mutants display normal limb and digit development indicating that the GLI3 is the major mediator of HH during limb development [150]. The digit and craniofacial defects in *Gli3* mutant mice mimic Greig cephalopolysyndactyly syndrome, a condition linked to mutations in *GLI3* [151].

1.34 Bone Morphogenetic Proteins

First appreciated for their ability to induce bone formation [152], BMPs mediate multiple processes during embryogenesis including cell proliferation, differentiation, and apoptosis (reviewed in [153]). BMP signaling is required in gastrulation, as knockout of *Bmp4* or *Bmpr1a* results in impaired mesoderm formation and embryonic lethality [154, 155]. Over 15 BMP ligands have been identified (reviewed in [153]), and many organs require one or more during development. For example, BMP7 is required for skeletal patterning, eye development, and kidney formation [156], while BMP8 and BMP12 have roles in spermatogenesis and seminal vesicle development, respectively [157, 158]. BMP signaling during gastrulation directs multipotent ectodermal cells towards an epidermal lineage [159, 160].

BMP ligand binding to a transmembrane BMP receptor (BMPR) complex activates the pathway (reviewed in [161, 162]). Ligand binding triggers a series of

phosphorylation events resulting in the activation of SMAD proteins. BMPs signal through SMAD 1/5/8 which then associate with SMAD 4 and move into the nucleus to affect gene transcription [163]. Relevant BMP transcriptional targets in hair follicle biology include Inhibitor of DNA Binding (*Id)* family members as well as the inner root sheath marker, *Gata3* [164, 165].

1.35 Notch

The Notch signaling pathway is a conserved cell-cell signaling cascade that plays diverse roles in development and adult homeostasis across many tissues (reviewed in [166, 167]). Notch is required for the development of multiple organs, including kidney, heart, and vasculature, as well as homeostasis of the epidermis, gut, and other tissues in postnatal life [86, 168-173].

The pathway is induced by contact between receptors and ligands on adjacent cells. In mammals, there are four Notch receptors (notch 1-4) and five Notch ligands (delta-like 1-3, jagged 1-2) that can interact with each other and initiate signaling (reviewed in [174, 175]). Receptor-ligand binding results in sequential cleavages of the Notch receptor, releasing an activated intracellular fragment (NICD). NICD enters the nucleus where it binds with RBPJ, releasing co-repressors and allowing association with co-activators, like mastermind-like to drive target gene expression. Transcriptional targets of the Notch pathway include *Hes* and *Hey* family members [176, 177].

The role of Notch signaling is dependent on the cellular context and can include proliferation, terminal differentiation, or lineage commitment. In the epidermis, Notch is an established regulator of terminal differentiation (reviewed in [178]). Notch receptors are

expressed in the differentiating layers of the skin and hair follicles [179, 180], and the

pathway is activated in cells undergoing or primed to differentiate. Epidermal-specific

ablation of Notch via *Rbpj*-knockout leads to impaired differentiation within the interfollicular

epidermis and hair follicles [181].

1.36 Hair Placode Induction

The Wnt/β-catenin pathway is necessary for hair placode induction **(Figure 1.5).**

Mice bearing a Wnt/β-catenin reporter gene (TOPGAL) show activation of the pathway

in forming placodes as well as the underlying dermal cells [96]. In epidermal-specific β-

catenin knock-out [182], and with constitutive overexpression of the Wnt inhibitor *Dkk1*

[183], hair follicle development is blocked. Conversely, in both chick and mouse

epidermis forced expression of a stabilized form of β-catenin results in the formation of

ectopic follicles [184-186].

In contrast to Wnt/β-catenin, BMP signaling plays an inhibitory role in hair

placode induction. BMP-2 and BMPR-1A are expressed throughout hair placodes, while

BMP-4 and the BMP inhibitor, NOG, are expressed in the forming dermal papilla [187-

190]. Dermal-derived NOG acts on the overlying epithelium to inhibit BMP signaling and

allow hair follicle development to proceed **(Figure 1.5)**. *Nog*-knockout mice lack 90% of

hairs and exhibit delayed development in the remaining follicles [63, 189]. Further, *Nog*

overexpression in basal keratinocytes leads to increased follicle density [191]. The

expression of LEF1, a readout of Wnt/β-catenin pathway and a critical player in hair

follicle induction, is decreased in *Nog*-deficient mice [189]. Conversely, primary

epidermal keratinocytes treated with NOG display elevated LEF1 levels compared to

untreated controls [192]. Together these findings suggest that BMP's inhibitory role in hair morphogenesis is at least partially due to repression of *Lef1*. BMP also plays a similar inhibitory role in the initial stages of tooth and feather development [193-195].

Shh signaling is not essential in hair induction. Hair follicles are specified in *Shh*^{-/-} mice, although they do not progress past the hair germ stage and lack a dermal counterpart [119, 190, 196]. *Shh*-deficient hair follicles exhibit Wnt reporter activity [197]. In contrast, in β-catenin^{-/-} epidermis, *Shh* and its target *Ptch1* are not expressed [182]. These data place the Wnt/β-catenin pathway upstream of Shh during the initial stages of hair follicle morphogenesis.

Ouspenskaia et al. further evaluated this relationship by examining domains of Shh and Wnt pathway activation [198]. They uncovered an antagonism between the two pathways wherein individual cells exhibit activation of one, but not both pathways. The Wnt/β-catenin pathway is high in the cells located at the bottom of the hair germ (basal), but low in their daughter cells, located directly above in the center (suprabasal). In contrast, the Shh pathway is activated in the suprabasal daughter cells via SHH ligand produced in the WNT^{hi} basal cells [198]. The lack of Shh pathway activity in LEF1 expressing basal cells suggests that elevated Wnt signaling may block autocrine Shh signaling or activation of the Shh pathway in those same (WNT^{hi}) cells. Overexpression of *Shh* within the epidermis during early development is sufficient to overcome WNT-mediated inhibition of autocrine signaling [198]. These samples also exhibit decreased levels of LEF1 in the epidermis, implying that elevated levels of SHH expression may also repress Wnt pathway activity [198]. In support of this notion, *Shh*^{-/-} hair follicles exhibit expanded LEF1 expression domains [197, 198]. The balance between Wnt and

Shh signaling is important for proper hair follicle development as the specification of both presumptive bulge stem cells and differentiated progeny requires the WNT[low]/SHH-pathway[high] domain of the center of the hair germ.

1.37 Hair Follicle Organogenesis and Differentiation

Following specification, follicles extend down into the dermis and prepare for hair shaft generation. This process requires a massive expansion of the epithelial-follicle lineage, as well as coordination with the forming dermal papilla. While SHH is dispensable for hair follicle specification, it is required for progression past stage 2 **(Figure 1.5)** [119, 190, 196]. *Gli2*-deficient hair follicles exhibit a comparable phenotype to that seen in *Shh^{-/-}* mice [196], providing evidence that Shh pathway activation is primarily driven by GLI2 in this context. Proliferation within the growing hair follicles is significantly lower than controls in both *Shh^{-/-}* and *Gli2^{-/-}* mice [190, 196]. Ectopic expression of a constitutively activated form of *Gli2* in the epidermis (*Keratin-5-Cre; ΔNGli2*) of *Shh^{-/-}* mice does not completely rescue the mutant phenotype [196]. One explanation for this result is the presence of GLI3-repressor in a *Shh*-deficient context. Elevated levels of GLI3 repressor are found in the developing neural tube and limb buds of *Shh^{-/-}* mice [148, 199]. SHH ligand is required to facilitate entry of SMO into the primary cilia where GLI transcription factors can be processed. Thus, the forced overexpression of constitutively active *ΔNGli2* is strongly opposed by high levels of GLI3 repressor. *Shh^{-/-}; Gli3^{-/-}* double mutants display partial rescue of the developmental and proliferation defects of *Shh^{-/-}* mice implicating GLI3 in hair follicle morphogenesis [200]. Analysis of *Shh^{-/-}; Gli3^{-/-}* mice overexpressing *ΔNGli2* throughout the epidermis

would facilitate the closer interrogation of GLI function during epidermal development. Epithelial-derived SHH controls dermal papilla formation and maintenance via induction of the BMP inhibitor, NOG [201]. As such, the limited rescue of epidermal-specific GLI2-activator expression in *Shh*^{-/-} may also be a result of impaired dermal papilla function.

Numerous genetic models have highlighted the requirement for Wnt/β-catenin, BMP, and Notch pathways for terminal differentiation of the inner root sheath (IRS) and hair shaft (HS) (**Figure 1.5)** [32, 33, 96, 173, 181, 202-204]. Wnt/β-catenin signaling is required for proper hair shaft differentiation [96], highlighted by the fact that many structural hair keratin genes have LEF/TCF DNA-binding domains [205, 206]. When BMP signaling is blocked throughout the epidermis and hair follicles (*Keratin-14-Cre; Bmpr1a*^{fl/fl}*)* the IRS and HS are not specified. Intriguingly, the companion layer (CL) is still formed in these mice [33]. While BMP is essential for the initial specification of IRS and HS, Notch appears to play a slightly different role in terminal differentiation. The Notch target gene, HES1 is present in the inner, suprabasal, cells of forming follicles and later in the presumptive IRS [181]. Disruption of Notch signaling throughout the epidermis and hair follicle (*Keratin-14-Cre; Rbpj*^{fl/fl}) results in hair loss, epidermal cyst formation, and barrier defects [173, 181, 204]. Blanpain et al. grafted epithelial-*Rbpj* knockout skin onto nude mice to study later stages of hair follicle development [181]. While both the IRS and HS are present at the time of grafting, they are not maintained and are unable to mature normally. Two weeks following grafting, controls exhibited external hair, while knockout hair canals were filled with keratinized material, not IRS and HS [181]. Most genetic manipulations to date have either not reported defects in CL specification [33] or have omitted them from their discussion. As such, the signaling

pathways required for CL specification and maintenance have yet to be determined. A closer examination of Notch, BMP and SHH mutant mice is needed to critically asses the involvement of these pathways in CL regulation.

1.38 Hair Follicle Regeneration

Hair regeneration largely recapitulates initial follicle formation **(Figure 1.3)**. Like development, anagen onset requires the coordination of Wnt/β-catenin activation with BMP inhibition within the bulge stem cells and SHG (**Figure 1.5)** [56, 207]. Indeed, BMP signaling is required to maintain bulge stem cells in their quiescent state during telogen [164, 208]. Intradermal adipocytes near the follicle express *Bmp2* during telogen which contributes to the inhibition of bulge stem cell activation [8]. Genetic-disruption of BMP signaling via *Bmpr1a*-deletion leads to ectopic activation of stem cells as well as the formation of epithelial tumors and cysts [32, 203, 207, 208]. BMP inhibition during the telogen-anagen transition is mediated by dermal-derived NOG [8, 209] and overexpression of *Nog* within the epidermis results in precocious anagen entry [191, 210]. In addition to NOG, the dermal papilla produces TGF-β2 and FGF7 which contribute to anagen onset [53-56]. TGF-β2 induces the expression of *Tmeff1* in the SHG during late telogen, counteracting BMPs inhibition of stem cell activation [54]. FGF7 promotes proliferation within the SHG, an initial step during anagen induction [56].

The Wnt/β-catenin pathway is activated in the bulge and SHG upon anagen induction [96]. Expression of a stabilized form of β-catenin within the epidermis and follicles results in premature entry into anagen [211, 212]. In contrast, β-catenin-

knockout results in the formation of epithelial cysts at the expense of new hair growth [182, 212].

Shh is expressed in the SHG during early anagen where it drives proliferation and downgrowth [72, 213]. Matrix-derived SHH promotes proliferation in bulge stem cells during early anagen when the two populations are near each other [72]. Treatment with a SHH-blocking antibody stops regeneration in early anagen [213], supporting its role in progression. Epithelial-derived SHH also regulates dermal adipocytes and fibroblasts [72, 119, 190, 201, 214]. Zhang et al.found that SHH promotes adipogenesis in the surrounding dermis during anagen progression [214]. Shh also functions in maintenance and maturation of the dermal papilla [72, 119, 190, 201]. Epithelial-derived SHH results in increased expression of Fgf7 and Nog within the dermal papilla, which promote anagen progression in the hair bulb [164, 201].

In both development and regeneration, the expression of Shh displays dynamic shifts. In early stages, Shh expression is symmetric throughout the forming matrix progenitor population [49] but becomes restricted to one side of the hair bulb at later stages. The exact mechanisms governing these shifts are not well understood, but likely involve niche-dependent signals. Interestingly, sustained activation of the Wnt pathway [184] or ectopic delivery of NOG results in expanded expression of Shh within the hair bulb [201, 209].

Differentiation of matrix progenitors into distinct cell lineages is again reliant on Wnt, BMP, and Notch signaling with many parallels to development **(Figure 1.3)** (reviewed in [1, 83]). Lef1 is expressed throughout the matrix with the highest signal in cells committed towards a hair shaft lineage that also exhibit Wnt reporter activity [96].

The BMP readout, phospho-SMAD 1/5/8, is also present in the matrix progenitor population [208]. Finally, early studies looking at the role of Notch in hair follicle biology identified the expression of jagged 1, jagged 2, and notch 1 in regions of the adult hair bulb [180, 215, 216]. The markers for these pathways are also expressed in the matrix of developing follicles, supporting the functional evidence for their role in terminal differentiation discussed earlier. Efforts in the field are currently focused on separating the matrix into sub-populations to glean information about the requirement of specific signaling pathways in cell-fate decisions.

1.4 Epidermal Barrier Formation and Harlequin Ichthyosis

1.41 Introduction

The formation of the epidermal barrier is a highly orchestrated process that when disrupted can lead to numerous human pathologies. These include blistering diseases such as, epidermolysis bullosa simplex and pemphigus, inflammatory disorders like psoriasis and atopic dermatitis, as well as various forms of ichthyoses (reviewed in [217-221]).

Mammalian skin is composed of a stratified squamous epithelium made up of four distinct cell layers. Proliferative cells of the basal layer sit directly above the dermis, anchored to the basement membrane. Barrier formation initiates when basal cells detach from the basement membrane and move towards the skin surface to produce the differentiated suprabasal layers (spinous, granular and the cornified) [65] (reviewed in [222]). These layers possess unique markers that reflect their differentiation status **(Figure 1.6A)**. Like the follicle, terminal differentiation in the epidermis is regulated by

Notch signaling (reviewed in [178]). Notch receptors (notch 1-3) as well as the ligand JAG1 are expressed in the suprabasal layers of the forming epidermis, while JAG2 is found in basal cells [173, 215]. Mutant mice lacking canonical Notch signaling are unable to form normal spinous or granular layers, highlighting its importance in differentiation [181, 223]. The Notch target gene, HES1, regulates differentiation from spinous to granular fate. Indeed, *Hes1*-knockout mice display premature differentiation of spinous cells into granular cells during early epidermal development [223]. Notch has also been implicated in downregulating the expression of integrins which are involved in anchoring basal cells to the basement membrane [181].

Cells of the epidermis are tightly linked by different types of cell-cell junctions including desmosomes, adherens junctions, and tight junctions (reviewed in [224]). Basal cells interface with the basement membrane via specialized desmosomes (hemidesmosomes) [225, 226]. Classical desmosomes and adherens junctions are found throughout the suprabasal epidermis. Disturbed desmosomal adhesion caused by autoantibodies against desmomsal cadherins underlies the blistering disesases of pemphigus [227, 228]. The physical skin barrier requires tight junctions which are located in the upper granular and cornified layers [229-231]. Mutant mice with impaired tight junctions display impaired barrier function and die shortly after birth [231].

Keratinocytes undergo a unique form of programmed cell death (cornification) to produce the dead corneocytes, often referred to as the building blocks of the epidermal barrier (reviewed in [232, 233]). Cornification involves extensive changes to the structure and molecular status of the cells, ultimately resulting in the replacement of intracellular organs with cytoskeletal material and the formation of the cornified

envelope, a mix of insoluble proteins that replaces the plasma membrane and acts as a

lipid scaffold **(Figure 1.6)** [232, 234]. This process begins with cells in the spinous layer

replacing the pre-existing keratin 14 (K14) and keratin 5 (K5) intermediate filament

network found in basal cells with keratin 1 (K1) and keratin 10 (K10) [235].

Desmosomes connect spinous cells to each other via K1/K10 filaments and provide

resistance to mechanical stress. Late differentiation markers, including cornified

envelope precursors, are expressed in the upper epidermal layers [236]. These include

involucrin (INVL) which is first expressed in the upper spinous layers as well as loricrin

(LOR) and filaggrin (FIL) which are found in the granular layer. The granular layer is

typified by the presence of keratohyalin granules which are aggregations of histidine

and cysteine-rich proteins that bind together keratin filaments. A major component of

keratohyalin granules is pro-filaggrin, the inactive precursor to FIL. Activation of pro-

filaggrin involves dephosphorylation and proteolytically cleavage, resulting in the

release of individual FIL monomers [237, 238]. These FIL monomers bind to keratin

filaments, contributing to the compaction of the cytoskeleton in cells of the upper

epidermis. Further compaction is accomplished by cross-linking of cornified envelope

components including LOR, INVL, and small proline-rich proteins (SPRRs) by

transglutaminases [239, 240] (reviewed in [241]). LOR accounts for over 80% of

cornified envelope content by weight [240, 242, 243]. SPRRs are proposed to act as

bridges linking together LOR and other precursors within the cornified envelope [243].

The cornified envelope of each corneocyte is connected to its neighbors via specialized

desmosomes called corneodesmosomes. Corneocytes at the top of the epidermis are

eventually shed in a process that requires proteases like kallikreins to degrade the cellular junctions [244, 245].

A vital component of the epidermal barrier is the intercellular lipid matrix found throughout the stratum corneum **(Figure 1.6B)**. Lipids and their precursors are packaged into membrane bound organelles called lamellar granules by transporter proteins in the granular layer and extruded into the intercellular space in the upper epidermis [246, 247]. Corneocytes and the surrounding lipids are often referred to as the "bricks and mortar" of the epidermis **(Figure 1.6B)** [248]. In this analogy the skin represents a wall constructed of individual corneocytes (bricks) which are stuck together by intercellular lipids (mortar) [249]. Epidermal homeostasis is maintained by desquamation, or sloughing off, of the upper cornified layer. Impaired desquamation leads to the characteristic thickened skin observed in Harlequin Ichthyosis (HI) [250].

1.42 Clinical Features of Harlequin Ichthyosis

HI is the most severe form of ichthyotic-diseases, characterized by fish-like scales covering the body [251]. First described in 1750 [252], HI patients have a massively expanded stratum corneum **(Figure 1.7)**, impairing barrier function and rendering neonates susceptible to infection, dehydration, and impaired thermoregulation [253-255] (reviewed in [251]). The extreme thickening of the epidermis pulls the skin tight, resulting in breaks or fissures in between the plate-like scales, as well as deformation of facial features, and autoamputation of digits [254, 255]. The HI phenotype appears in the hair canal, before the epidermis [255], raising the question of whether the hair follicle plays a role in the pathogenesis of HI. Patients with HI exhibit

28

generalized poor hair growth [254], potentially a result of impaired hair exit from the canals. The involvement of the hair follicle in the pathogenesis of this disease has yet to be rigorously tested.

Previously thought to be invariably fatal, survival rates for HI patients have increased recently. Rajpopat et al. reported a 56% survival rate in a retrospective study of 45 cases of HI. These survivors' ages ranged from 10 months to 25 years. Improved survival can be attributed to better quality of care and possibly treatment with oral retinoids (vitamin A derivatives), although patients not treated with retinoids have survived as well [253, 254, 256, 257]. Surviving patients exhibit a dramatic phenotypic improvement, resembling non-bullous congenital ichthyosis erythroderma, a less severe form of ichthyosis [254, 256, 258]. Understanding the molecular mechanisms underlying this phenotype improvement should be an area of focus in the field in the coming years.

1.43 Mutations in ABCA12 Underlie Harlequin Ichthyosis

Mutations in the lipid transporter, ATP binding cassette subfamily A member 12 (ABCA12), result in HI [251, 254, 259-261]. Over 55 distinct loss-of-function mutations have been reported in patients. These mutations are most frequently nonsense or deletions, and are distributed throughout the *ABCA12* gene [254, 261]. Survival rate and disease severity are linked to the type of *ABCA12* mutation. Patients with a compound heterozygote mutation are more likely to survive than those bearing homozygote mutations [262].

ABCA12 is a member of the ATP-binding cassette transporter family of proteins which transport lipids and other molecules across membranes or into organelles [263,

264]. Akiyama et al. found that ABCA12 localized to lamellar granules throughout the granular layer in human skin. ABCA12 loads lipids into these lamellar granules which are then released into the intercellular space in the stratum corneum **(Figure 1.6A)** [259]. Lamellar granules are abnormal, or absent in the epidermis of HI patients **(Figure 1.7)** [259]. Many mature lipids that constitute the epidermal barrier are derived from glucosylceramide (GlyCer) delivered in lamellar granules. Epidermal cells derived from HI patients harboring *ABCA12* mutations show impaired ability to transport GlyCer in a cell culture system [259]. Remarkably, this phenotype can be corrected via *ABCA12* gene transfer [259], indicating that ABCA12 is required for proper transport of the barrier lipid pre-cursor, GlyCer. The expression of desquamation-specific proteases, kallikrein 5 and cathepsin D, is dramatically reduced in the epidermis of HI patients (**Figure 1.7)** [265]. Loss of these proteins which break cell-cell connections required for sloughing off dead cells, may underlie the massive expansion of the stratum corneum in HI patients.

Normal epidermal differentiation is also disrupted in HI patient skin **(Figure 1.7)**. Using a 3D human organ culture system, Fleckman et al., showed HI keratinocytes exhibited reduced expression of the differentiation marker, keratin 1 (K1), as well as impaired conversion of pro-filaggrin to filaggrin. Further evidence is needed to understand whether this abnormal differentiation is a direct result of ABCA12 loss or an indirect consequence of impaired barrier function. The development of the HI phenotype begins in utero, preceding introduction to a dry environment where a functioning barrier is required [255]. This observation suggests that impaired differentiation is not a result of impaired barrier function, but rather a direct consequence of ABCA12 loss.

1.44 Mouse Models of Harlequin Ichthyosis

Researchers have turned to mouse models to examine the disease mechanisms of HI in more detail. To date, four whole-body *Abca12-* knockout mouse models have been generated [250, 267-269] **(Table 1.1)**. These models differ in location and type of ABCA12 mutation, but all recapitulate the gross phenotype of human HI patients. They also display severe barrier deficiencies and have abnormal differentiation programs and lamellar granules [250, 267-269].

Yanagi et al., reported ABCA12 expression in the lung of wild-type mice. Further, in their *Abca12*-deficient model the lungs are unable to inflate due to decreased expression of pulmonary surfactant protein B [268]. They speculated that respiratory failure might lead to death. However, Zuo et al. failed to find a lung phenotype in their model, so the precise role of ABCA12 in the lung remains unclear. Respiratory distress is a leading cause of death in HI human patients [254] and rare cases of lung abnormalities including incomplete development (pulmonary hypoplasia) have been reported [254, 270]. These lung defects have yet to be directly linked to respiratory failure in HI patients. Rather, chest compression caused by the tightness of the skin is postulated to contribute to the high rates of respiratory distress [254].

One limitation of these mouse models is the severity of their phenotype causes them to die shortly after birth. To circumvent this issue, Yanagi et al. transplanted *Abca12*-knockout skin onto nude mice to follow the phenotypic changes that occur postnatally [271]. Intriguingly, both differentiation and barrier defects were rescued in transplantation experiments, mirroring the improvements in phenotype observed in human patients. This result highlights the need for genetic models that facilitate

postnatal studies. Further, most studies using these mice have focused at the skin surface, largely ignoring the hair follicle. Given that human patients exhibit hair follicle-abnormalities prior to epidermal phenotype, it is important to evaluate this possibility, as well.

1.5 Dissertation Summary

The advent of new mouse models and molecular tools has resulted in significant advances in the field of epidermal and hair follicle biology in the past 20 years. Much of this work focused on the adult stem cells in the bulge and their contribution to follicle biology and skin pathologies (reviewed in [272]). My thesis aims to shed light on other aspects of hair follicle biology that are less understood, including temporal aspects of terminal differentiation within the follicle, and the link between hair canal development and the human barrier disease, Harlequin Ichthyosis.

In Chapter II, I evaluate the timing of matrix cell differentiation within the follicle, as well as the importance of mesenchymal-derived signals from the dermal papilla during cell-fate decisions [273]. In Chapter III, I shift my focus up the hair follicle from the bulb to the canal. Here, I evaluate the role of migratory Keratin 79+ cells during hair canal generation, following up a previous report from my lab [21]. This chapter also highlights the link between follicular and interfollicular development which is the focus of Chapter IV. In Chapter IV, I develop a genetic tool for studying the role of the lipid transporter, ABCA12, in epidermal and hair follicle development. The overarching uses for this tool are two-fold: (1) understand the role of ABCA12 in normal hair follicle biology and (2) to evaluate the involvement of the hair follicle in the pathogenesis of HI

and barrier function. In addition, this tool may be useful to study the role of ABCA12 in

other organ systems.

1.6 Figures
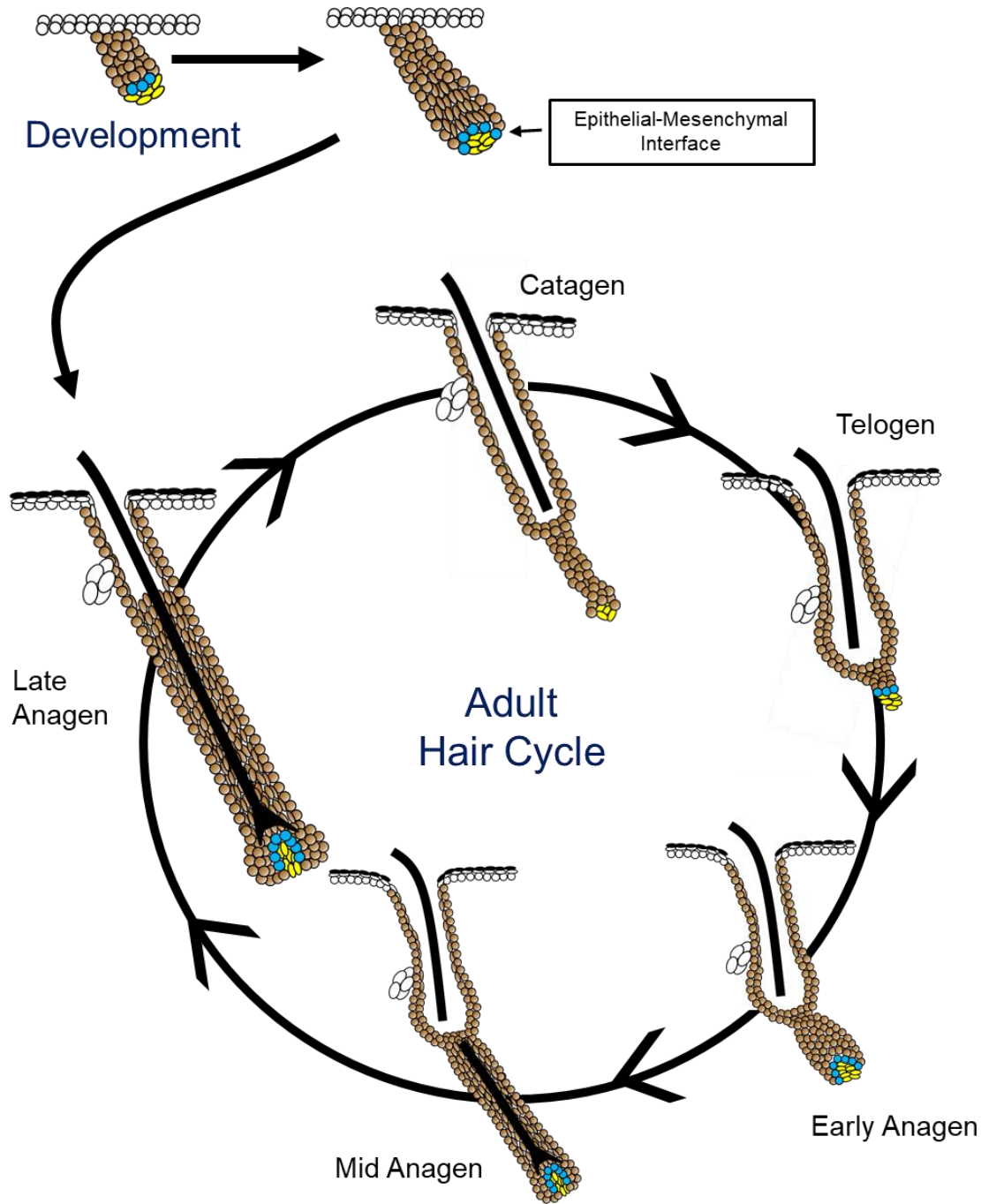
Figure 1.1 Overview of Hair Follicle Biology. Hair follicles (brown) form early in development, growing down from the overlying epidermis (white). Hair follicles formed in development undergo cyclical phases of anagen (growth), catagen (regression), and telogen (rest). Hairs grown during postnatal cycling emerge from the same hair canal formed in development. Blue: Matrix progenitor cells (epithelial). Yellow: Dermal Papilla (mesenchymal). Sebaceous glands (white) are attached to the hair follicles.
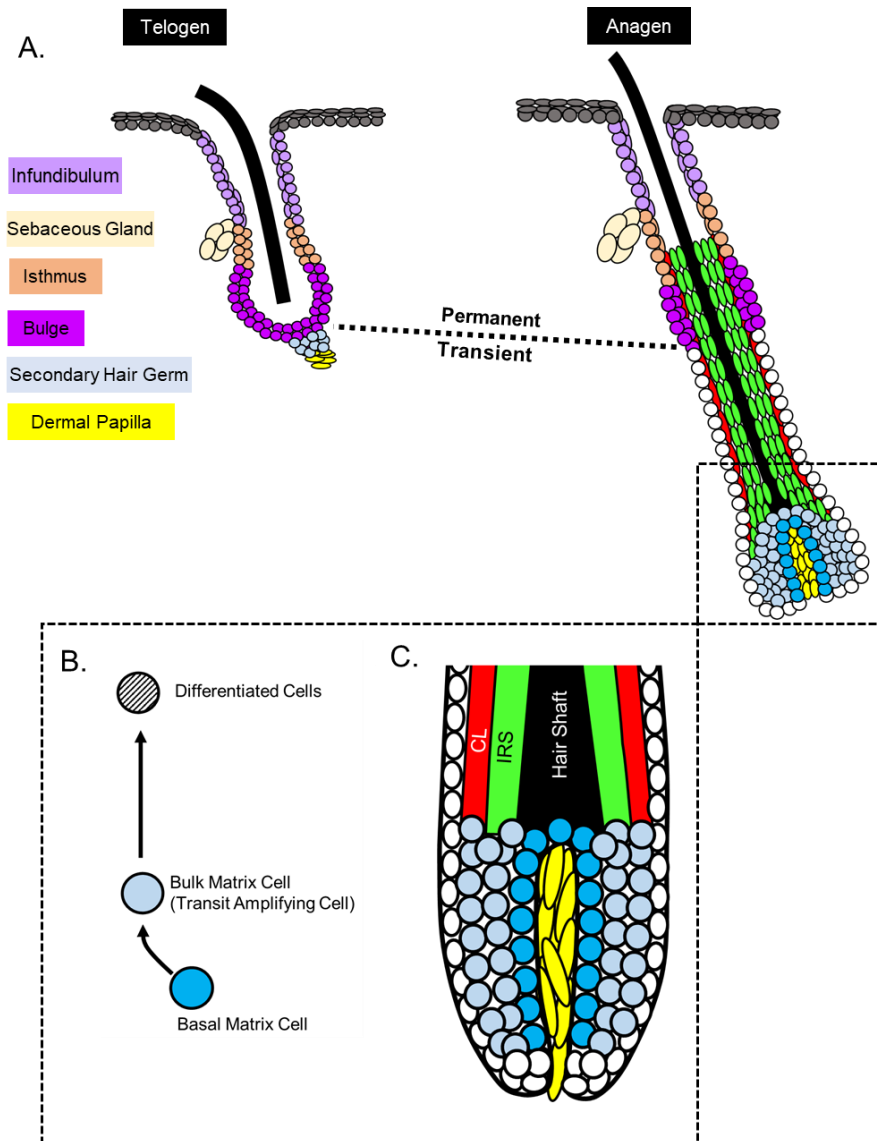
Figure 1.2. Cellular Domains of a Hair Follicle. A. Telogen and Anagen Domains. Left: The telogen follicle contains the permanent regions of the hair follicle which are not lost during the catagen period of the hair cycle. Right: The anagen follicle contains the cellular domains of the telogen follicle as well as cell populations that are distinct to the growth phase. The secondary hair germ (light blue) of the telogen follicle becomes the matrix of the growing follicle, a proliferative domain that is in the anagen bulb (dotted box) and gives rise to differentiated cells within the follicle. Dotted line indicates separation from the permanent, non-cycling portion (above), and transient portion (below). **B. Matrix Progenitor Hierarchy**. Basal matrix cells sit along the epithelial-mesenchymal interface and divide asymmetrically to produce bulk matrix cells (light blue) that ultimately differentiate. **C. Structure of a Mature Anagen Bulb**. Differentiated cell layers produced by matrix cells are arranged in concentric rings and include the companion layer (CL, red), inner root sheath (IRS, green), and hair shaft (black).

35
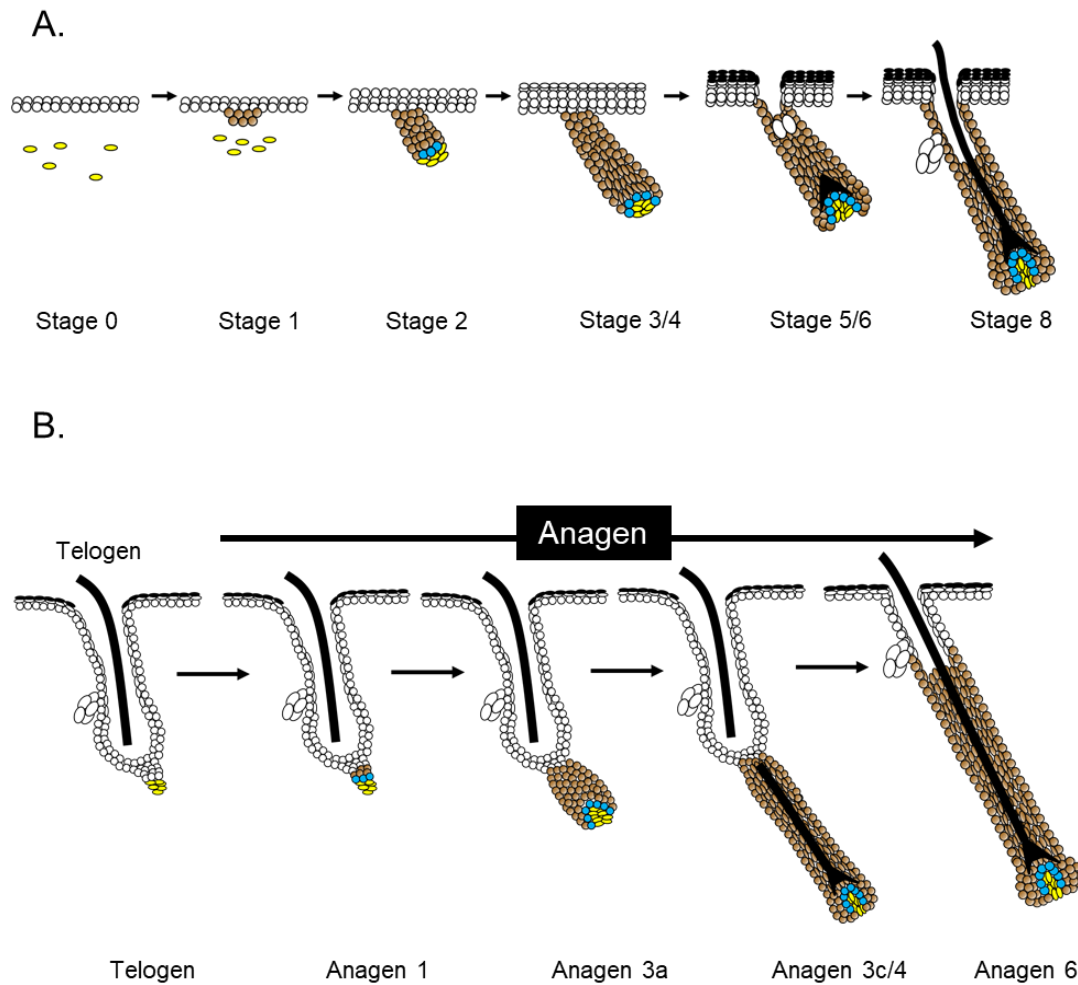
Figure 1.3. Hair Follicle Development and Regeneration. **A. Major Steps in Hair Follicle Development.** This process begins with induction as the follicle (brown) placode forms below the epidermis. As morphogenesis continues, the follicle grows down and associates closer with the developing dermal papilla (yellow). Matrix cells (blue) located in the bottom of the follicle progressively wrap around the dermal papilla as development continues. The first differentiation event, specification of the inner root sheath (IRS), is thought to occur late in development (stage 4) and require a mature dermal papilla. As hair follicle development progresses, the epidermis undergoes a specialized differentiation process to produce a complete barrier (black layer, Details in Figure 6). Hair canal formation occurs at stage 6, at the same time as epidermal barrier completion. Shortly following birth, the hair shaft emerges from the canal**. B. Major Stages of Anagen**. The transition from telogen to anagen causes (1) proliferation of cells in the secondary hair germ (matrix, blue) and (2) stem cell activation in the bulge. As anagen proceeds, matrix cells proliferate and at later stages, differentiate. Like development, differentiation is thought to require mature dermal papilla (yellow) signals and occur with specification of the IRS at Anagen 3a. By anagen 6, the nascent hair shaft emerges from the old hair canal. Adapted from [9,64].
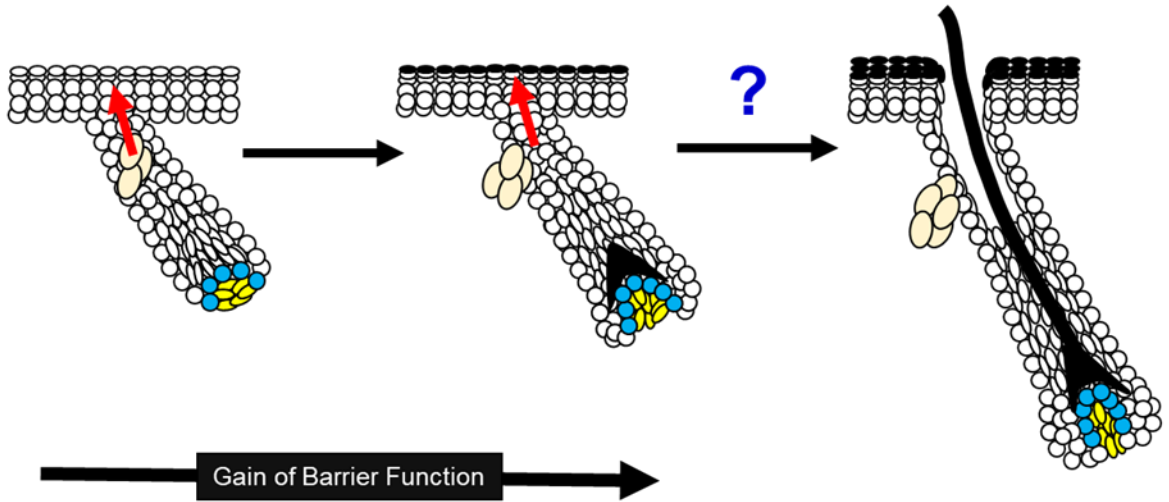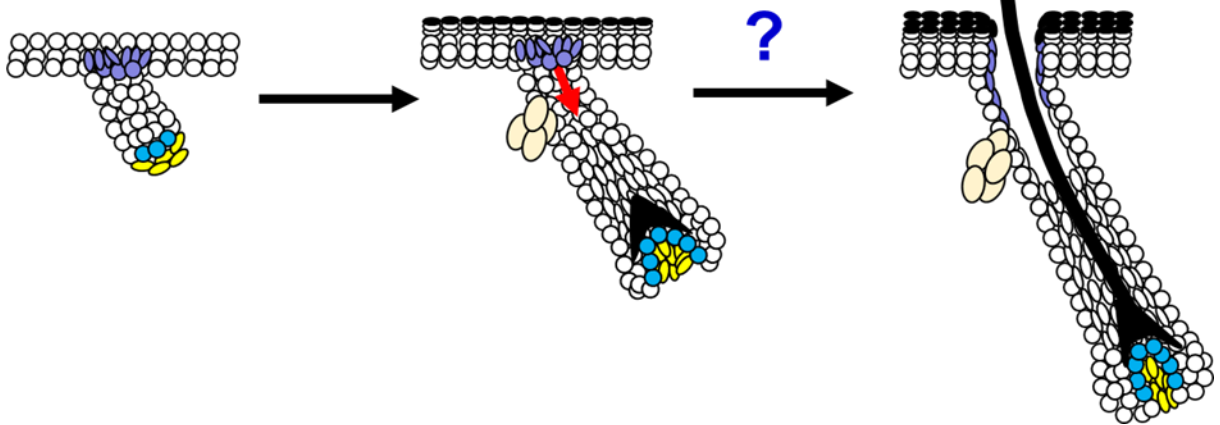
Figure 1.4. Models for Hair Canal Generation. **A. Model 1**. Cells attached to developing sebocytes move out of the hair follicle, keratinize, ultimately resulting in canal formation. **B. Model 2**. During stage 3 of follicle development spinous epidermal cells above the follicle reorient themselves to initiate canal specification. In contrast to the model in (A), this model is thought to proceed from the epidermis down into the follicle. Note that the epidermal barrier is forming concurrently with canal generation and that in both models the canal is formed after acquisition of barrier function. The precise mechanisms leading to canal generation are not well understood.
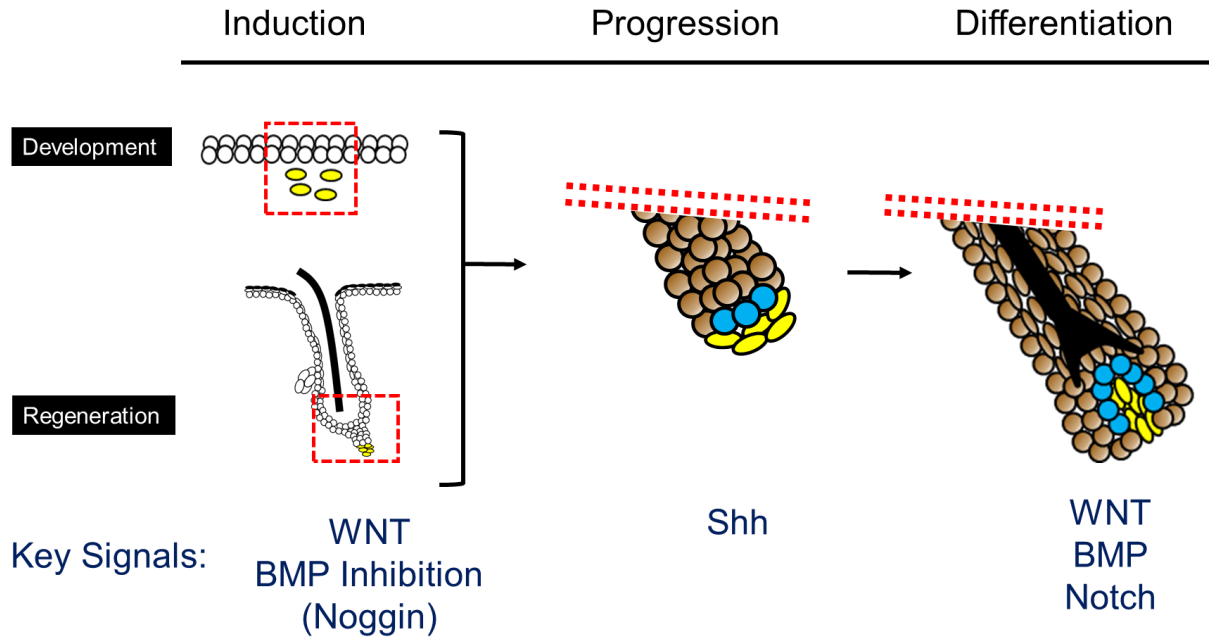
Figure 1.5. Key Signals Involved in Regulating Hair Development and Regeneration. WNT activation and BMP inhibition are required for induction of hair development and hair regeneration. Dermal-derived noggin is the primary source of BMP inhibition in this context. Red dotted box represents zoomed in area for both development and regeneration. SHH expression is required for both development and regeneration to continue as it promotes proliferation in hair follicle epithelium and is also essential for dermal papilla maintenance and maturation. Matrix cell (blue) differentiation requires the WNT (HS), BMP (IRS, HS) and Notch (IRS, HS) pathways. Specific pathways required for specifying and maintaining the companion layer (CL) remain unknown. Note: This schematic only represents the roles of WNT, BMP, Shh, and Notch. These processes are very complex, requiring many signals not discussed here (reviewed in [4,83]). Abbreviations: HS: Hair Shaft; IRS: Inner Root Sheath; CL: Companion Layer.
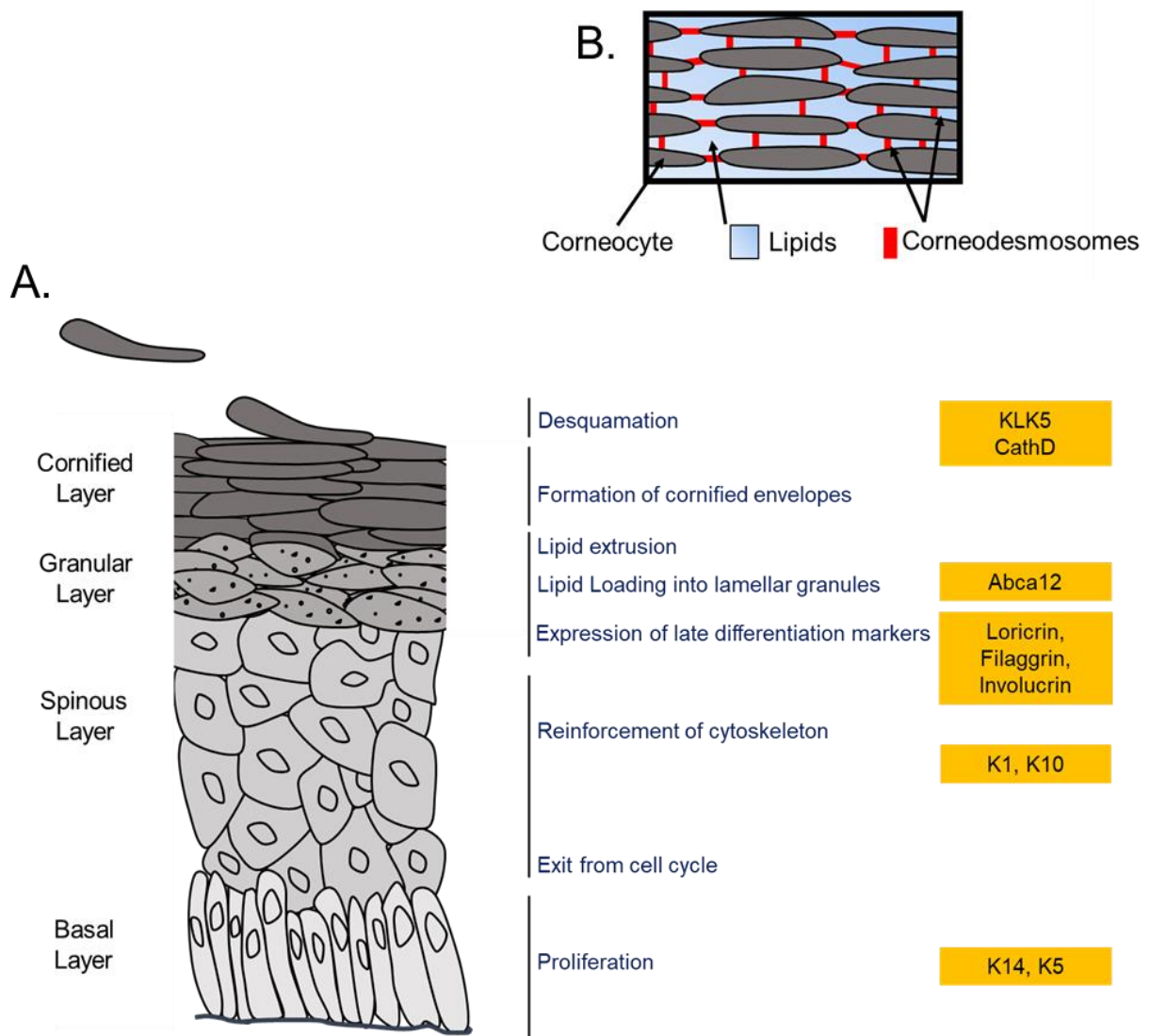
Figure 1.6. Epidermal Differentiation. A. **Structure of Epidermis.** Proliferative cells in the basal layer express K5 and K14 and are attached to the basement membrane via specialized cell junctions including hemidesmosomes. Differentiation initiates when basal cells detach from the basement membrane, move into the spinous layer and stop proliferating. The spinous layer is marked by the expression of K1 and K10 throughout, and Involucrin in the upper region. In the granular layer late differentiation markers loricrin and filaggrin are expressed. Cells of this layer contain lamellar granules which are packed with lipids by transporter proteins, including ABCA12. At the transition from the granular to cornified layer the content of the lamellar granules is extruded into the intercellular space. Desmosomes which connect cells in the basal through granular layers are replaced corneodesmosomes which link the corneocytes together. **B. Close-Up View of Cornified Layer.** The plasma membrane of corneocytes is replaced by an insoluble protein mass (cornified envelope) tightly connected to neighboring cells via corneodesmosomes. The epidermal barrier requires both corneocytes as well as the lipid component. To maintain a constant thickness, corneocytes at the top of the cornified layer are shed in a process that requires desquamation enzymes such as KLK5, and CATHD. Abbreviations: K5: keratin 5; K14: keratin 14; K1: keratin 1; K10: keratin 10; KLK5: kallikrien 5; CathD: cathepsin D. Adapted from [232-234].
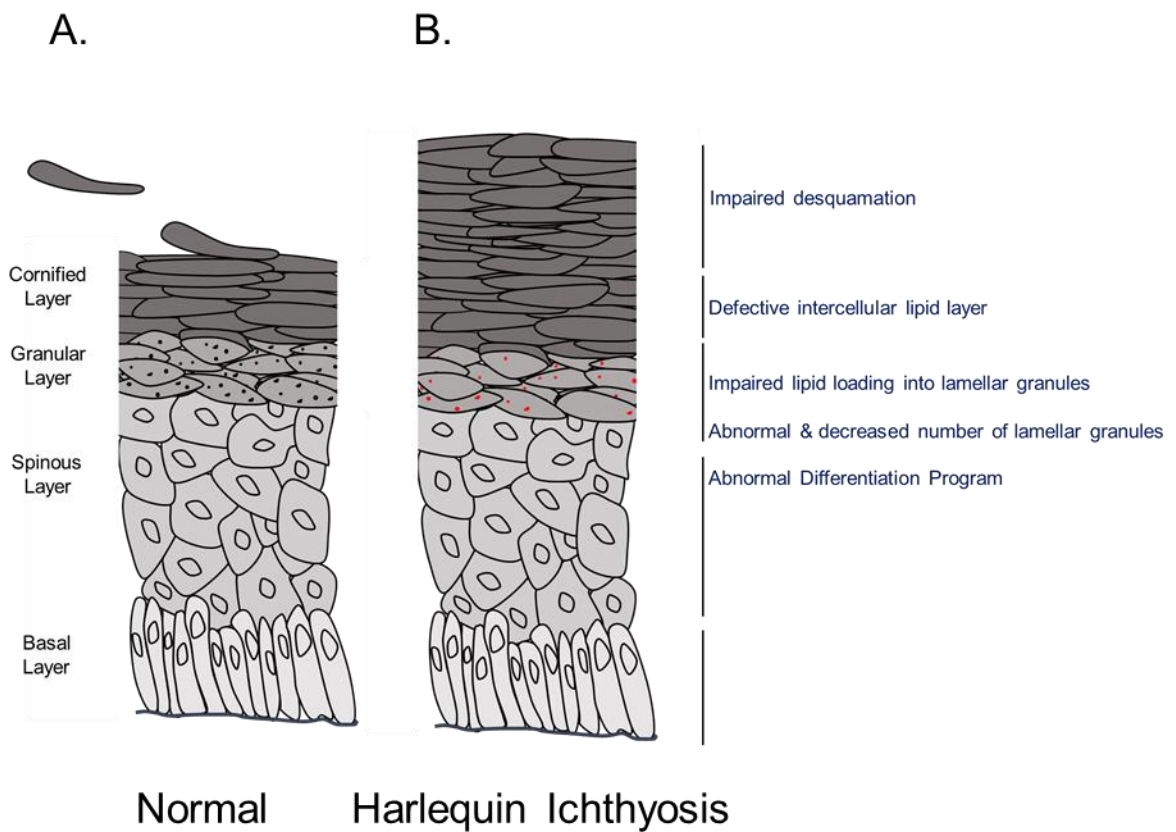
Figure 1.7. Graphical Depiction of Epidermal Defects in Harlequin Ichthyosis Patients. A. Normal Epidermis. See Figure 1.6 for details. **B. Harlequin Ichthyosis (HI)** patients exhibit expansion of cornified layer due to impaired desquamation, potentially a result of decreased expression of kallikrein 5 and cathepsin D. HI patients exhibit some defects in differentiation, namely impaired conversion of pro-filaggrin to filaggrin. Lamellar granules are abnormal (red) or completely absent from the granular layer. Lamellar granules that are present do not contain normal lipid content. The cornified layer has decreased levels of lipids between the corneocytes, which combined with the massive expansion of this layer contributes to barrier dysfunction. Adapted from [232-234].

Reference Number	Author	Targeting scheme	HI Phenocopy*	Noted Differentiation Defects	Lung Phenotype
268,271	Yanagi	Exon 30 deleted	Yes	- Decreased^: loricrin, kallikrein 5, transglutaminase 1 - Defective pro-filaggrin to filaggrin conversion	Yes
269	Zuo	Exon 9 replaced with neo cassette	Yes	- Defective release of filaggrin (normal conversion of pro-filaggrin and expression levels) - Parakeratosis	No
267	Smyth	Exon 41 Missence Mutation (G1997D)	Yes	- Defective filaggrin processing - Premature differentiation (filaggrin, K10 overlap with K14 basal layer)	ND
250	Zhang	Exon 29 deleted	Yes	- Decreased: K1, corneodesmosin, kallikerein 5/7 - Parakeratosis	ND

Table 1.1. Summary of *Abca12*-deficient Mouse Models. Note that all 4 models target different regions of the *Abca12* gene, yet all recapitulate the HI phenotype. The status of differentiation and lung defects differs slightly across the models. These discrepancies may be a result of different targeting strategies or could reflect differences in experimental design and interpretation. *HI Phenocopy: determined by appearance, histology, barrier dysfunction, decreased intercellular lipids in stratum corneum, absent/abnormal lamellar granules. ^: Decreased at protein level, higher expression at mRNA level. Abbreviations: ND: Not determined; K: Keratin.

1.7 Reference List

1. Blanpain, C. and E. Fuchs, *Epidermal stem cells of the skin.* Annu Rev Cell Dev Biol, 2006. **22**: p. 339-73.
2. Adolphe, C. and B. Wainwright, *Pathways to improving skin regeneration.* Expert Reviews in Molecular Medicine, 2005. **7**(20): p. 1-14.
3. Schneider, M.R., R. Schmidt-Ullrich, and R. Paus, *The hair follicle as a dynamic miniorgan.* Current Biology, 2009. **19**(3): p. R132-R142.
4. Millar, S.E., *Molecular mechanisms regulating hair follicle development.* Journal of Investigative Dermatology, 2002. **118**(2): p. 216-225.
5. Hardy, M.H., *The secret life of the hair follicle.* Trends in Genetics, 1992. **8**(2): p. 55-61.
6. Oh, J.W., et al., *A guide to studying human hair follicle cycling in vivo.* Journal of Investigative Dermatology, 2016. **136**(1): p. 34-44.
7. Plikus, M.V., et al., *Self-organizing and stochastic behaviors during the regeneration of hair stem cells.* Science, 2011. **332**(6029): p. 586-9.
8. Plikus, M.V., et al., *Cyclic dermal bmp signalling regulates stem cell activation during hair regeneration.* Nature, 2008. **451**(7176): p. 340-4.
9. Muller-Rover, S., et al., *A comprehensive guide for accurate classification of murine hair follicles in distinct hair cycle stages.* J Invest Dermatol, 2001. **117**(1): p. 3-15.
10. Halloy, J., et al., *Modeling the dynamics of human hair cycles by a follicular automaton.* Proc Natl Acad Sci U S A, 2000. **97**(15): p. 8328-8333.
11. Dawber, R.R.R., *Diseases of the hair and scalp* 1997: Wiley.
12. Tumbar, T., et al., *Defining the epithelial stem cell niche in skin.* Science, 2004. **303**(5656): p. 359-63.
13. Trempus, C.S., et al., *Enrichment for living murine keratinocytes from the hair follicle bulge with the cell surface marker cd34.* J Invest Dermatol, 2003. **120**(4): p. 501-11.
14. Ohyama, M., et al., *Characterization and isolation of stem cell-enriched human hair follicle bulge cells.* J Clin Invest, 2006. **116**(1): p. 249-60.
15. Niemann, C. and V. Horsley, *Development and homeostasis of the sebaceous gland.* Semin Cell Dev Biol, 2012. **23**(8): p. 928-36.
16. Nirmal, B., et al., *Evaluation of perifollicular inflammation of donor area during hair transplantation in androgenetic alopecia and its comparison with controls.* International Journal of Trichology, 2013. **5**(2): p. 73-76.
17. Zhang, B., et al., *Early stage alopecia areata is associated with inflammation in the upper dermis and damage to the hair follicle infundibulum.* Australasian Journal of Dermatology, 2013. **54**(3): p. 184-191.
18. Bellew, S., D. Thiboutot, and J.Q. Del Rosso, *Pathogenesis of acne vulgaris: What's new, what's interesting and what may be clinically relevant.* Journal of Drugs in Dermatology, 2011. **10**(6): p. 582-585.
19. van der Zee, H.H., et al., *Hidradenitis suppurativa: Viewpoint on clinical phenotyping, pathogenesis and novel treatments.* Exp Dermatol, 2012. **21**(10): p. 735-9.

20. Schneider, M.R. and R. Paus, *Deciphering the functions of the hair follicle infundibulum in skin physiology and disease.* Cell Tissue Res, 2014.

21. Veniaminova, N.A., et al., *Keratin 79 identifies a novel population of migratory epithelial cells that initiates hair canal morphogenesis and regeneration.* Development, 2013. **140**(24): p. 4870-80.

22. Oshima, H., et al., *Morphogenesis and renewal of hair follicles from adult multipotent stem cells.* Cell, 2001. **104**(2): p. 233-245.

23. Cotsarelis, G., T.-T. Sun, and R.M. Lavker, *Label-retaining cells reside in the bulge area of pilosebaceous unit: Implications for follicular stem cells, hair cycle, and skin carcinogenesis.* Cell, 1990. **61**(7): p. 1329-1337.

24. Morris, R.J., et al., *Capturing and profiling adult hair follicle stem cells.* Nat Biotechnol, 2004. **22**(4): p. 411-7.

25. Sequeira, I. and J.F. Nicolas, *Redefining the structure of the hair follicle by 3d clonal analysis.* Development, 2012. **139**(20): p. 3741-51.

26. Ellis, T., et al., *The transcriptional repressor cdp (cutl1) is essential for epithelial cell differentiation of the lung and the hair follicle.* Genes Dev, 2001. **15**: p. 2307-2319.

27. Langbein, L., et al., *A novel epithelial keratin, hk6irs1, is expressed differentially in all layers of the inner root sheath, including specialized huxley cells (flugelzellen) of the human hair follicle.* J Invest Dermatol, 2002. **118**: p. 789-799.

28. Gu, L.H. and P.A. Coulombe, *Keratin expression provides novel insight into the morphogenesis and function of the companion layer in hair follicles.* J. Invest. Dermatol., 2007. **127**: p. 1061-1073.

29. Morioka, K., *Outer rooth sheath and companion layer*, in *Hair follicle*, K. Morioka, Editor. 2005, Springer Tokyo: Tokyo. p. 89-106.

30. Rothnagel, J.A. and D.R. Roop, *Hair follicle companion layer: Reacquainting an old friend.* Journal of Investigative Dermatology, 1995. **104**(5): p. 42-43.

31. Winter, H., et al., *A novel human type ii cytokeratin, k6hf, specifically expressed in the companion layer of the hair follicle.* J Invest Dermatol, 1998. **111**(6): p. 955-62.

32. Andl, T., et al., *Epithelial bmpr1a regulates differentiation and proliferation in postnatal hair follicles and is essential for tooth development.* Development, 2004. **131**(10): p. 2257-68.

33. Kobielak, K., et al., *Defining bmp functions in the hair follicle by conditional ablation of bmp receptor ia.* J Cell Biol, 2003. **163**(3): p. 609-23.

34. Seldin, L., A. Muroyama, and T. Lechler, *Numa-microtubule interactions are critical for spindle orientation and the morphogenesis of diverse epidermal structures.* Elife, 2016. **5**.

35. Kaufman, C.K., et al., *Gata-3: An unexpected regulator of cell lineage determination in skin.* Genes Dev, 2003. **17**(17): p. 2108-22.

36. Hanakawa, Y., et al., *Desmogleins 1 and 3 in the companion layer anchor mouse anagen hair to the follicle.* J Invest Dermatol, 2004. **123**(5): p. 817-22.

37. Jaks, V., M. Kasper, and R. Toftgard, *The hair follicle-a stem cell zoo.* Exp Cell Res, 2010. **316**(8): p. 1422-8.

38. Kobayashi, K., A. Rochat, and Y. Barrandon, *Segregation of keratinocyte colony-forming cells in the bulge of the rat vibrissa.* PNAS, 1993. **90**(15): p. 7391-7395.

39. Rochat, A., K. Kobayashi, and Y. Barrandon, *Location of stem cells of human hair follicles by clonal analysis.* Cell, 1994. **76**(6): p. 1063-1073.

40. Blanpain, C., et al., *Self-renewal, multipotency, and the existence of two cell populations within an epithelial stem cell niche.* Cell, 2004. **118**(5): p. 635-48.

41. Jaks, V., et al., *Lgr5 marks cycling, yet long-lived, hair follicle stem cells.* Nat Genet, 2008. **40**(11): p. 1291-9.

42. Trempus, C.S., et al., *Comprehensive microarray transcriptome profiling of cd34-enriched mouse keratinocyte stem cells.* J Invest Dermatol, 2007. **127**(12): p. 2904-7.

43. Liu, Y., et al., *Keratin 15 promoter targets putative epithelial stem cells in the hair follicle bulge.* J Invest Dermatol, 2003. **121**(5): p. 963-8.

44. Barker, N., et al., *Lgr5(+ve) stem cells drive self-renewal in the stomach and build long-lived gastric units in vitro.* Cell Stem Cell, 2010. **6**(1): p. 25-36.

45. Barker, N., et al., *Identification of stem cells in small intestine and colon by marker gene lgr5.* Nature, 2007. **449**(7165): p. 1003-7.

46. D.S., K., et al., *Characterization of murine cd34, a marker for hematopoietic progenitor and stem cells.* Blood, 1994. **84**(3): p. 691-701.

47. Ito, M., et al., *Stem cells in the hair follicle bulge contribute to wound repair but not to homeostasis of the epidermis.* Nat Med, 2005. **11**(12): p. 1351-4.

48. Hoeck, J.D., et al., *Stem cell plasticity enables hair regeneration following lgr5(+) cell loss.* Nat Cell Biol, 2017. **19**(6): p. 666-676.

49. Levy, V., et al., *Distinct stem cell populations regenerate the follicle and interfollicular epidermis.* Dev Cell, 2005. **9**(6): p. 855-61.

50. Jensen, K.B., et al., *Lrig1 expression defines a distinct multipotent stem cell population in mammalian epidermis.* Cell Stem Cell, 2009. **4**(5): p. 427-39.

51. Jensen, U.B., et al., *A distinct population of clonogenic and multipotent murine follicular keratinocytes residing in the upper isthmus.* J Cell Sci, 2008. **121**(Pt 5): p. 609-17.

52. Aragona, M., et al., *Defining stem cell dynamics and migration during wound healing in mouse skin epidermis.* Nat Commun, 2017. **8**: p. 14684.

53. Rezza, A., et al., *Signaling networks among stem cell precursors, transit-amplifying progenitors, and their niche in developing hair follicles.* Cell Rep, 2016. **14**(12): p. 3001-18.

54. Oshimori, N. and E. Fuchs, *Paracrine tgf-beta signaling counterbalances bmp-mediated repression in hair follicle stem cell activation.* Cell Stem Cell, 2012. **10**(1): p. 63-75.

55. Rosenquist, T.A. and G.R. Martin, *Fibroblast growth factor signalling in the hair growth cycle: Expression of the fibroblast growth factor receptor and ligand genes in the murine hair follicle.* Developmental Dynamics, 1996. **205**(4): p. 379-386.

56. Greco, V., et al., *A two-step mechanism for stem cell activation during hair regeneration.* Cell Stem Cell, 2009. **4**: p. 155-169.

57. Sunberg, J.P., *Handbook of mouse mutations with skin and hair abnormalities: Animal models and biomedical tools.* 1994, Boca Raton, FL: CRC Press.

58. Duverger, O. and M.I. Morasso, *Epidermal patterning and induction of different hair types during mouse embryonic development.* Birth Defects Res C Embryo Today, 2009. **87**(3): p. 263-72.

59. Ferguson, B.M., et al., *Cloning of tabby, themurine homolog of the human eda: Evidence for a membrane-associated protein with a short collagenous domain.* Hum Mol Genet, 1997. **6**(9): p. 1589-94.

60. Srivastava, A.K., et al., *The tabby phenotype is caused by mutation in a mouse homologue of the eda gene that reveals novel mouse and human exons and encodes a protein (ectodysplasin-a) with collagenous domains.* Proceedings of the National Academy of Sciences, 1997. **94**(24): p. 13069-13074.

61. Headon, D.J. and P.A. Overbeek, *Involvement of a novel tnf receptor homologue in hair follicle induction.* Nat Genet, 1999. **22**(4): p. 370-4.

62. Yan, M., et al., *Identification of a novel death domain-containing adaptor molecule for ectodysplasin-a receptor that is mutated in crinkled mice.* Current Biology, 2002. **12**(5): p. 409-413.

63. Botchkarev, V.A., et al., *Modulation of bmp signaling by noggin is required for induction of the secondary (nontylotrich) hair follicles.* J Invest Dermatol, 2002. **118**(1): p. 3-10.

64. Paus, R., et al., *A comprehensive guide for the recognition and classification of distinct stages of hair follicle morphogenesis.* J Invest Dermatol, 1999. **113**(4): p. 523-534.

65. Lechler, T. and E. Fuchs, *Asymmetric cell divisions promote stratification and differentiation of mammalian skin.* Nature, 2005. **437**(7056): p. 275-80.

66. Gibbs, H.F., *A study of the development of the skin and hair of the australian opossum, trichosurus vulpecula.* Proc. Zool. Soc. Lond., 1938. **108B**: p. 611-648.

67. Wildman, A.B., *Coat and fibre development in some british sheep.* Proc. Zool. Soc. Lond., 1932. **102**: p. 257-285.

68. Hardy, M.H., *The development of mouse hair in vitro with some observations on pigmentation.* J. Anat., 1949. **83**(3): p. 364-384.

69. Pinkus, H., *Embryology of hair.* 1958, New York, NY: Academic Press.

70. Maximow, A.A. and W. Bloom, *A textbook of histology*, ed. W.B. Saunders. 1934, Philadelphia, PA.

71. Hsu, Y.C., H.A. Pasolli, and E. Fuchs, *Dynamics between stem cells, niche, and progeny in the hair follicle.* Cell, 2011. **144**(1): p. 92-105.

72. Hsu, Y.C., L. Li, and E. Fuchs, *Transit-amplifying cells orchestrate stem cell activity and tissue regeneration.* Cell, 2014. **157**(4): p. 935-49.

73. Milner, Y., et al., *Exogen, shedding phase of the hair growth cycle: Characterization of a mouse model.* J Invest Dermatol, 2002. **119**(3): p. 639-44.

74. Stenn, K., *Exogen is an active, separately controlled phase of the hair growth cycle.* J Am Acad Dermatol, 2005. **52**(2): p. 374-5.

75. Higgins, C.A., G.E. Westgate, and C.A. Jahoda, *From telogen to exogen: Mechanisms underlying formation and subsequent loss of the hair club fiber.* J Invest Dermatol, 2009. **129**(9): p. 2100-8.

76. Rompolas, P., K.R. Mesa, and V. Greco, *Spatial organization within a niche as a determinant of stem-cell fate.* Nature, 2013. **502**(7472): p. 513-8.

77.   Zhang, Y.V., et al., *Distinct self-renewal and differentiation phases in the niche of infrequently dividing hair follicle stem cells.* Cell Stem Cell, 2009. **5**: p. 1-12.

78.   Panteleyev, A.A., C.A. Jahoda, and A.M. Christiano, *Hair follicle predetermination.* J Cell Sci, 2001. **114**: p. 3419-3431.

79.   Legue, E. and J.F. Nicolas, *Hair follicle renewal: Organization of stem cells in the matrix and the role of stereotyped lineages and behaviors.* Development, 2005. **132**(18): p. 4143-54.

80.   Yang, H., et al., *Epithelial-mesenchymal micro-niches govern stem cell lineage choices.* Cell, 2017. **169**(3): p. 483-496 e13.

81.   Botchkarev, N.V. and R. Paus, *Molecular biology of hair morphogenesis:Development and cycling.* J Exp Zool, 2003. **298**(1): p. 164-180.

82.   Nakamura, M., S. J.P., and R. Paus, *Mutant laboratory mice with abnormalities in hair follicle morphogenesis, cycling, and/or structure: Annotated tables.* Exp Dermatol, 2001. **10**(6): p. 369-390.

83.   Rishikaysh, P., et al., *Signaling involved in hair follicle morphogenesis and development.* Int J Mol Sci, 2014. **15**(1): p. 1647-70.

84.   Oro, A.E., et al., *Basal cell carcinomas in mice overexpressing sonic hedgehog.* Science, 1997. **276**(5313): p. 817-821.

85.   Grachtchouk, M., et al., *Basal cell carcinomas in mice overexpressing gli2 in skin.* Nat Genet, 2000. **24**(3): p. 216-7.

86.   Nicolas, M., et al., *Notch1 functions as a tumor suppressor in mouse skin.* Nat Genet, 2003. **33**(3): p. 416-21.

87.   Malanchi, I., et al., *Cutaneous cancer stem cell maintenance is dependent on beta-catenin signalling.* Nature, 2008. **452**(7187): p. 650-3.

88.   Sharov, A.A., et al., *Bone morphogenetic protein antagonist noggin promotes skin tumorigenesis via stimulation of the wnt and shh signaling pathways.* Am J Pathol, 2009. **175**(3): p. 1303-14.

89.   Nusse, R., et al., *Mode of proviral activation of a putative mammary oncogene (int-1) on mouse chromosome 15.* Nature, 1984. **307**(5947): p. 131-136.

90.   Sharma, R.P., *Wingless, a new mutant in d. Melanogaster.* Drosophila Inf. Serv, 1973. **50**(134).

91.   Rijsewijk, F., et al., *The drosophila homology of the mouse mammary oncogene int-1 is identical to the segment polarity gene wingless.* Cell, 1987. **50**(4): p. 649-657.

92.   Korinek, V., et al., *Depletion of epithelial stem-cell compartments in the small intestine of mice lacking tcf-4.* Nat Genet, 1998. **19**(4): p. 379-83.

93.   Fevr, T., et al., *Wnt/beta-catenin is essential for intestinal homeostasis and maintenance of intestinal stem cells.* Mol Cell Biol, 2007. **27**(21): p. 7551-9.

94.   van Es, J.H., et al., *A critical role for the wnt effector tcf4 in adult intestinal homeostatic self-renewal.* Mol Cell Biol, 2012. **32**(10): p. 1918-27.

95.   Ireland, H., et al., *Inducible cre-mediated control of gene expression in the murine gastrointestinal tract: Effect of loss of β-catenin.* Gastroenterology, 2004. **126**(5): p. 1236-1246.

96.   DasGupta, R. and E. Fuchs, *Multiple roles for activated lef/tcf transcription complexes during hair follicle development and differentiation.* Development, 1999. **126**: p. 4557-4568.

97. Lien, W.H., et al., *In vivo transcriptional governance of hair follicle stem cells by canonical wnt regulators.* Nat Cell Biol, 2014. **16**(2): p. 179-90.

98. Lim, X., et al., *Axin2 marks quiescent hair follicle bulge stem cells that are maintained by autocrine wnt/beta-catenin signaling.* Proc Natl Acad Sci U S A, 2016. **113**(11): p. E1498-505.

99. Polakis, P., *Wnt signaling in cancer.* Cold Spring Harb Perspect Biol, 2012. **4**(5).

100. Wood, L.D., et al., *The genomic landscapes of human breast and colorectal cancers.* Science, 2007. **318**(5853): p. 1108-1113.

101. Zeng, X., et al., *A dual-kinase mechanism for wnt co-receptor phosphorylation and activation.* Nature, 2005. **438**(7069): p. 873-7.

102. Logan, C.Y. and R. Nusse, *The wnt signaling pathway in development and disease.* Annu Rev Cell Dev Biol, 2004. **20**: p. 781-810.

103. van de Wetering, M., et al., *The beta-catenin/tcf-4 complex imposes a crypt progenitor phenotype on colorectal cancer cells.* Cell. **111**(2): p. 241-250.

104. Nüsslein-Volhard, C. and E. Wieschaus, *Mutations affecting segment number and polarity in drosophila.* Nature, 1980. **287**(5785): p. 795-801.

105. Goodrich, L.V., et al., *Conservation of the hedgehog/patched signaling pathway from flies to mice: Induction of a mouse patched gene by hedgehog.* Genes & Development, 1996. **10**(3): p. 301-312.

106. Ruiz i Altaba, A., V. Palma, and N. Dahmane, *Hedgehog-gli signalling and the growth of the brain.* Nat Rev Neurosci, 2002. **3**(1): p. 24-33.

107. Tickle, C. and M. Towers, *Sonic hedgehog signaling in limb development.* Front Cell Dev Biol, 2017. **5**: p. 14.

108. Aberger, F. and A.M. Frischauf, *Gli genes and their targets in epidermal development and disease*, in *Madame Curie Bioscience Database*. 2000-2013, Landes Bioscience: Austin (Tx).

109. Briscoe, J. and P.P. Therond, *The mechanisms of hedgehog signalling and its roles in development and disease.* Nat Rev Mol Cell Biol, 2013. **14**(7): p. 416-29.

110. St-Jacques, B., B. Hammerschmidt, and A.P. McMahon, *Indian hedgehog signaling regulates proliferation and differentiation of chondrocytes and is essential for bone formation.* Genes Dev, 1999. **13**: p. 2072-2086.

111. Bitgood, M.J., L. Shen, and A.P. McMahon, *Sertoli cell signaling by desert hedgehog regulates the male germline.* Current Biology, 1996. **6**(3): p. 298-304.

112. Chiang, C., et al., *Cyclopia and defective axial patterning in mice lacking sonic hedgehog gene function.* Nature, 1996. **383**(6599): p. 407-13.

113. Wallis, D. and M. Muenke, *Mutations in holoprosencephaly.* Human Mutation, 2000. **16**(2): p. 99-108.

114. Nanni, L., et al., *The mutational spectrum of the sonic hedgehog gene in holoprosencephaly: Shh mutations cause a significant proportion of autosomal dominant holoprosencephaly.* Human Molecular Genetics, 1999. **8**(13): p. 2479-2488.

115. Hayhurst, M. and S.K. McConnell, *Mouse models of holoprosencephaly.* Curr Opin Neurol, 2003. **16**(2): p. 135-41.

116. Washington Smoak, I., et al., *Sonic hedgehog is required for cardiac outflow tract and neural crest cell development.* Dev Biol, 2005. **283**(2): p. 357-72.

117. Hildreth, V., et al., *Left cardiac isomerism in the sonic hedgehog null mouse.* J Anat, 2009. **214**(6): p. 894-904.

118. Litingtung, Y., et al., *Sonic hedgehog is essential to foregut development.* Nat Genet, 1998. **20**(1): p. 58-61.

119. Chiang, C., et al., *Essential role for sonic hedgehog during hair follicle morphogenesis.* Dev Biol, 1999. **205**(1): p. 1-9.

120. Mullor, J.L., P. Sánchez, and A.R.i. Altaba, *Pathways and consequences: Hedgehog signaling in human disease.* Trends in Cell Biology, 2002. **12**(12): p. 562-569.

121. Pietsch, T., et al., *Medulloblastomas of the desmoplastic variant carry mutations of the human homologue of drosophila patched.* Cancer Research, 1997. **57**(11): p. 2085-2088.

122. Raffel, C., et al., *Sporadic medulloblastomas contain ptch mutations.* Cancer Research, 1997. **57**(5): p. 842-845.

123. Xie, J., et al., *Activating smoothened mutations in sporadic basal-cell carcinoma.* Nature, 1998. **391**: p. 90.

124. Wolter, M., et al., *Mutations in the human homologue of the drosophila segment polarity gene patched (ptch) in sporadic basal cell carcinomas of the skin and primitive neuroectodermal tumors of the central nervous system.* Cancer Research, 1997. **57**(13): p. 2581.

125. Aszterbaum, M., et al., *Identification of mutations in the human patched gene in sporadic basal cell carcinomas and in patients with the basal cell nevus syndrome.* Journal of Investigative Dermatology. **110**(6): p. 885-888.

126. Epstein, E.H., *Basal cell carcinomas: Attack of the hedgehog.* Nat Rev Cancer, 2008. **8**(10): p. 743-54.

127. Singla, V. and J.F. Reiter, *The primary cilium as the cell's antenna: Signaling at a sensory organelle.* Science, 2006. **313**(5787): p. 629-633.

128. Huangfu, D., et al., *Hedgehog signalling in the mouse requires intraflagellar transport proteins.* Nature, 2003. **426**: p. 83.

129. Alcedo, J., et al., *The drosophila smoothened gene encodes a seven-pass membrane protein, a putative receptor for the hedgehog signal.* Cell, 1996. **86**(2): p. 221-232.

130. Taipale, J., et al., *Patched acts catalytically to suppress the activity of smoothened.* Nature, 2002. **418**(6900): p. 892-7.

131. van den Heuvel, M. and P.W. Ingham, *Smoothened encodes a receptor-like serpentine protein required for hedgehog signalling.* Nature, 1996. **382**(6591): p. 547-51.

132. Rohatgi, R., L. Milenkovic, and M.P. Scott, *Patched1 regulates hedgehog signaling at the primary cilium.* Science, 2007. **317**(5836): p. 372-376.

133. Stone, D.M., et al., *The tumour-suppressor gene patched encodes a candidate receptor for sonic hedgehog.* Nature, 1996. **384**(6605): p. 129-34.

134. Marigo, V., et al., *Biochemical evidence that patched is the hedgehog receptor.* Nature, 1996. **384**(6605): p. 176-9.

135. Corbit, K.C., et al., *Vertebrate smoothened functions at the primary cilium.* Nature, 2005. **437**(7061): p. 1018-21.

136. Bai, C.B., et al., *Gli2, but not gli1, is required for initial shh signaling and ectopic activation of the shh pathway.* Development, 2002. **129**(20): p. 4753-4761.
137. Mo, R., et al., *Specific and redundant functions of gli2 and gli3 zinc finger genes in skeletal patterning and development.* Development, 1997. **124**: p. 113-123.
138. Park, H.L., et al., *Mouse gli1 mutants are viable but have defects in shh signaling in combination with a gli2 mutation.* Development, 2000. **127**: p. 1593-1605.
139. Bai, C.B. and A.L. Joyner, *Gli1can rescue the in vivo function of gli2.* Development, 2001. **128**: p. 5161-5172.
140. Ding, Q., et al., *Diminished sonic hedgehog signaling and lack of floor plate differentiation in gli2 mutant mice.* Development, 1998. **125**: p. 2533-2543.
141. Motoyama, J., et al., *Essential function of gli2 and gli3 in the formation of lung, trachea and oesophagus.* Nat Genet, 1998. **20**(1): p. 54-57.
142. Ingham, P.W. and A.P. McMahon, *Hedgehog signaling in animal development: Paradigms and principles.* Genes Dev, 2001. **15**: p. 3059-3087.
143. Matise, M.P., et al., *Gli2 is required for induction of floor plate and adjacent cells, but not most ventral neurons in the mouse central nervous system.* Development, 1998. **125**(15): p. 2759-2770.
144. Hu, M.C., et al., *Gli3-dependent transcriptional repression of gli1, gli2 and kidney patterning genes disrupts renal morphogenesis.* Development, 2006. **133**(3): p. 569-78.
145. Büscher, D., et al., *Evidence for genetic control of sonic hedgehog by gli3 in mouse limb development.* Mechanisms of Development, 1997. **62**(2): p. 175-182.
146. Ruiz i Altaba, A., *Combinatorial gli gene function in floor plate and neuronal inductions by sonic hedgehog.* Development, 1998. **125**(12): p. 2203.
147. Masuya, H., et al., *A duplicated zone of polarizing activity in polydactylous mouse mutants.* Genes & Development, 1995. **9**(13): p. 1645-1653.
148. Litingtung, Y., et al., *Shh and gli3 are dispensable for limb skeleton formation but regulate digit number and identity.* Nature, 2002. **418**: p. 979.
149. Hui, C.-c. and A.L. Joyner, *A mouse model of greig cephalo–polysyndactyly syndrome: The extra–toesj mutation contains an intragenic deletion of the gli3 gene.* Nature Genetics, 1993. **3**: p. 241.
150. Park, H.L., et al., *Mouse gli1 mutants are viable but have defects in shh signaling in combination with a gli2 mutation.* Development, 2000. **127**(8): p. 1593-1605.
151. Vortkamp, A., M. Gessler, and K.-H. Grzeschik, *Gli3 zinc-finger gene interrupted by translocations in greig syndrome families.* Nature, 1991. **352**: p. 539.
152. Urist, M.R., *Bone: Formation by autoinduction.* Clinical orthopaedics and related research, 1965(395): p. 4.
153. Wang, R.N., et al., *Bone morphogenetic protein (bmp) signaling in development and human diseases.* Genes Dis, 2014. **1**(1): p. 87-105.
154. Winnier, G., et al., *Bone morphogenetic protein-4 is required for mesoderm formation and patterning in the mouse.* Genes Dev, 1995. **9**: p. 2105-2116.
155. Mishina, Y., et al., *Bmpr encodes a type i bone morphogenetic protein receptor that is essential for gastrulation during mouse embryogenesis.* Genes & Development, 1995. **9**(24): p. 3027-3037.
156. Luo, G., et al., *Bmp-7 is an inducer of nephrogenesis, and is also required for eye development and skeletal patterning.* Genes Dev, 1995. **9**(22): p. 2808-2020.

157. Settle, S., et al., *The bmp family member gdf7 is required for seminal vesicle growth, branching morphogenesis, and cytodifferentiation.* Dev Biol, 2001. **234**(1): p. 138-50.

158. Zhao, G.Q., L. Liaw, and B.L.M. Hogan, *Bone morphogenetic protein 8a plays a role in the maintenance of spermatogenesis and the integrity of the epididymis.* Development, 1998. **125**(6): p. 1103-1112.

159. Nikaido, M., et al., *In vivo analysis using variants of zebrafish bmpr-ia: Range of action and involvement of bmp in ectoderm patterning.* Development, 1999. **126**(1): p. 181-190.

160. Hemmati-Brivanlou, A. and D. Melton, *Vertebrate embryonic cells will become nerve cells unless told otherwise.* Cell, 1997. **88**(1): p. 13-17.

161. Miyazono, K., K. Kusanagi, and H. Inoue, *Divergence and convergence of tgf-beta/bmp signaling.* J Cell Physiol, 2001. **187**(3): p. 265-76.

162. Massagué, J. and Y.G. Chen, *Controlling tgf-β signaling.* Genes Dev, 2000. **14**: p. 627-644.

163. Shi, Y. and J. Massagué, *Mechanisms of tgf-β signaling from cell membrane to the nucleus.* Cell, 2003. **113**(6): p. 685-700.

164. Genander, M., et al., *Bmp signaling and its psmad1/5 target genes differentially regulate hair follicle stem cell lineages.* Cell Stem Cell, 2014. **15**(5): p. 619-33.

165. Hollnagel, A., et al., *Id genes are direct targets of bone morphogenetic protein induction in embryonic stem cells.* Journal of Biological Chemistry, 1999. **274**(28): p. 19838-19845.

166. Hansson, E.M., U. Lendahl, and G. Chapman, *Notch signaling in development and disease.* Semin Cancer Biol, 2004. **14**(5): p. 320-8.

167. Bray, S.J., *Notch signalling: A simple pathway becomes complex.* Nat Rev Mol Cell Biol, 2006. **7**(9): p. 678-89.

168. Lawson, N.D., et al., *Notch signaling is required for arterial-venous differentiation during embryonic vascular development.* Development, 2001. **128**(19): p. 3675-3683.

169. Timmerman, L.A., et al., *Notch promotes epithelial-mesenchymal transition during cardiac development and oncogenic transformation.* Genes Dev, 2004. **18**(1): p. 99-115.

170. Riccio, O., et al., *Loss of intestinal crypt progenitor cells owing to inactivation of both notch1 and notch2 is accompanied by derepression of cdk inhibitors p27kip1 and p57kip2.* EMBO Rep, 2008. **9**(4): p. 377-83.

171. Pellegrinet, L., et al., *Dll1- and dll4-mediated notch signaling are required for homeostasis of intestinal stem cells.* Gastroenterology, 2011. **140**(4): p. 1230-1240.e7.

172. McLaughlin, K.A., M.S. Rones, and M. Mercola, *Notch regulates cell fate in the developing pronephros.* Developmental Biology, 2000. **227**(2): p. 567-580.

173. Pan, Y., et al., *Gamma-secretase functions through notch signaling to maintain skin appendages but is not required for their patterning or initial morphogenesis.* Dev Cell, 2004. **7**(5): p. 731-43.

174. Andersson, E.R., R. Sandberg, and U. Lendahl, *Notch signaling: Simplicity in design, versatility in function.* Development, 2011. **138**(17): p. 3593-3612.

175.   D'Souza, B., L. Meloty-Kapella, and G. Weinmaster, *Chapter three - canonical and non-canonical notch ligands*, in *Current topics in developmental biology*, R. Kopan, Editor. 2010, Academic Press. p. 73-129.

176.   Iso, T., L. Kedes, and Y. Hamamori, *Hes and herp families: Multiple effectors of the notch signaling pathway.* J Cell Physiol, 2003. **194**(3): p. 237-55.

177.   Iso, T., et al., *Herp, a novel heterodimer partner of hes/e(spl) in notch signaling.* Molecular and Cellular Biology, 2001. **21**(17): p. 6080-6089.

178.   Watt, F.M., S. Estrach, and C.A. Ambler, *Epidermal notch signalling: Differentiation, cancer and adhesion.* Curr Opin Cell Biol, 2008. **20**(2): p. 171-9.

179.   Favier, B., et al., *Localisation of members of the notch system and the differentiation of vibrissa hair follicles: Receptors, ligands, and fringe modulators.* Developmental Dynamics, 2000. **218**(3): p. 426-437.

180.   Kopan, R., *Mouse notch: Expression in hair follicles correlates with cell fate determination.* The Journal of Cell Biology, 1993. **121**(3): p. 631-641.

181.   Blanpain, C., et al., *Canonical notch signaling functions as a commitment switch in the epidermal lineage.* Genes Dev, 2006. **20**(21): p. 3022-35.

182.   Huelsken, J., et al., *B-catenin controls hair follicle morphogenesis and stem cell differentiation in the skin.* Cell, 2001. **105**(4): p. 533-545.

183.   Andl, T., et al., *Wnt signals are required for the initiation of hair follicle development.* Developmental Cell, 2002. **2**(5): p. 643-653.

184.   Gat, U., et al., *De novo hair follicle morphogenesis and hair tumors in mice expressing a truncated β-catenin in skin.* Cell, 1998. **95**(5): p. 605-614.

185.   Noramly, S., A. Freeman, and B.A. Morgan, *B-catenin signaling can initiate feather bud development.* Development, 1999. **126**: p. 3509-3521.

186.   Widelitz, R.B., et al., *Beta-catenin in epithelial morphogenesis: Conversion of part of avian foot scales into feather buds with a mutated beta-catenin.* Dev Biol, 2000. **219**(1): p. 98-114.

187.   Lyons, K.M., R.W. Pelton, and B. Hogan, *Organogenesis and pattern formation in the mouse: Rna distribution patterns suggest a role for bone morphogenetic protein-2a (bmp-2a.* Development, 1990. **109**: p. 833-844.

188.   Lyons, K.M., R.W. Pelton, and B. Hogan, *Patterns of expression of murine vgr-1 and bmp-2a rna suggest that transforming growth factor-p-like genes coordinately regulate aspects of embryonic development.* Genes Dev, 1989. **3**: p. 1657-1668.

189.   Botchkarev, V.A., *Noggin is a mesenchymally derived stimulator of hair-follicle induction.* Nat Cell Biol, 1999. **1**: p. 158-163.

190.   St-Jacques, B., et al., *Sonic hedgehog signaling is essential for hair development.* Current Biology, 1998. **8**(19): p. 1058-1069.

191.   Plikus, M., et al., *Morpho-regulation of ectodermal organs: Integument pathology and phenotypic variations in k14-noggin engineered mice through modulation of bone morphogenic protein pathway.* The American Journal of Pathology, 2004. **164**(3): p. 1099-1114.

192.   Jamora, C., et al., *Links between signal transduction, transcription and adhesion in epithelial bud development.* Nature, 2003. **422**: p. 317.

193. Neubüser, A., et al., *Antagonistic interactions between fgf and bmp signaling pathways: A mechanism for positioning the sites of tooth formation.* Cell, 1997. **90**(2): p. 247-255.

194. Jung, H.S., et al., *Local inhibitory action of bmps and their relationships with activators in feather formation: Implications for periodic patterning.* Dev Biol, 1998. **196**(1): p. 11-23.

195. Noramly, S. and B.A. Morgan, *Bmps mediate lateral inhibition at successive stages in feather tract development.* Development, 1998. **125**: p. 3775-3787.

196. Mill, P., et al., *Sonic hedgehog-dependent activation of gli2 is essential for embryonic hair follicle development.* Genes Dev, 2003. **17**: p. 282-294.

197. Cui, C.Y., et al., *Shh is required for tabby hair follicle development.* Cell Cycle, 2011. **10**(19): p. 3379-86.

198. Ouspenskaia, T., et al., *Wnt-shh antagonism specifies and expands stem cells prior to niche formation.* Cell, 2016. **164**(1-2): p. 156-169.

199. Litingtung, Y. and C. Chiang, *Specification of ventral neuron types is mediated by an antagonistic interaction between shh and gli3.* Nature Neuroscience, 2000. **3**: p. 979.

200. Mill, P., et al., *Shh controls epithelial proliferation via independent pathways that converge on n-myc.* Dev Cell, 2005. **9**(2): p. 293-303.

201. Woo, W.M., H.H. Zhen, and A.E. Oro, *Shh maintains dermal papilla identity and hair morphogenesis via a noggin-shh regulatory loop.* Genes Dev, 2012. **26**(11): p. 1235-46.

202. Kulessa, H., G. Turk, and B.L. Hogan, *Inhibition of bmp signaling affects growth and differentiation in the anagen hair follicle.* EMBO J, 2000. **19**(24): p. 6664-74.

203. Yuhki, M., et al., *Bmpr1a signaling is necessary for hair follicle cycling and hair shaft differentiation in mice.* Development, 2004. **131**(8): p. 1825-33.

204. Yamamoto, N., et al., *Notch/rbp-j signaling regulates epidermis/hair fate determination of hair follicular stem cells.* Curr Biol, 2003. **13**: p. 333-338.

205. Merrill, B.J., et al., *Tcf3 and lef1 regulate lineage differentiation of multipotent stem cells in skin.* Genes Dev, 2001. **15**: p. 1688-1705.

206. Zhou, P., et al., *Lymphoid enhancer factor 1 directs hair follicle patterning and epithelial cell fate.* Genes & Development, 1995. **9**(6): p. 700-713.

207. Kandyba, E., et al., *Competitive balance of intrabulge bmp/wnt signaling reveals a robust gene network ruling stem cell homeostasis and cyclic activation.* Proc Natl Acad Sci U S A, 2013. **110**(4): p. 1351-6.

208. Kobielak, K., et al., *Loss of a quiescent niche but not follicle stem cells in the absence of bone morphogenetic protein signaling.* Proc Natl Acad Sci U S A, 2007. **104**(24): p. 10063-8.

209. Botchkarev, V.A., et al., *Noggin is required for induction of the hair follicle growth phase in postnatal skin.* FASEB, 2001. **15**: p. 2205-2214.

210. Guha, U., et al., *Bone morphogenetic protein signaling regulates postnatal hair follicle differentiation and cycling.* The American Journal of Pathology, 2004. **165**(3): p. 729-740.

211. Van Mater, D., et al., *Transient activation of beta -catenin signaling in cutaneous keratinocytes is sufficient to trigger the active growth phase of the hair cycle in mice.* Genome Res, 2003. **17**(19): p. 1219-1224.

212. Lowry, W.E., et al., *Defining the impact of beta-catenin/tcf transactivation on epithelial stem cells.* Genes Dev, 2005. **19**(13): p. 1596-611.

213. Wang, L.C., et al., *Conditional disruption of hedgehog signaling pathway defines its critical role in hair development and regeneration.* J Invest Dermatol, 2000. **114**(5): p. 901-8.

214. Zhang, B., et al., *Hair follicles' transit-amplifying cells govern concurrent dermal adipocyte production through sonic hedgehog.* Genes Dev, 2016. **30**(20): p. 2325-2338.

215. Powell, B.C., et al., *The notch signalling pathway in hair growth.* Mech Dev, 1998. **78**(1-2): p. 189-192.

216. Lin, M.H., et al., *Activation of the notch pathway in the hair cortex leads to aberrant differentiation of the adjacent hair-shaft layers.* Development, 2000. **127**(11): p. 2421-32.

217. Roop, D.R., *Defects in the barrier.* Science, 1995. **267**(5197): p. 474-475.

218. Segre, J.A., *Epidermal barrier formation and recovery in skin disorders.* J Clin Invest, 2006. **116**(5): p. 1150-8.

219. Agrawal, R. and J.A. Woodfolk, *Skin barrier defects in atopic dermatitis.* Curr Allergy Asthma Rep, 2014. **14**(5): p. 433.

220. Sprecher, E., *Epidermolysis bullosa simplex.* Dermatologic Clinics, 2010. **28**(1): p. 23-32.

221. Yeh, S.W., et al., *Blistering disorders: Diagnosis and treatment.* Dermatologic Therapy, 2003. **16**(3): p. 214-223.

222. Simpson, C.L., D.M. Patel, and K.J. Green, *Deconstructing the skin: Cytoarchitectural determinants of epidermal morphogenesis.* Nat Rev Mol Cell Biol, 2011. **12**(9): p. 565-80.

223. Moriyama, M., et al., *Multiple roles of notch signaling in the regulation of epidermal development.* Developmental Cell. **14**(4): p. 594-604.

224. Sumigray, K.D. and T. Lechler, *Cell adhesion in epidermal development and barrier formation.* Current topics in developmental biology, 2015. **112**: p. 383-414.

225. Carter, W.G., et al., *Distinct functions for integrins alpha 3 beta 1 in focal adhesions and alpha 6 beta 4/bullous pemphigoid antigen in a new stable anchoring contact (sac) of keratinocytes: Relation to hemidesmosomes.* The Journal of Cell Biology, 1990. **111**(6): p. 3141.

226. Tsuruta, D., B. Hopkinson Susan, and C.R. Jones Jonathan, *Hemidesmosome protein dynamics in live epithelial cells.* Cell Motility, 2003. **54**(2): p. 122-134.

227. Eyre, R.W. and J.R. Stanley, *Human autoantibodies against a desmosomal protein complex with a calcium-sensitive epitope are characteristic of pemphigus foliaceus patients.* J Exp Med, 1987. **165**(6): p. 1719-24.

228. Amagai, M., V. Klaus-Kovtun, and J.R. Stanley, *Autoantibodies against a novel epithelial cadherin in pemphigus vulgaris, a disease of cell adhesion.* Cell, 1991. **67**(5): p. 869-877.

229. Morita, K., et al., *Subcellular distribution of tight junction-associated proteins (occludin, zo-1, zo-2) in rodent skin.* Journal of Investigative Dermatology, 1998. **110**(6): p. 862-866.

230.   Schlüter, H., et al., *Sealing the live part of the skin: The integrated meshwork of desmosomes, tight junctions and curvilinear ridge structures in the cells of the uppermost granular layer of the human epidermis.* European Journal of Cell Biology, 2004. **83**(11): p. 655-665.

231.   Furuse, M., et al., *Claudin-based tight junctions are crucial for the mammalian epidermal barrier: A lesson from claudin-1-deficient mice.* J Cell Biol, 2002. **156**(6): p. 1099-111.

232.   Eckhart, L., et al., *Cell death by cornification.* Biochim Biophys Acta, 2013. **1833**(12): p. 3471-80.

233.   Candi, E., R.A. Knight, and G. Melino, *Cornification of the skin: A non-apoptotic cell death mechanism.* 2009.

234.   Candi, E., R. Schmidt, and G. Melino, *The cornified envelope: A model of cell death in the skin.* Nat Rev Mol Cell Biol, 2005. **6**(4): p. 328-40.

235.   Fuchs, E. and H. Green, *Changes in keratin gene expression during terminal differentiation of the keratinocyte.* Cell, 1980. **19**(4): p. 1033-1042.

236.   Kypriotou, M., M. Huber, and D. Hohl, *The human epidermal differentiation complex: Cornified envelope precursors, s100 proteins and the 'fused genes' family.* Exp Dermatol, 2012. **21**(9): p. 643-9.

237.   Resing, K.A., B.A. Dale, and K.A. Walsh, *Multiple copies of phosphorylated filaggrin in epidermal profilaggrin demonstrated by analysis of tryptic peptides.* Biochemistry, 1985. **24**(15): p. 4167-4175.

238.   Resing, K.A., R.S. Johnson, and K.A. Walsh, *Characterization of protease processing sites during conversion of rat profilaggrin to filaggrin.* Biochemistry, 1993. **32**(38): p. 10036-10045.

239.   Nemes, Z., L.N. Marekov, and P.M. Steinert, *Involucrin cross-linking by transglutaminase 1.* Journal of Biological Chemistry, 1999. **274**(16): p. 11013-11021.

240.   Steinert, P.M. and L.N. Marekov, *The proteins elafin, filaggrin, keratin intermediate filaments, loricrin, and small proline-rich proteins 1 and 2 are isodipeptide cross-linked components of the human epidermal cornified cell envelope.* Journal of Biological Chemistry, 1995. **270**(30): p. 17702-17711.

241.   Eckert, R.L., et al., *Transglutaminase function in epidermis.* Journal of Investigative Dermatology, 2005. **124**(3): p. 481-492.

242.   Kalinin, A., L.N. Marekov, and P.M. Steinert, *Assembly of the epidermal cornified cell envelope.* Journal of Cell Science, 2001. **114**(17): p. 3069.

243.   Steinert, P.M., T. Kartasova, and L.N. Marekov, *Biochemical evidence that small proline-rich proteins and trichohyalin function in epithelia by modulation of the biomechanical properties of their cornified cell envelopes.* Journal of Biological Chemistry, 1998. **273**(19): p. 11758-11769.

244.   Borgoño, C.A., et al., *A potential role for multiple tissue kallikrein serine proteases in epidermal desquamation.* Journal of Biological Chemistry, 2007. **282**(6): p. 3640-3652.

245.   Hachem, J.-P., et al., *Acute acidification of stratum corneum membrane domains using polyhydroxyl acids improves lipid processing and inhibits degradation of corneodesmosomes.* The Journal of investigative dermatology, 2010. **130**(2): p. 500-510.

246.	Freinkel, R.K. and T.N. Traczyk, *Lipid composition and acid hydrolase content of lamellar granules of fetal rat epidermis.* Journal of Investigative Dermatology, 1985. **85**(4): p. 295-298.

247.	Landmann, L., *The epidermal permeability barrier.* Anatomy and Embryology, 1988. **178**(1): p. 1-13.

248.	Elias, P.M., *Epidermal lipids, barrier function, and desquamation.* J Invest Dermatol, 1983. **80**(1 Suppl): p. 44s-9s.

249.	Nemes, Z. and P.M. Steinert, *Bricks and mortar of the epidermal barrier.* Experimental &Amp; Molecular Medicine, 1999. **31**: p. 5.

250.	Zhang, L., et al., *Defects in stratum corneum desquamation are the predominant effect of impaired abca12 function in a novel mouse model of harlequin ichthyosis.* PLoS One, 2016. **11**(8): p. e0161465.

251.	Richard, G. *Autosomal recessive congenital ichthyosis* Gene Reviews [Internet] 2001 May 18, 2017; Available from: https://www.ncbi.nlm.nih.gov/books/NBK1420/.

252.	Waring, J.I., *Early mention of a harlequin fetus in america.* Archives of Pediatrics & Adolescent Medicine, 1932. **43**(2): p. 442.

253.	Kun-Darbois, J.D., et al., *Facial features in harlequin ichthyosis: Clinical findings about 4 cases.* Rev Stomatol Chir Maxillofac Chir Orale, 2016. **117**(1): p. 51-3.

254.	Rajpopat, S., et al., *Harlequin ichthyosis: A review of clinical and molecular findings in 45 cases.* Arch Dermatol, 2011. **147**(6): p. 681-6.

255.	Akiyama, M., Dale, B. A., Smith, L. T. , Shimuzu, S., and Holbrook, K. A. , *Regional difference in expression of characterstic abnormality of harlequin ichthyosis in affected fetuses* Prenatal Diagnosis 1998. **18**: p. 425-436.

256.	Mithwani, A.A., et al., *Harlequin ichthyosis: A case report of prolonged survival.* BMJ Case Rep, 2014. **2014**.

257.	Haftek, M., et al., *A longitudinal study of a harlequin infant presenting clinically as non-bullous congenital ichthyosiform erythroderma.* Brit J of Derm, 1996. **135**(3): p. 448-453.

258.	Roberts, L.J., *Long-term survival of a harlequin fetus* J Am Acad Dermatol, 1989. **21**(2): p. 335-339.

259.	Akiyama, M., et al., *Mutations in lipid transporter abca12 in harlequin ichthyosis and functional recovery by corrective gene transfer.* J Clin Invest, 2005. **115**(7): p. 1777-84.

260.	Kelsell, D.P., et al., *Mutations in abca12 underlie the severe congenital skin disease harlequin ichthyosis.* Am J Hum Genet, 2005. **76**(5): p. 794-803.

261.	Thomas, A.C., et al., *Abca12 is the major harlequin ichthyosis gene.* J Invest Dermatol, 2006. **126**(11): p. 2408-13.

262.	Akiyama, M., *Abca12 mutations and autosomal recessive congenital ichthyosis: A review of genotype/phenotype correlations and of pathogenetic concepts.* Hum Mutat, 2010. **31**(10): p. 1090-6.

263.	Annilo, T., et al., *Identification and characterization of a novel abca subfamily member, abca12, located in the lamellar ichthyosis region on 2q34.* Cytogenet Genome Res, 2002. **98**(2-3): p. 169-76.

264.	Borst, P. and R.O. Elferink, *Mammalian abc transporters in health and disease.* Annu Rev Biochem, 2002. **71**: p. 537-92.

265. Thomas, A.C., et al., *Premature terminal differentiation and a reduction in specific proteases associated with loss of abca12 in harlequin ichthyosis.* Am J Pathol, 2009. **174**(3): p. 970-8.

266. Fleckman, P., B. Hager, and B.A. Dale, *Harlequin ichthyosis keratinocytes in lifted culture differentiate poorly by morphologic and biochemical criteria.* Journal of Investigative Dermatology, 1997. **109**(1): p. 36-38.

267. Smyth, I., et al., *A mouse model of harlequin ichthyosis delineates a key role for abca12 in lipid homeostasis.* PLoS Genet, 2008. **4**(9): p. e1000192.

268. Yanagi, T., et al., *Harlequin ichthyosis model mouse reveals alveolar collapse and severe fetal skin barrier defects.* Hum Mol Genet, 2008. **17**(19): p. 3075-83.

269. Zuo, Y., et al., *Abca12 maintains the epidermal lipid permeability barrier by facilitating formation of ceramide linoleic esters.* J Biol Chem, 2008. **283**(52): p. 36624-35.

270. Rathore, S., et al., *Harlequin ichthyosis: Prenatal diagnosis of a rare yet severe genetic dermatosis.* J Clin Diagn Res, 2015. **9**(11): p. QD04-6.

271. Yanagi, T., et al., *Self-improvement of keratinocyte differentiation defects during skin maturation in abca12-deficient harlequin ichthyosis model mice.* Am J Pathol, 2010. **177**(1): p. 106-18.

272. Rompolas, P. and V. Greco, *Stem cell dynamics in the hair follicle niche.* Semin Cell Dev Biol, 2014. **25-26**: p. 34-42.

273. Mesler, A.L., et al., *Hair follicle terminal differentiation is orchestrated by distinct early and late matrix progenitors.* Cell Rep, 2017. **19**(4): p. 809-821.

Chapter II: Hair Follicle Terminal Differentiation is Orchestrated by Distinct Early and Late Matrix Progenitors[1]

2.1 Summary

During development and regeneration, matrix progenitors undergo terminal differentiation to form the concentric layers of the hair follicle. These differentiation events are thought to require signals from the mesenchymal dermal papilla (DP); however, it remains unclear how DP-progenitor cell interactions govern specific cell fate decisions. Here, we show that the hair follicle differentiated layers are specified asynchronously, with early matrix progenitors initiating differentiation prior to surrounding the DP. Uniquely, these early matrix cells can undergo terminal differentiation in the absence of Shh, BMP signaling, and DP maturation. Whereas early matrix progenitors form the hair follicle companion layer, later matrix populations progressively form the inner root sheath and hair shaft. Together, our findings identify unexpectedly early terminal differentiation events in the hair follicle, and reveal that the matrix progenitor pool can be divided into early and late phases based on distinct temporal, molecular and functional characteristics.

2.2 Introduction

The hair on our skin is a mammalian innovation that serves numerous functions, including thermoregulation, sensation and protection against the environment [274,

---

275]. Hair follicles, which house the differentiated cells of the hair shaft, are initially

formed from placodes that condense throughout the epidermis during embryonic

development [276]. In mice, these placodes appear in several waves commencing at

embryonic day 14.5 and ending at around birth. These epithelial buds subsequently

extend into the underlying dermis (hair germ and hair peg stages) and surround the

mesenchymal dermal papilla (DP), a key signaling and organizing center at the base of

the follicle [277-279].

Although hair follicle specification ceases around the time of birth, existing

follicles are periodically renewed throughout life. This process, known as the hair cycle,

consists of cyclic phases of rest (telogen), growth (anagen) and regression (catagen),

and recapitulates many of the events seen during initial hair follicle development [280].

During regeneration, hair follicle stem cells within the lower bulge and secondary hair

germ contribute to the outer root sheath (ORS) and matrix progenitors, respectively [56,

77, 78, 281]. Eventually, these matrix progenitors will terminally differentiate into cells

that form the concentric layers of the hair shaft, the inner root sheath (IRS) and the

companion layer (CL).

How is the intricate and stereotyped radial configuration of these different layers

achieved? Detailed lineage tracing studies have suggested that matrix cells, which

juxtapose and receive anagen-inducing signals from the DP, display a spatial

organization that determines their fate [27, 282, 283]. Matrix cells located more

centrally in the anagen hair bulb form the innermost layers that comprise the hair shaft,

whereas more peripherally-located matrix cells generate the outer differentiated layers,

the IRS and CL [282].

These observations suggest that the location of matrix progenitors along the hair follicle medial-lateral axis largely governs their fate. However, it is important to note that these progenitors are not a static population, but rather one that expands and changes shape as the lower hair bulb envelopes the DP during development and regeneration [284, 285] (**Figure 2.1A-B**). Thus, these progenitor populations may make varying cell fate decisions that hinge upon evolving spatial and temporal cues.

Among the terminally differentiated cells in the growing hair follicle, the IRS and CL are thought to arise from adjacently-located matrix progenitors, and have been reported to share similar growth kinetics, morphology and expression of markers such as Cutl1/CDP [26, 28, 29, 282, 286, 287]. Elaborate desmosomal and gap junction contacts between the CL and IRS have also been noted [27], which may enable upward-moving IRS cells to "pull" CL cells up alongside the anagen follicle [288, 289]. Given the extensive similarities and physical connections between the IRS and CL, this has led to speculation that these layers may act as an interdependent complex, with the CL essentially serving as the outermost layer of the IRS [26, 282].

Our previous studies identified Keratin 79 (K79) as a marker of early differentiating cells that form the CL [290]. We now show that CL cells are specified prior to other terminally differentiated cells in the hair follicle. Given the early appearance of these cells, we traced their origins back to a primitive matrix population that unexpectedly differentiates both prior to DP engulfment and independently of BMP signaling and Shh. Finally, we provide evidence that K79 is not required for hair growth, that the CL is distinct from the IRS, and that CL cells are lost during hair regression.

2.3 Experimental Procedures

2.31 Mice

The following strains were used: $Shh^{tm1(EGFP/cre)Cjt}$/J (*Shh-EGFP-Cre*) and *B6.129S6-Shh^{tm2(cre/ERT2)Cjt}*/J (*Shh-Cre^{ERT2}*) [291]; *Bmpr1a^{flox}* [292]; and $Gt(ROSA)26Sor^{tm1(EYFP)Cos}$ (*ROSA26-YFP*) [293]. To generate *Shh*-null animals, *Shh-EGFP-Cre* mice were inter-crossed. To generate $K79^{tm2a}$ mice, embryonic stem cells from clone EPD0179-4-A12 were purchased from KOMP and microinjected into blastocysts. Founder animals were crossed with *E2a-Cre* mice to remove the *neomycin* cassette. $K79^{tm2a}$ mice were inter-crossed to generate *K79*-null mice. To generate *K79-Cre* mice, the 5,789 bp sequence upstream of the *K79* transcriptional start site was PCR-amplified using BAC # RP24-152H23 and cloned into pCAG-Cre:GFP (Addgene #13776). Finally, the insert was purified and microinjected into (C57BL/6 x SJL) F2 mouse eggs and transferred into recipients. All studies were performed in accordance with regulations established by the University of Michigan Unit for Laboratory Animal Medicine.

2.32 5E1 Experiments

One day prior to depilation, 8-week-old mice were either uninjected, or injected with purified 5E1 anti-Shh antibody (Developmental Studies Hybridoma Bank), or purified IgG1 isotype-matched control antiserum (BioLegend). Mice received 200 µg of purified antibody daily for up to 15 days after depilation, similar to previously described [294].

2.33 Immunohistochemistry

In most cases, skin biopsies were fixed for 1 hour in cold 3.7% paraformaldehyde,
incubated overnight in 30% sucrose at 4°C, before embedding in OCT. Frozen sections
were rehydrated with PBS, blocked and stained using standard conditions. For the Shh
antibody from R&D, frozen sections prepared similarly to above were exposed to heat-
mediated antigen retrieval at 98°C in citrate buffer (Biogenex Laboratories) (pH 6.0) for
1 minute. Following this treatment, standard staining protocols were followed. For the
5E1 Shh antibody, skin biopsies were harvested and directly embedded into OCT
without fixation. Frozen sections were incubated in 100% acetone for 15 minutes at
room temperature, rinsed with PBS and air dried for 30 minutes. Following this
treatment, standard staining protocols were followed. For images containing
GFP/EGFP/YFP, fluorescence was visualized by antibody staining, except for the
epifluorescent whole mount images shown in **Figure 2.1E**. In *K79-Cre;R26R-YFP*
mice, which harbor both GFP and YFP alleles, we did not distinguish between these
signals for our analyses. Antibodies and procedures used for immunohistochemistry are
listed below in section 2.34.

2.34 Antibodies

Table 2.1: Antibodies used in Chapter II

Antigen	Vendor	Clone # or Product #	Dilution	Usage Notes
AE15	Santa Cruz	M-215	1:500	
Gata3	Santa Cruz	HG3-31	1:200	

Gata6	Cell Signaling	D61E4	1:300	
GFP/YFP	Aves Labs	GFP-1020	1:1,000	Used in most figures.
GFP/YFP	Abcam	ab6673	1:500	Used in Fig. 8C only
K6	BioLegend	PRB-169P	1:500	
K14	Santa Cruz	C-14	1:500	
K75	American Research Products	03-GP-CK6HF	1:400	
K79	Santa Cruz	Y-17	1:250	Lot #J2412.
K79	Abcam	Ab7195	1:500	This antibody, originally generated against mouse Gli2, is known to cross-react with K79 [290].
Lef1	Cell Signaling	C12A5	1:200	
Lrig1	R&D Systems	AF3688	1:300	
Msx2	Santa Cruz	M-70	1:200	
pSmad1/5	Cell Signaling	D5B10	1:100	
Shh	R&D Systems	AF464	1:1,000	Antigen retrieval (see text)
Shh	DSHB	5E1	1:1,000	Acetone fixation (see text)
Sox9	Santa Cruz	H-90	1:150	

2.35 Quantitating Shh+/EGFP+ Matrix Cell Contribution to Differentiated Cell Layers

Shh-EGFP-Cre mice were depilated at 8 weeks of age, and dorsal biopsies were harvested between 6-10 days afterwards. Non-consecutive sections were scored for potential overlap between EGFP and differentiation markers. The CL was identified by K79 expression in Anagen II follicles, and by K75 expression at more advanced stages.

The IRS was identified by AE15 expression at all stages. For each stage (Anagen II, IIIa-b or IIIc-IV) and marker combination, at least 25 hair follicles were scored.

For Anagen II follicles, sections were initially examined in the EGFP channel, and hair follicles were analyzed only if there were at least 3 EGFP$^+$ cells within the secondary hair germ. Hair follicles were subsequently scored as positive if there was at least 1 EGFP$^+$ cell that overlapped with the differentiation marker. For Anagen IIIa-b and IIIc-IV, sections were initially examined in the EGFP channel, and only hair follicles that were longitudinally cut, harbored at least 10 EGFP$^+$ cells in the hair bulb, and displayed expression of the differentiated marker, were used for analysis. Hair follicles were scored as positive if there were cells that displayed overlap between EGFP and the differentiation marker, and appeared as a continuous stream originating directly from the Shh$^+$ matrix cell pool (similar to **Figure 2.7E**). Occasionally, hair follicles contained isolated EGFP$^+$ cells that possessed marker expression but were not continuous with the Shh$^+$ matrix cell pool. Since these cells may have arisen during earlier stages, they were not scored as positive. All follicles that met the above scoring criteria were evaluated, independent of hair subtype.

2.36 Lineage Tracing and Quantitating Shh-Cre^{ERT2};R26R-YFP Matrix Cell Contribution to Differentiated Cell Layers

Shh-Cre^{ERT2};R26R-YFP mice were depilated at 8 weeks of age and induced with a single dose of tamoxifen (1 mg per 40 grams body weight, dissolved in corn oil), 8 days post-depilation. Dorsal skin biopsies were harvested 3 days after induction and non-consecutive sections were scored for potential overlap between YFP and the IRS

marker, AE15. Sections were initially examined in the YFP channel and hair follicles were analyzed only if there were at least 10 YFP$^+$ cells present. The contribution of Shh$^+$ matrix cells to each differentiation layer (CL, IRS, HS) was evaluated based on the spatial relationship between YFP$^+$ and AE15$^+$ cells. If YFP$^+$ cells were present to the outside of the AE15$^+$ cell domain, they was scored as CL. If YFP$^+$ cells were observed to the interior of the AE15$^+$ cell domain, they were scored as HS. Instances of YFP/AE15 overlay were scored as IRS. These categories were not mutually exclusive, as a given follicle could display Shh$^+$ matrix cell contributions to multiple differentiated cell layers. For this analysis, a total of 45 hair follicles were scored from 3 independent mice (**Figure 2.8C**). All follicles that met the above scoring criteria were evaluated, independent of hair subtype.

2.4 Results

2.41 Asynchronous Formation of Terminally Differentiated Cell Layers in the Hair Follicle

We previously reported that K79 identifies an early population of terminally differentiated cells within hair germs during development and secondary hair germs during regeneration [290]. In both instances, K79$^+$ cells form columns that extend outwards. To place the appearance of these cells in the context of other events that occur during hair growth, we began by assessing the specification of K79$^+$ cells relative to other differentiated cells in the hair follicle.

IRS cells first appear in Stage 4 hair pegs and in Anagen IIIa regenerating follicles, which have fully engulfed the DP at this point [284, 295]. Interestingly, in

earlier stage hair germs and in Anagen II regenerating follicles, K79+ cells already formed a solid column (**Figure 2.1C-D**). In contrast, IRS cells were not detected at these stages, as assessed by the markers trichohyalin (AE15) and Gata3 [296] (**Figure 2.1C-D**). When IRS cells eventually did appear in later stage follicles, these IRS cells pushed upwards through the middle of the existing K79+ column, causing those cells to separate into a cone-like configuration at the proximal end (**Figure 2.1C-D**).

We next generated transgenic mice expressing a Cre-GFP fusion protein under the control of the *K79* promoter (*K79-Cre*) to better visualize these differentiated cells. When coupled with a Cre-inducible *YFP* reporter allele (*K79-Cre;R26R-YFP*), P2.5 animals displayed epifluorescent follicles (**Figure 2.1E**). Upon imaging the under-surface of freshly excised skin by confocal microscopy, we observed K79+ columns that appeared wider at the base, where the IRS cone was forming, and narrower at the tip (**Figure 2.1E**). Although the thickness of adult skin precluded us from performing similar imaging studies during regeneration, serial sections confirmed that K79+ cells also formed a wide, cone-like shape at the base that was continuous with a narrow column of cells extending up around the club hair bulge (**Figure 2.1F-G**). Altogether, these observations indicate that terminal differentiation occurs asynchronously in the growing hair follicle, and that K79+ cells are specified earlier than other terminally differentiated cell types.

2.42 The CL is Specified Prior to Canonical K75 and K6 Expression

Our previous studies suggested that K79+ cells become the CL, which is comprised of a flat layer of cells that initially expresses Keratin 75 (K75) and then

65

Keratin 6 (K6) [28, 287, 297-299]. Although the cellular origins of the CL have been somewhat controversial, several studies have argued that the CL is related to the IRS and that the two layers form concomitantly [28, 288, 289]. However, since K79$^+$ cells appear prior to the IRS, we decided to reassess whether canonical CL markers such as K75 and K6 might also be expressed in the early regenerating follicle.

Surprisingly, early K79$^+$ cell columns did not express K75 (**Figure 2.2A**). Rather, we detected K75/K79 co-localization only in more advanced anagen follicles, with K75 expression originating proximally in the hair bulb and extending outward in a "bulb to bulge" direction, consistent with prior reports [28] (**Figure 2.2B-C**). We made similar observations with K6, which co-localized with K79$^+$ cells in the CL only in later stage follicles, but whose expression extended in an opposing inward "bulge to bulb" direction, as has also previously been observed [28] (**Figure 2.2D-E**).

By mid-anagen, we further noted that K79 is largely lost from the CL, which now expresses only K75 and K6 (**Figure 2.2C, 2.2F-G**). To confirm these shifts in K79 expression, we generated mice in which a *lacZ* cassette, encoding β-galactosidase (β-gal), was inserted into the endogenous *K79* locus, thereby inactivating the allele but also serving as a reporter for *K79* promoter activity (*K79^{tm2a}* mice) (**Figure 2.2H**). *K79$^{tm2a/+}$* mice did not display any overt abnormalities, while β-gal activity recapitulated the expression pattern for *K79* in the skin [290, 300]. This included strong activity in columns extending out from hair germs; in the sebaceous glands and suprabasal cells of the infundibulum in adult follicles; and in the early CL (**Figure 2.2I-J**). β-gal activity, however, was absent from the lower late anagen follicle, consistent with the loss of K79 expression from the mature CL (**Figure 2.2K**). These observations indicate that the CL

undergoes a dynamic maturation process throughout anagen, and that the CL is already specified before gaining canonical K75 and K6 expression. These findings may possibly explain why the exact origins of the CL have been difficult to elucidate, and also why asynchronous formation of this cell layer has not been previously documented (**Figure 2.2L**).

2.43 Early Matrix Progenitors Give Rise to K79+ Cells

Terminal differentiation in the hair follicle is thought to occur only after matrix cells have surrounded the DP [284, 295]. However, since K79$^+$ cells appear earlier than other differentiated cells, this suggested to us that a primitive matrix population might be functioning even prior to DP engulfment. We therefore delved deeper into the origins of K79$^+$ cells, reasoning that if we can identify the earliest differentiation events that occur within the follicle, this will enable us to pinpoint the moment when matrix cells first become functional.

Previous studies have shown that *Sonic hedgehog* (*Shh*) is expressed in hair placodes and later restricted to the base of developing follicles [301-303]. Using mice that express EGFP-Cre from the endogenous *Shh* locus (*Shh-EGFP-Cre*), coupled with a Cre-inducible reporter allele, Levy et al., demonstrated that *Shh*$^+$ progenitors give rise to the hair follicle, but not to the interfollicular epidermis [304]. Even in the absence of a conditional reporter allele, *Shh-EGFP-Cre* mice display highly fluorescent *Shh*$^+$ matrix progenitors [291, 304]. Importantly, we took advantage of the fact that the immediate, *Shh*-negative progeny of these cells are also weakly fluorescent, likely due to the transient persistence of EGFP-Cre fusion protein. This is illustrated by the slightly

67

expanded territory of EGFP$^+$ cells relative to the Shh$^+$ domain at the base of the hair germ (**Figure 2.3A**). Therefore, in contrast to conventional lineage tracing strategies where a cell progenitor and all its direct and indirect descendents become permanently marked, these *Shh-EGFP-Cre* mice provided us a convenient snapshot of *Shh*$^+$ progenitors and only their most direct, weakly fluorescent progeny at all times.

Using P2.5 *Shh-EGFP-Cre* newborn skin, we focused on hair germs that had initiated at around the time of birth and had not surrounded the DP. We observed that single K79$^+$, EGFP-weak suprabasal cells were often centrally located immediately above EGFP-high, *Shh*$^+$ matrix cell clusters (**Figure 2.3B**). We confirmed that these K79$^+$ cells were *Shh*-negative, thereby suggesting that *Shh*$^+$ matrix cells directly give rise to overlying K79$^+$ suprabasal cells (**Figure 2.4**). Similarly, in slightly later stage hair germs, columns of K79$^+$ cells were observed, with only the most proximal 1-2 cells retaining weak EGFP (**Figure 2.3B**). We further noted that the base of K79$^+$ columns was comprised of Sox9$^+$ cells that lacked Wnt pathway activity, as assessed by Lef1 expression (**Figure 2.3C-E** and **Figure 2.4**). As Sox9$^+$/Wnt-negative cells in the early hair bud have been reported to specify future bulge stem cells [305, 306], our findings here suggest that at least a subset of these cells, directly derived from early *Shh*$^+$ progenitors and expressing K79, are already terminally differentiated.

Finally, we observed using Oncomine that expression of *K79* is highly correlated with *Gata6* mRNA levels in vulvar intraepithelial neoplasia [307]. *Gata6* mRNA is also enriched in sorted hair follicle stem cells [308], in particular those expressing Lrig1 [309], which give rise to K79$^+$ cells in the infundibulum [290]. In late stage hair pegs, we determined that Gata6 is expressed in distal K79$^+$ cells, but is not present in earlier

stage hair germs (**Figure 2.3F**). Furthermore, Gata6^{+} cells did not directly originate

from *Shh*[+] progenitors, but did overlay with Lrig1^{+} stem cells in the adult hair follicle

isthmus [310] (**Figure 2.3F-G**). Taken together, these data suggest that early matrix

cells can undergo terminal differentiation even prior to DP engulfment. Subsequently,

K79^{+} differentiated cells gain some markers (Gata6) while losing others (*Shh*, Sox9,

Lef1) during maturation (**Figure 2.3H**).

2.44 Early and Late Matrix Progenitors Exhibit Molecular Differences

Thus far, we have defined early matrix progenitors based on their ability to form

K79^{+} cells prior to surrounding the DP. To determine whether these progenitors are

molecularly distinct from later matrix populations in the anagen bulb, we assessed the

expression of canonical matrix markers, including nuclear localization of Lef1, Msx2 and

phosphorylated Smad1/5 (pSmad).

To examine cycling hair follicles in synchrony, we focused our analysis on adult

anagen follicles from *Shh-EGFP-Cre* mice that were depilated for either 6 or 8 days,

timepoints before and after DP engulfment, respectively. Similar to during development,

we confirmed that early *Shh*[+] progenitors in the secondary hair germ directly give rise to

K79^{+} cells by 6 days post-depilation (**Figure 2.5A**). We next co-localized canonical

matrix markers with *Shh* expression, and observed that this early population exhibited

strong Lef1 nuclear localization, confirming that these are true matrix cells (**Figure

2.5B**). For Msx2, we observed occasional nuclear staining, typically in cells located at

the periphery of the *Shh*[+] cell cluster (**Figure 2.5C**). Importantly, although we observed

strong nuclear pSmad in the bulge, as previously reported [311, 312], early *Shh*[+] matrix

progenitors typically displayed only diffuse pSmad staining (**Figure 2.5D**). In contrast,

later matrix cells surrounding the DP exhibited nuclear localization of all 3 markers

(**Figure 2.5B-D**). These findings suggest that early and late matrix progenitors activate

overlapping but also distinct pathways, possibly due to evolving interactions with the

DP, and that this may influence their subsequent cell fate decisions.

2.45 Neither BMP signaling, Shh nor DP Maturation is Required for Early Matrix Cell

Differentiation

The absence of nuclear pSmad in early matrix progenitors suggests that these

cells do not require BMP signaling to initiate differentiation. To test this functionally, we

generated mice expressing *Keratin 5* promoter-driven Cre recombinase coupled with

conditional floxed and deleted alleles of *BMP receptor 1A* (*K5;Bmpr1a$^{flox/-}$*). These

mutants, which exhibited hind limb defects [311] (**Figure 2.6A**), developed hair pegs

which specifically lacked epithelial BMP signaling (**Figure 2.6B**). Consistent with our

hypothesis that early matrix progenitors lack nuclear pSmad but are nonetheless

functional, *K5;Bmpr1A$^{flox/-}$* follicles possessed normal K79$^+$ cells, but no AE15$^+$ IRS

cells, even in later stage hair pegs (**Figure 2.6B**). Since early-arising K79$^+$ cells

eventually form the CL, these observations may explain why ablating BMP signaling in

the hair follicle specifically disrupts IRS differentiation, while sparing the CL [292, 311,

313].

Given that early matrix progenitors initiate differentiation prior to surrounding the

DP, this then led us to wonder whether these early progenitors depend upon DP

maturation for function. Since Shh is required for DP maturation and maintenance [278,

301, 302], we examined whether specification of K79$^+$ cells is perturbed in *Shh*$^{-/-}$ animals. As previously reported, P0 *Shh*$^{-/-}$ mutants display gross abnormalities in the head, tail and appendages, but possess largely normal epidermis (**Figure 2.6C**) [301, 302]. Although hair germs were initiated, these buds were enlarged and deformed, did not extend into the deeper dermis, and were juxtaposed by deteriorated or non-existant DPs. In spite of these defects, K79$^+$ cells were still specified (**Figure 2.6D**). Interestingly, a subset of K79$^+$ cells co-expressed AE15 (**Figure 2.6E**), markers that do not typically overlap (**Figure 2.1C**). These findings suggest that early matrix progenitors can undergo terminal differentiation into K79$^+$ cells even in the absence of DP maturation, and that some of these cells subsequently gain aberrant AE15 expression.

To reassess these findings in the context of adult hair regeneration, we used the monoclonal antibody 5E1 to neutralize Shh prior to and after depilation. As previously shown, animals injected daily with 5E1 do not regenerate hair [314], in contrast to mice that were either uninjected or injected with an isotype-matched IgG1 antiserum (**Figure 2.6F**). In 5E1-injected depilated mice, cells in the secondary hair germ underwent initial expansion, similar to *Shh*$^{-/-}$ hair germs, but did not progress past Anagen II. As was seen during development, Shh suppression did not prevent K79 specification at 10 or 15 days after depilation (**Figure 2.6G**); however, specification of IRS cells was fully inhibited by the 5E1 antibody (**Figure 2.6G**). Since similarly staged hair follicles were observed at both timepoints in 5E1-injected mice, this confirmed that these follicles were fully halted in early anagen, and not merely progressing through the hair cycle more slowly. Altogether, these results indicate that early matrix progenitors do not

71

require BMP signaling, Shh or DP maturation to undergo terminal differentiation into K79$^+$ cells. In contrast, later matrix populations require these signals to form the IRS.

2.46 Asynchronous Maturation of Terminally Differentiated Cell Layers

Having now shown that early and late matrix populations initiate CL and IRS specification at different times, we next tested whether these progenitors also finish forming these layers asynchronously. Prior evidence supporting this possibility comes from electron microscopy studies by Morioka et al., who showed that the ORS directly abuts IRS cells without an intervening CL at the most proximal end of advanced follicles [29] (diagrammed in **Figure 2.7A**). Thus, at the base of late anagen follicles, CL cells are effectively sealed off from direct contact with matrix progenitors, implying that no new CL cells are being created at this point.

Consistent with these observations, we noted that in early anagen follicles, K79$^+$ cell columns are directly juxtaposed with their Lef1$^+$ matrix progenitors (**Figure 2.7B**). At later stages, however, only IRS cells, which are themselves partially Lef1$^+$, directly contacted matrix cells (**Figure 2.7C**). Importantly, we also noticed that the IRS extends lower down the anagen bulb than does the CL (**Figure 2.7D**). This again suggests that, as the configuration of matrix progenitors and their differentiated progeny changes during anagen progression, CL cells are eventually blocked off from direct contact with progenitor cells.

This lack of direct contact suggested to us that not only do primitive matrix progenitors initiate CL formation earlier than that of the other layers, but that these progenitors may also finish forming the CL earlier as well. To directly test this

hypothesis, we again used the *Shh-EGFP-Cre* allele as a "timing mechanism" to trace only the most immediate contributions made by *Shh+* matrix cells to the growing hair follicle.

In depilated skin from adult mice, *Shh+* cells within Anagen II follicles formed only CL cells, since IRS cells are not present at this point (**Figure 2.7E-F**). In Anagen IIIa-b follicles, we observed efficient labeling of both the CL and IRS, indicating that *Shh+* progenitors are directly forming both cell types. In more advanced Anagen IIIc-IV follicles, however, labeling was observed in the IRS and hair shaft, but only rarely in the CL. These labeling shifts were not due to selective expression of *Shh* in specific hair follicle layers, since Shh was restricted to the asymmetric lateral disc region of the lower anagen bulb (**Figure 2.8A-B**). In addition, we performed more conventional lineage tracing experiments by inducibly and permanently labeling *Shh+* progenitors during mid/late-anagen, and observed that these cells formed IRS and hair shaft, but not CL (**Figure 2.8C**). Altogether, these results, obtained using both permanent and transient fate mapping strategies, support a model whereby matrix progenitors progressively form and complete the inner layers of the growing hair follicle asynchronously.

2.47 Fate of Terminally Differentiated CL Cells

At the conclusion of anagen, the hair follicle regresses during catagen to re-enter telogen. This is accompanied by the upward movement of terminally differentiated cells, which are eventually expelled into the hair canal [315, 316].

To trace the fate of CL cells during catagen, we turned back to *K79-Cre;R26R-YFP* mice described above (**Figure 2.1E**). These animals enable permanent labeling of

73

cells that, at any given time, expressed K79. As expected, we observed fluorescent suprabasal cells within the K79$^+$ domain of the infundibulum, but also efficient labeling of the entire mature CL, whose elongated cells and nuclei manifest a "beads on a string" morphology (**Figure 2.9A-B**). The permanent labeling of the entire mature CL occurred in spite of the apparent absence of K79 protein and *K79* promoter/β-gal activity in this domain (**Figure 2.9C**, **2.2K**). This suggests that mature CL cells, identified by K75 expression, may either express very low levels of K79 (enough to drive functional Cre expression), or at one time expressed K79 and subsequently downregulated its expression.

In *K79-Cre;R26R-YFP* mice during early catagen, we observed labeled CL cells being drawn up the regressing follicle (**Figure 2.9D**). These cells maintained their elongated morphology, even after the IRS had begun to deteriorate and had partially evacuated the hair bulb (**Figure 2.9D**). Intriguingly, the base of the regressing CL appeared continuous with the future inner bulge, which also expresses K75 (**Figure 2.9E**). As follicles re-entered telogen, we observed that the inner bulge was mostly unlabeled, consistent with previous reports that the CL does not give rise to these cells [317] (**Figure 2.9F**). However, we occasionally noticed persistent fluorescent cells within the upper domain of the inner bulge, possibly due to weak re-expression of K79 in these cells specifically during catagen (**Figure 2.9F-G**). As for the ultimate fate of the CL, we observed thin YFP$^+$K79$^-$ cells shed into the hair canal, suggesting that these are likely the remnants of this layer (**Figure 2.10**). In summary, we have lineage traced a discrete layer in the hair follicle and confirmed that K79$^+$ cells form the CL. During catagen, the CL is eliminated, while cells immediately proximal to the CL persist in the

upper reaches of the inner bulge, a region that has recently been reported to harbor at least 3 molecularly distinct cell subpopulations [318].

2.48 Functional Testing of K79

Given that K79 is a defining marker of the earliest differentiating cells in the hair follicle, we lastly tested the requirement for this keratin in development and regeneration. To do this, we generated *K79*^{tm2a/tm2a} homozygous mice, where both alleles of *K79* are disrupted by *lacZ* coding sequences, and confirmed that K79 was fully ablated throughout the skin (**Figure 2.11**).

K79^{tm2a/tm2a} newborn mice developed hair normally and did not exhibit any overt skin phenotypes. Upon challenging adult mice to 2 consecutive cycles of depilation or hair plucking, wherein K79 gene expression recapitulates that which is seen during physiological hair cycling [21], mutant animals entered anagen and regrew hair similarly to littermate controls (**Figures 2.11, 2.12**). We also did not notice any obvious histological differences between mutant and control skin at different hair cycle stages, except that *K79*^{tm2a/tm2a} mice possess disordered sebaceous glands (data not shown; manuscript in preparation). During anagen, expression of K75 and K6 in the CL was unaffected by loss of K79. Finally, we confirmed that the cells which normally express K79 are still present and located within the expected domains of mutant follicles in *K79*^{tm2a/tm2a} mice, as determined by β-gal expression from the endogenous *K79* locus. Altogether, these findings indicate that K79 is not required for hair growth, possibly due to functional redundancy with related keratin family members.

2.5 Discussion

During morphogenesis and regeneration, the DP promotes hair growth by secreting factors such as TGF-β, Fgf7/10, Noggin and possibly Eda to responding cells at the base of the follicle [278, 308, 319-321]. These signals are thought to initially drive early cell proliferation in the hair germ or secondary hair germ [56, 77, 78], with terminal differentiation occurring later as the expanding follicle envelopes the DP [280, 284]. Once this occurs, matrix progenitors are thought to assume different cell fates along the hair follicle medial-lateral axis [283]. How these choices are made remains unclear, although signaling gradients may lead to differential expression of matrix transcription factors such as Msx2, Dlx3 and Foxn1 [313, 322, 323].

Our findings here offer several new insights into this complicated process (**Figure 2.9H**). First, we show that K79 is the earliest terminal differentiation marker in the growing hair follicle, and that matrix progenitors unexpectedly initiate differentiation prior to surrounding the DP. Second, we find that specification of the differentiated layers of the follicle both commences and terminates asynchronously, as determined using *Shh-EGFP-Cre* mice. Third, we propose that the matrix progenitor pool can be divided into early and late phases that are distinguishable temporally (anagen stage), morphologically (physical relationship to the DP) and molecularly (BMP status). Although terminal differentiation occurs throughout both phases, specific cell fate choices evolve over time and rely on distinct signaling inputs, as proven functionally by analyzing *Shh* and *Bmpr1a* mutant mice, as well as by antibody-mediated Shh neutralization. Fourth, we observe using *K79^{tm2a}* and *K79-Cre;R26R-YFP* mice that the CL undergoes a dynamic maturation process, and that CL-derived cells do not persist

into telogen. Finally, fifth, we report that K79 is not required for normal hair growth, as assessed using *K79* null animals.

In developing hair placodes, basal *Shh*^{+} cells divide perpendicularly to the basement membrane to generate proliferative Sox9^{+} cells that will eventually become the bulge [305, 306]. We also observed early specification of basal layer future bulge cells in *Shh-EGFP-Cre* placodes (**Figure 2.13**). In later stage hair germs and secondary hair germs, we noted that basal *Shh*^{+} cells form overlying, terminally differentiated K79^{+} suprabasal cells, firmly establishing that matrix progenitors are functional at this point. These findings are consistent with the observation that early cell divisions in the secondary hair germ are often oriented perpendicularly to both the basement membrane and the axis of hair growth, which may be a mechanism for generating K79^{+} cells [324].

Here, we have used *Shh-EGFP-Cre* mice, in the absence of a traditional reporter allele, to visualize direct cellular relationships between *Shh*[+] progenitors and their progeny. One limitation of this technique is that during anagen, *Shh*[+] progenitors represent only a subset of the entire mature matrix pool (**Figure 2.4**). Indeed, we have occasionally noticed in late anagen follicles that *Shh*^{+} matrix cells appear to possess reduced pSmad, relative to adjacent non-*Shh* matrix (**Figure 2.8D**). In spite of this, gene expression studies have also indicated that *Shh*[+] progenitors are very similar to the overall matrix population [308], suggesting that the behavior of this sub-population may be generally representative of the whole.

Earlier studies have questioned the origins of the CL, a structure hypothesized to function either as a slippage plane for hair growth, or as an anchor for the hair shaft

[286, 325]. More recent reports have argued that the CL arises from matrix progenitors [282, 317], a conclusion supported here by our studies. Given the intimate cellular connections between the CL and IRS, including specialized structures termed "*Flügelzellen*" [27], it has also been proposed that growth of the CL depends upon the upward movement of the IRS [288, 289]. Our findings, however, argue against this since the CL clearly forms before the other differentiated layers. Compellingly, hair follicles lacking *Gata3*, *Bmpr1a* or functional NuMA possess abnormal IRS without obvious defects in the CL [296, 311, 313, 326]. Altogether, these findings unequivocally indicate that the CL can form independently of the IRS.

An important lingering question relates to how the matrix progenitor pool expands throughout anagen. In particular, it remains unclear how early and late matrix populations are related, how these cells assume their final medial-lateral positions along the DP axis, and how *Shh* expression becomes restricted [282, 283, 317]. Although we have divided the matrix progenitor pool into early and late phases here, it is also possible that matrix cells with varying innate potentials may co-exist even early on, or exist along a continuum. In addition, further studies will be needed to determine whether early matrix progenitors can directly become later matrix cells, give rise to later matrix cell progeny, or remain as separate and independent populations throughout anagen.

2.6 Author Contributions

A.L.M, N.A.V and M.V.L. conceived and performed experiments. S.Y.W. conceived and performed experiments, wrote the manuscript and secured funding.

2.7 Acknowledgements

This chapter was published in Cell Reports (see citation below).

2.8 Figures

Figure 2.1. Asynchronous Specification of Terminally Differentiated Cell Layers. A. Schematic of early hair development. The mesenchymal dermal condensate (DC) matures into the dermal papilla (DP), which is surrounded by the growing hair germ (brown). Matrix progenitors (blue) are thought to differentiate only after surrounding the DP. B. Similarly, the secondary hair germ (brown) engulfs the DP during hair regeneration. Images not drawn to scale. C. K79 precedes AE15 during hair development and regeneration. D. K79 precedes Gata3. E. K79-Cre;R26R-YFP mice possess epifluorescent hair canals in P2.5 whole-mount skin viewed from the surface (top right). Bottom panels, confocal imaging from the underside of the skin, with K79+ cells (green) forming a cone that is wider at the base and narrower at the tip. The epidermis is colored gold (bottom left). Bottom right, magnified views of individual follicles. p, proximal; d, distal. F. Serial sections through an adult early anagen follicle, with K79+ cells (green) forming a cone-like shape that narrows into a solid column near the bulge (asterisk). G. Schematic of K79+ cone and column in the regenerating follicle. P, postnatal day. DEP, days post-depilation.
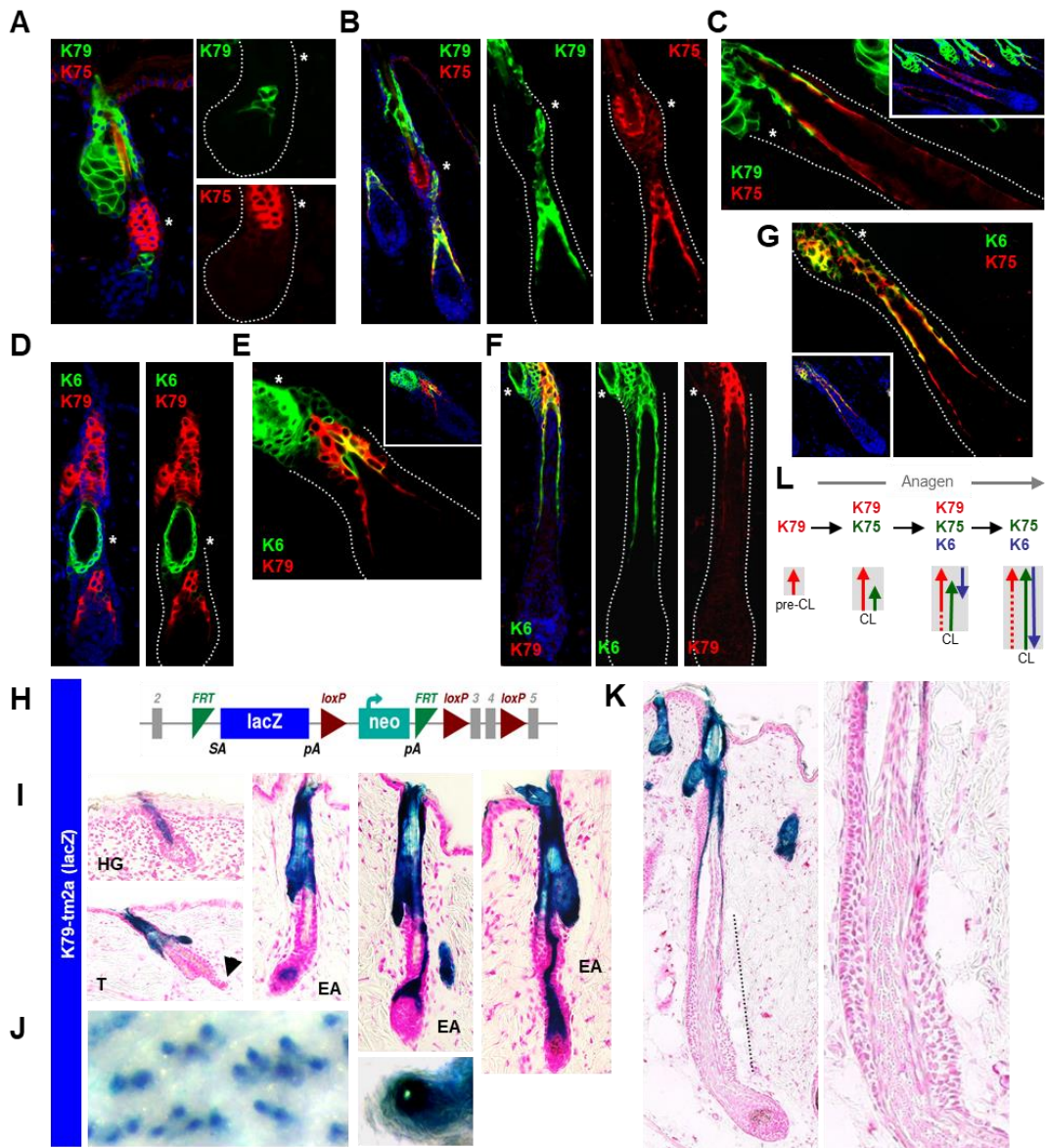
Figure 2.2. The CL Undergoes a Dynamic Maturation Process. A. K79 appears prior to K75 in anagen II regenerating follicles. B. K79 and K75 co-localize in the CL during Anagen III. C. K79 is lost from the K75+ CL in later follicles. D. K79 precedes K6 in Anagen II follicles. E. K6 later overlays with K79, beginning at the distal CL. F. K79 is lost from the K6+ CL in later follicles. G. The mature CL is K75+K6+K79-. H. Schematic of the K79tm2a allele, where LacZ is inserted into the endogenous K79 locus. I. β-gal activity in K79tm2a/+ skin recapitulates K79 expression in developing hair germs (HG), during telogen (T) and early anagen (EA). Note the absence of β-gal/K79 in the telogen secondary hair germ (arrowhead). J. Whole-mount K79tm2a/+ telogen skin, showing labeled hair canals. K. β-gal activity is absent in the lower late anagen follicle (dotted line), reflecting loss of K79 from the CL. Right, magnified view of lower follicle. L. Schematic summarizing keratin shifts in the growing CL (gray box), with arrows indicating direction by which keratin expression appears. Dotted lines indicate weak or no expression. In panels with multiple boxes, these are separated channel views with the bulge indicated by an asterisk.

81
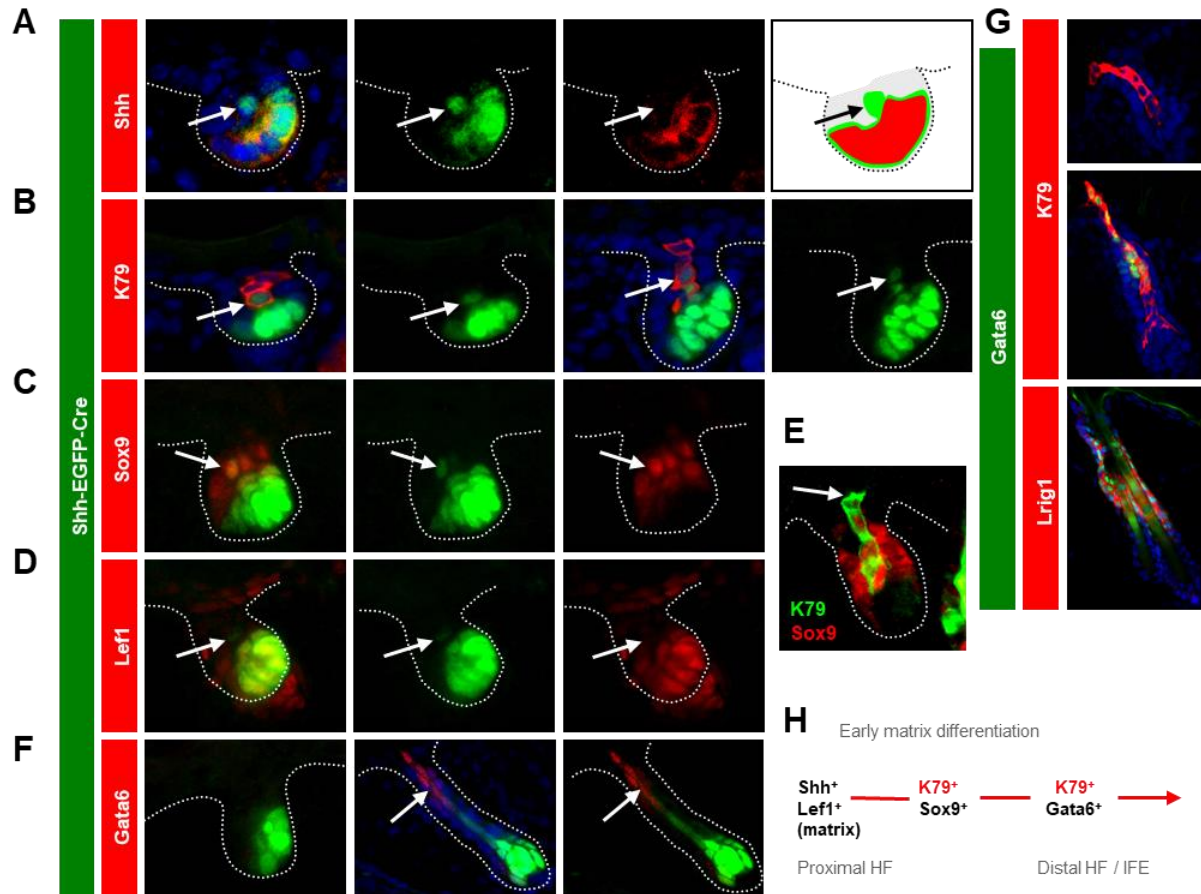
Figure 2.3. Early Matrix Progenitors Initiate Terminal Differentiation in Hair Germs. A-D. P2.5 hair germs from Shh-EGFP-Cre skin display EGFP expression in early matrix progenitors (bright green) and in their immediate progeny (light green, arrows). These progeny are Shh-, K79+, Sox9+ and Lef1-, as indicated (red). E. K79+ columns lose Sox9 distally in later stage hair germs (arrow). F. Gata6 is not in hair germs (left), but is present in distal cells in hair pegs (middle and right, arrows). G. Gata6 is not in hair germs (top), overlays with distal K79+ cells in hair pegs (middle), and overlays with Lrig1 in adult telogen follicles. H. Schematic of early matrix cell differentiation. In panels with multiple boxes, these are separated channel views.
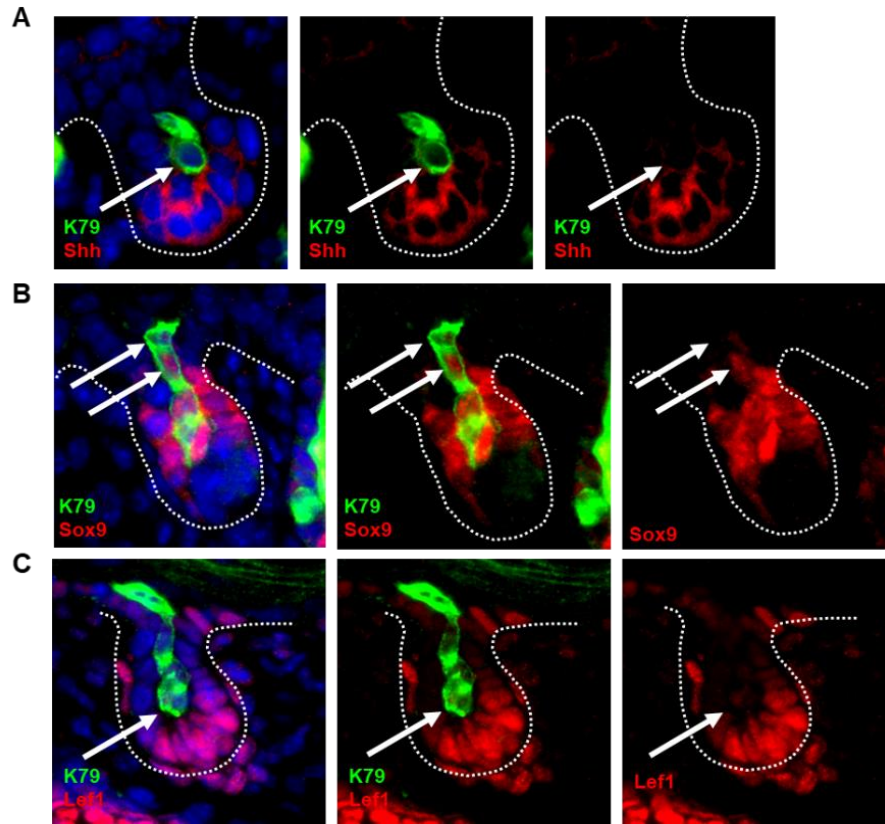
Figure 2.4. Differentiated K79+ Cells in P2.5 Hair Germs Initially Express Sox9, but Not Shh or Lef1. Related to Figure 3. A. K79+ cells (green, arrow) do not express Shh (red). B. K79+ cell columns overlay with Sox9 proximally (lower arrows), but lose Sox9 distally (upper arrows). C. K79+ cell columns do not express Lef1 (arrow). Middle and right boxes are separated channel views of the left boxes. The middle image in (B) is also depicted in Figure 3E.
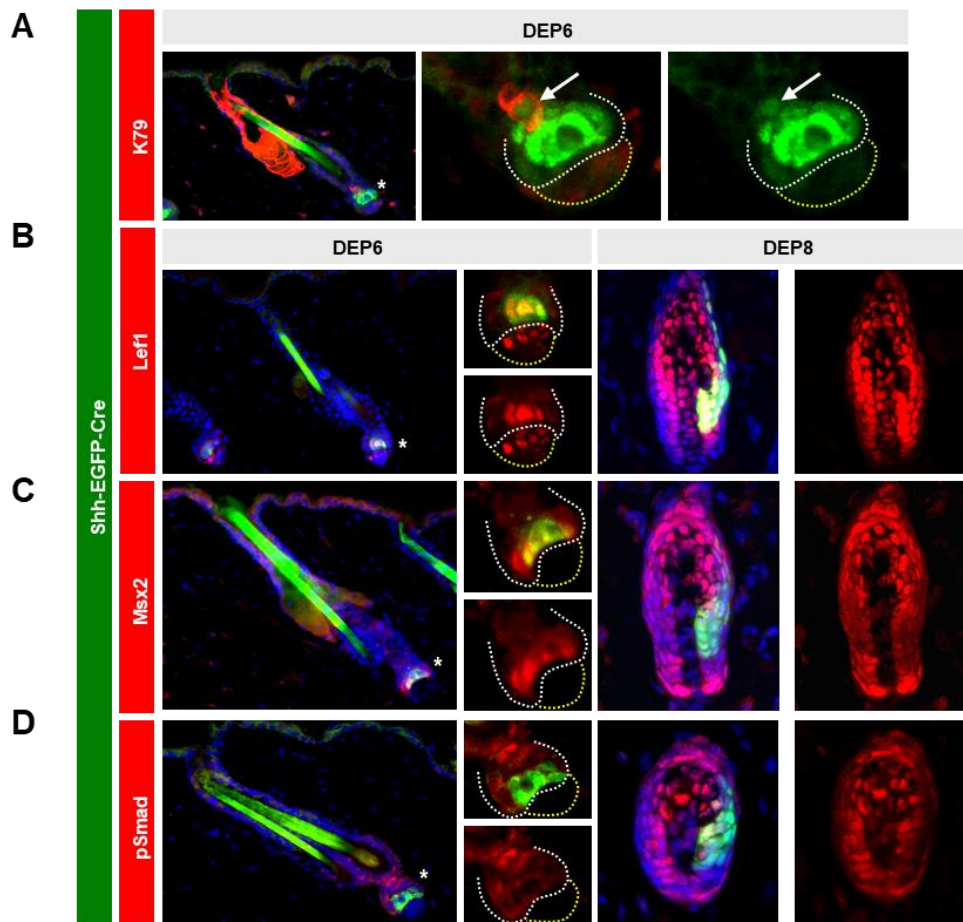
Figure 2.5. Early Matrix Progenitors are Molecularly Distinct from Later Matrix Populations. A. Six days post-depilation, regenerating follicles from adult Shh-EGFP-Cre mice display EGFP expression in early matrix progenitors (bright green) and in their immediate progeny (light green), which express K79 (arrows). B-D. Left boxes, early matrix cells (green) from Shh-EGFP-Cre skin exhibit nuclear localization of Lef1, occasional nuclear localization of Msx2, and no pSmad nuclear localization, as indicated. Right boxes, later matrix cells display nuclear localization of all 3 canonical matrix markers. In panels with multiple boxes, these are separated channel views, magnified from the region of the lower hair follicle indicated by an asterisk. White broken lines, lower regenerating follicle. Yellow broken lines, DP. DEP, days post-depilation.
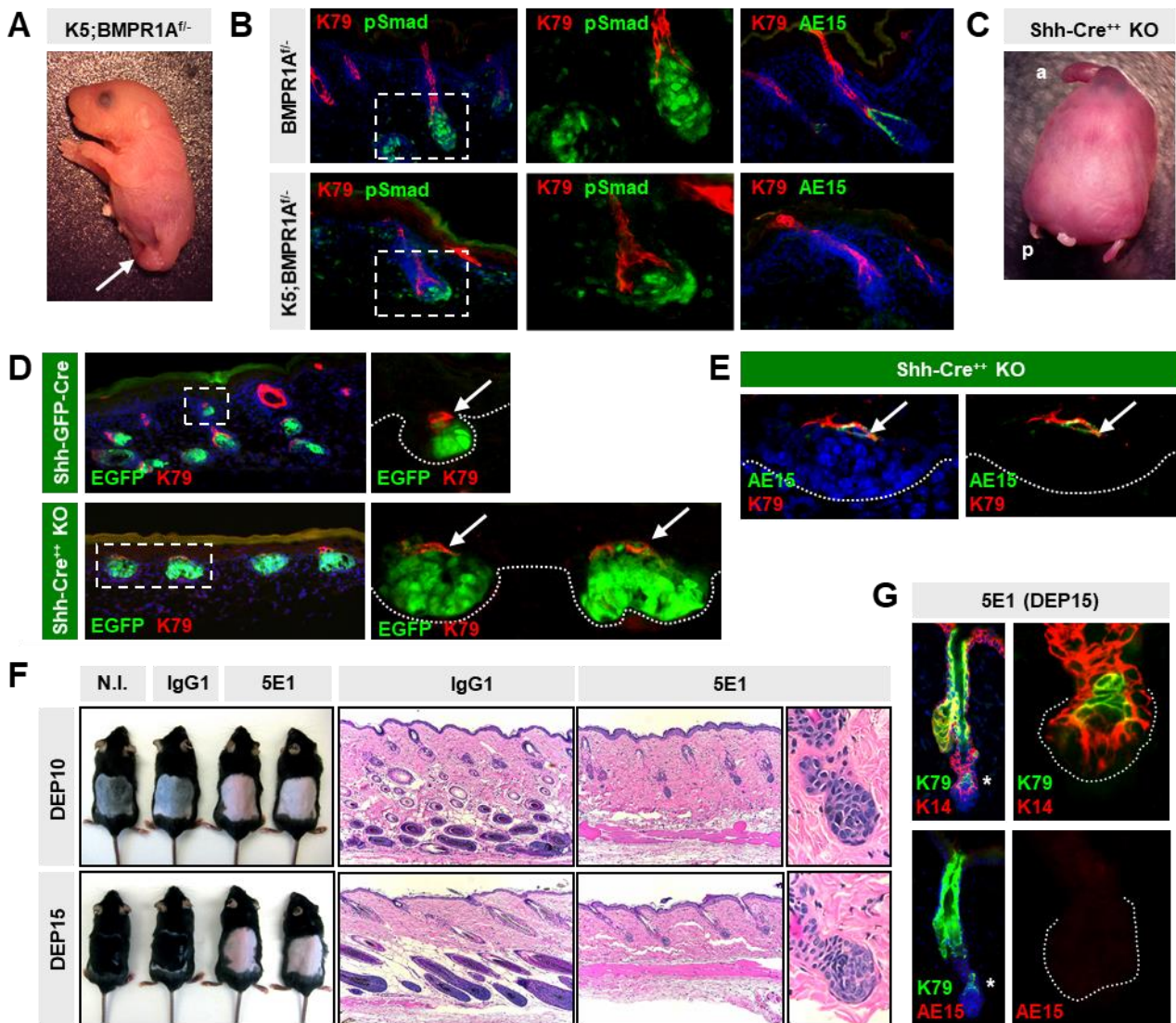
Figure 2.6. Early Matrix Progenitors Differentiate Independently of Bmpr1a, Shh and DP Maturation. A. Newborn K5;Bmpr1a$^{flox/-}$ mutant with defective hindlimbs (arrow). B. K5;Bmpr1a$^{flox/-}$ mutant follicles lack pSmad specifically in the epithelial compartment, with normal pSmad in the DP. Mutant follicles form K79+ cells, but not AE15+ IRS. C. Newborn Shh-deficient mutant, generated by homozygosing the Shh-EGFP-Cre allele (Shh-Cre++) (a, anterior; p, posterior). D. K79+ cells (arrows) are specified in aberrant Shh-deficient hair germs (bottom). Control littermates harboring a single Shh-EGFP-Cre allele develop normal follicles (top). E. A subset of K79+ cells aberrantly co-expresses AE15 (arrows) in Shh-deficient follicles. F. Mice injected with anti-Shh neutralizing antibody (5E1) do not re-enter anagen, in contrast to depilated mice injected with isotype control IgG1 (IgG), or not injected (N.I.). G. Early matrix progenitors in 5E1-injected depilated skin can differentiate into K79+ cells, but do not form IRS. In panels with multiple images, these are separated channel views, magnified from either the boxed regions (B and D) or from the lower follicle (G) (asterisk). DEP, days post-depilation.

85
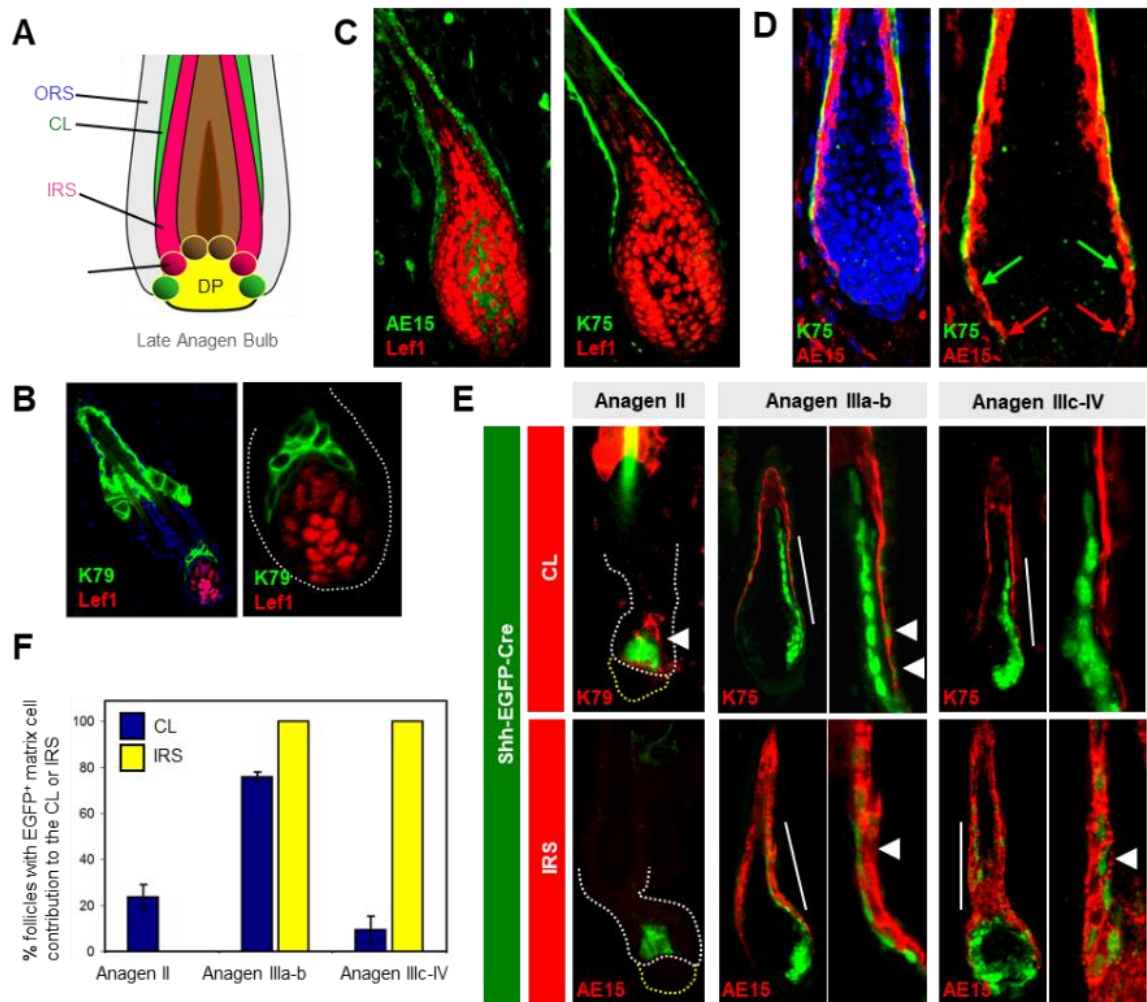
Figure 2.7. Matrix Cells Asynchronously Complete the Inner Layers of the Hair Follicle. A. Schematic of the mature anagen hair bulb, adapted from Morioka et al., 2005. Note the lack of direct contact between the mature CL (green) and matrix. B. K79+ cells are juxtaposed with Lef1+ matrix progenitors in Anagen II follicles. C. IRS (left), but not mature CL (right), directly contacts matrix progenitors in Anagen IV-V follicles. D. IRS cells (red arrows) extend more proximally down the anagen bulb than does the CL (green arrows) in Anagen IV-V follicles. E. Left, in Anagen II follicles from Shh-EGFP-Cre mice, early matrix cells contribute only to the CL (arrowhead). Middle, in Anagen IIIa-b follicles, matrix cells contribute to both CL and IRS (arrowheads). Right, in Anagen IIIc-IV follicles, matrix cells contribute to IRS (arrowhead), but not to CL. For (B) and (D), right boxes are magnified views of the lower follicle without DAPI. For (E), magnified views are of areas indicated by the solid white line. White broken lines, lower follicle. Yellow broken line, DP. F. Quantitation of results from (E), scoring EGFP+ matrix cell contribution to the indicated layers at different hair stages. For scoring methodology, see Experimental Procedures.
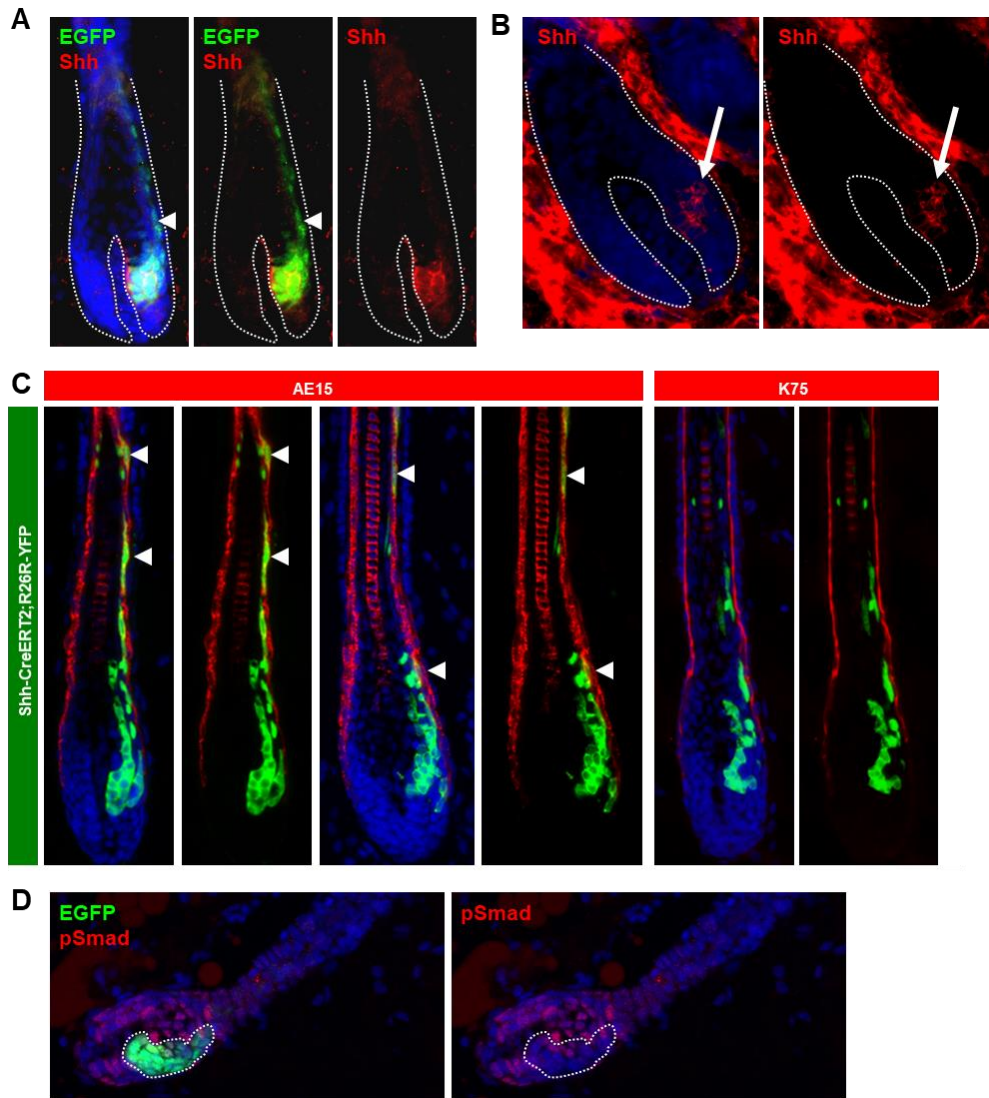
Figure 2.8. The CL is Completed Prior to Other Differentiated Layers During Hair Regeneration. A. In Shh-EGFP-Cre anagen follicles, 8 days post-depilation, EGFP+ cells overlap with, and extend beyond (arrowhead), the domain of Shh protein expression, as assessed by IHC using an anti-Shh antibody (R&D Systems). B. A similar domain of Shh expression (arrow) is seen using an independent anti-Shh antibody (clone 5E1). C. In Shh-CreERT2;R26R-YFP mice, Shh+ matrix progenitors and their progeny were permanently labeled upon treatment with tamoxifen, administered 8 days post-depilation. In biopsies harvested 3 days subsequently, labeled matrix cells formed AE15+ IRS (left, arrowheads; 2 examples depicted), but not K75+ CL (right). No matrix contribution to the CL was observed in a total of 45 follicles from 3 independent Shh-CreERT2;R26R-YFP mice treated in this manner. D. In Shh-EGFP-Cre anagen follicles, 8 days post-depilation, Shh+ matrix progenitors (dotted lines) sometimes continued to exhibit reduced pSmad, similar to what is seen during earlier stages of anagen. In all panels, separated channel views are also depicted.

87
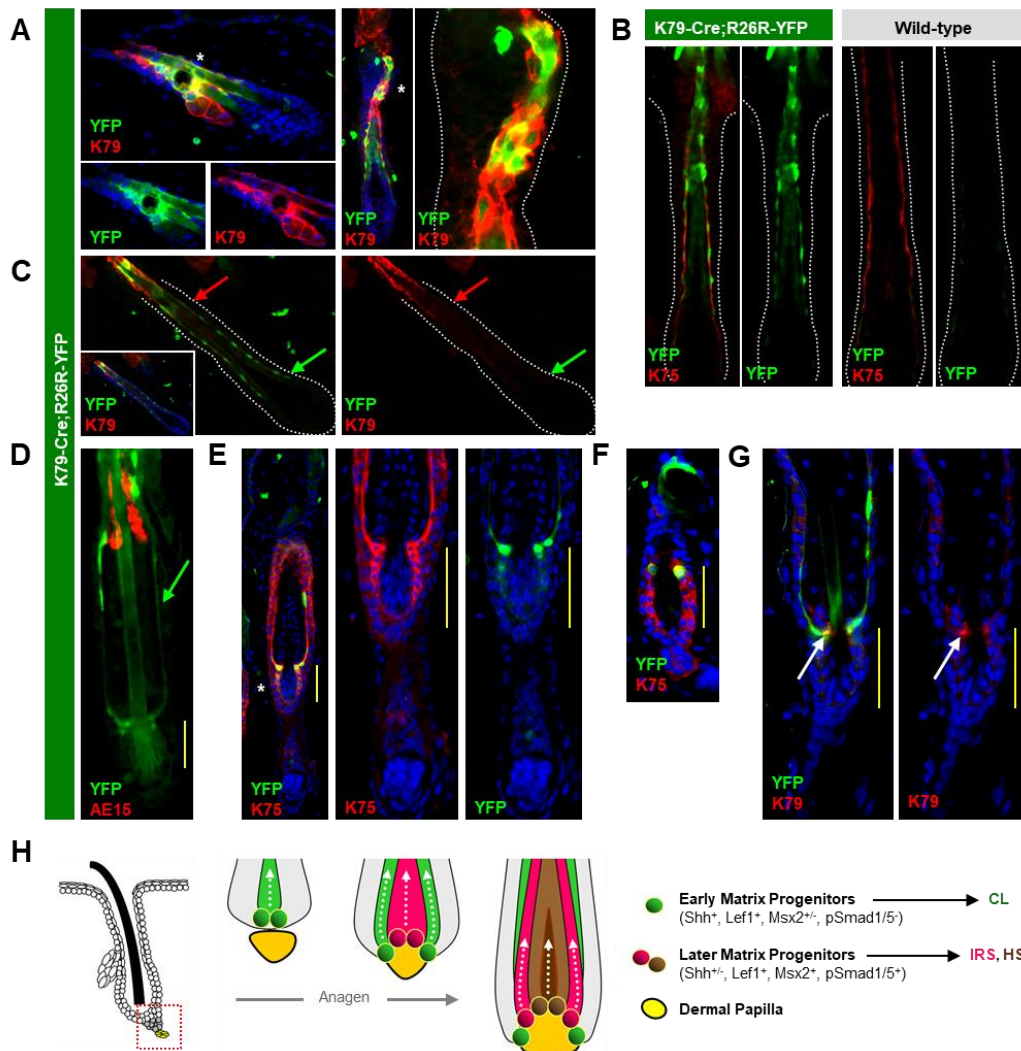
Figure 2.9. CL Cells Are Eliminated During Hair Regression. A. K79-Cre;R26R-YFP mice exhibit labeling (green) in a subset of K79+ suprabasal cells in the infundibulum during telogen (left) and in the CL of Anagen III follicles (right). B. The mature CL, identified by K75 (red), is labeled in these mice (left boxes, green), but not in control animals (right boxes), from Anagen IV-V follicles. C. CL labeling persists (arrows, green), even as K79 recedes (arrows, red) in Anagen IV-V follicles. D. In early catagen, the CL persists (green arrow), with partially evacuated IRS remnants (red). E. The regressing CL (green) appears continuous with upper cells of the future inner bulge (yellow lines), both identified by K75 (red), during early catagen. F. In telogen, labeling persists in upper cells of the inner bulge (green). G. This is possibly due to weak re-expression of K79 (red) at the base of the CL during catagen (arrows). H. Schematic of hair regeneration, where early matrix cells (green) initially form the CL prior to surrounding the DP (yellow). After the DP has been engulfed, later matrix cells (red and brown) occupy more central regions of the hair bulb and form the IRS and HS, with no further contribution to the CL. This model incorporates observations from Sequeira and Nicolas, 2012. Alternative models, where matrix cells of varying innate differentiation potentials may co-exist in early anagen, are not depicted here for the sake of simplicity. In panels with multiple images, these are separated channel views, in some cases magnified from areas indicated by asterisks.
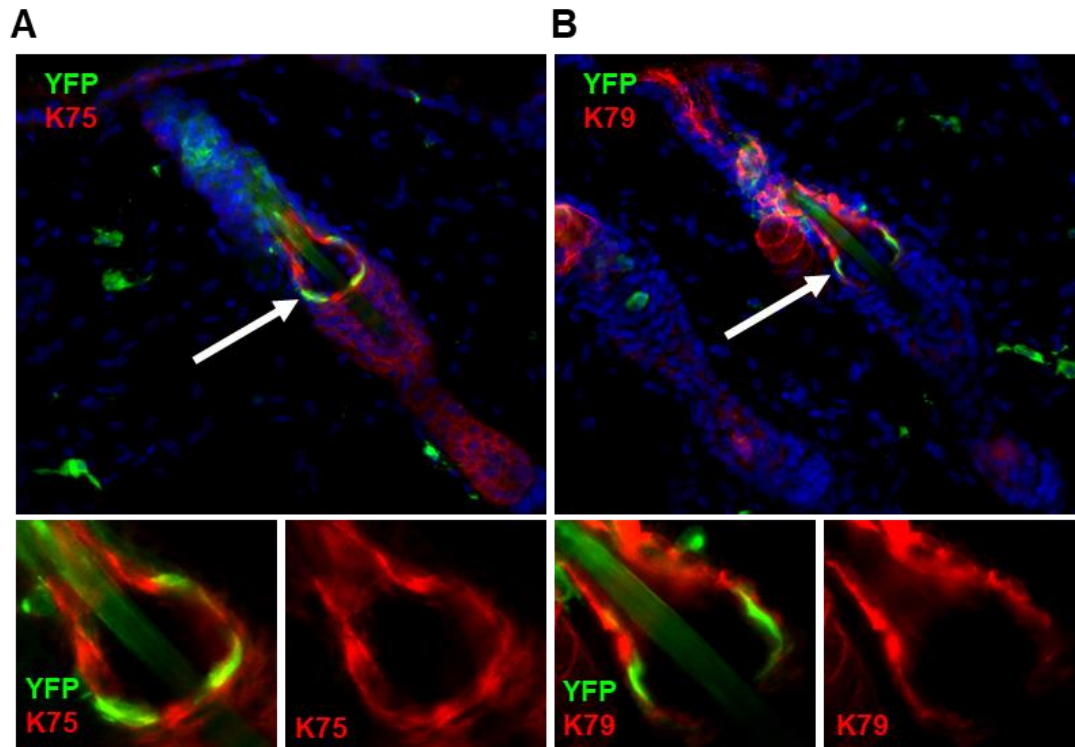
Figure 2.10. CL Cells Are Shed Into the Hair Canal During Catagen. Related to Figure 7. A. In K79-Cre;R26R-YFP catagen skin, labeled CL cells (green) continue to express K75 (red) as these cells move up and are shed into the hair canal. B. These same labeled cells do not express K79 (red), and are located to the inside of K79+ suprabasal cells lining the infundibulum. Lower panels are separated channel views of the regions indicated by the arrows.
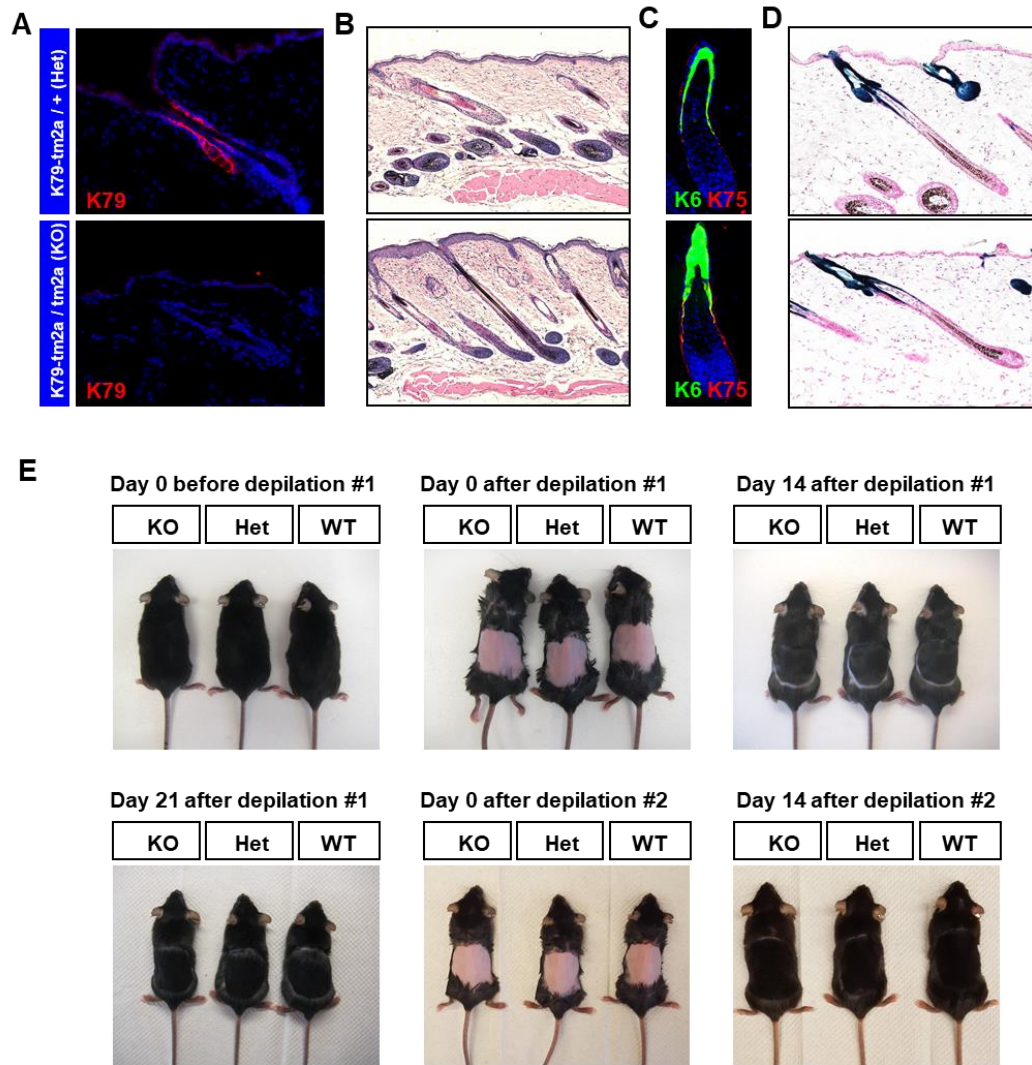
Figure 2.11. Functional Testing of K79. A. Complete loss of K79 (red) was validated in K79tm2a/tm2a mice (KO) compared to K79tm2a/+ control mice (Het). B. Hematoxylin and eosin staining of anagen skin from K79-Het and K79-KO skin, both from adult mice depilated 10 days prior to biopsy. C. Loss of K79 does not affect canonical expression of K75/K6 in the CL. D. LacZ activity, which identifies cells expressing K79, is unchanged between K79-Het and K79-KO animals during anagen. E. Loss of K79 does not affect hair regeneration in depilated adult mice.
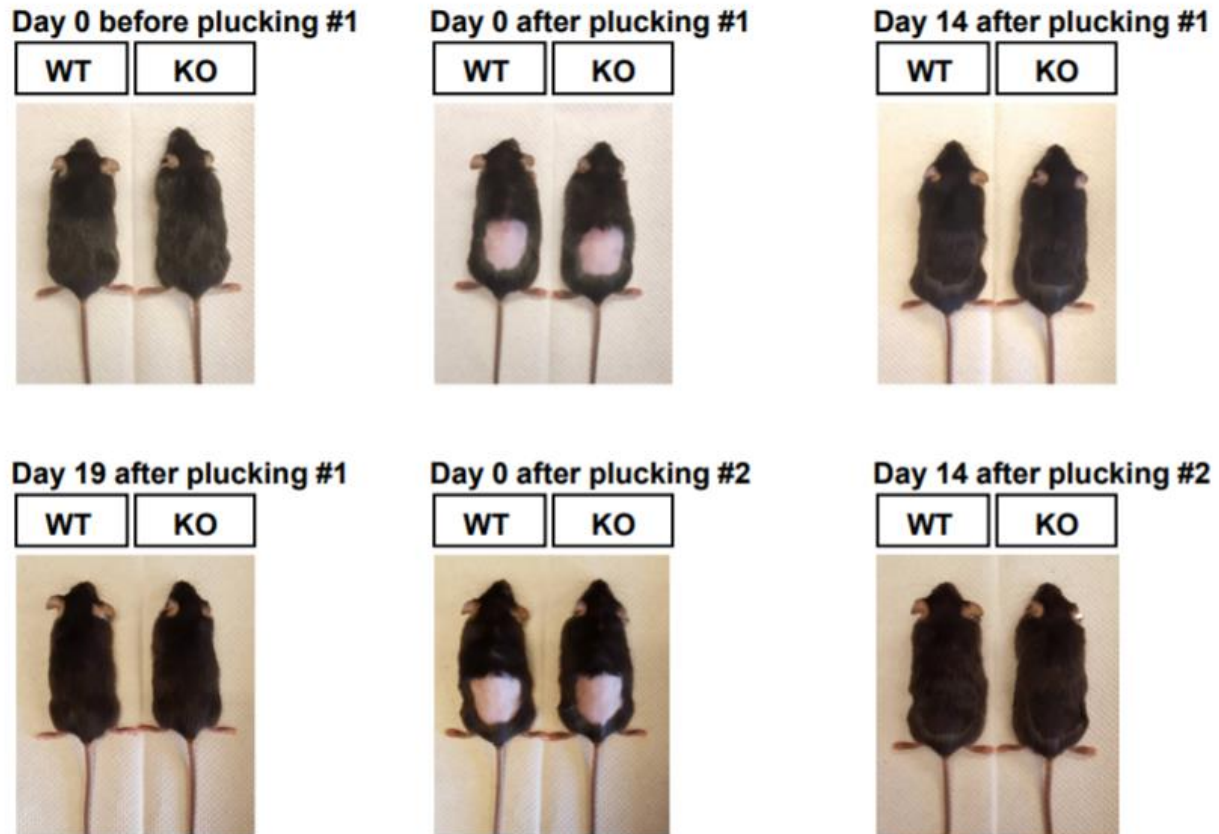
Figure 2.12. Loss of K79 Does Not Affect Plucking-Induced Hair Regeneration. Similar to in Figure 11, K79 is not required for hair regeneration induced by 2 consecutive cycles of hair plucking.
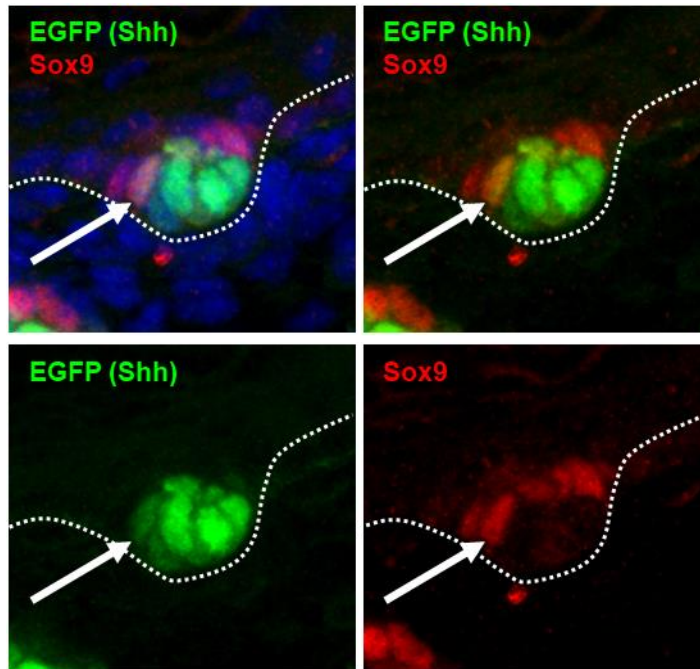
Figure 2.13. Early Formation of Basal Layer Future Bulge Cells. Related to Figure 3. Hair follicle placodes from newborn *Shh-EGFP-Cre* mice display strong EGFP at the base of the developing follicle and weak EGFP in overlying basal layer future bulge cells (Sox9+, arrow), suggesting a direct lineage relationship. Individual panels represent separated channels of the same image, as indicated.

2.9 Reference List

1.   Blanpain, C. and E. Fuchs, *Epidermal homeostasis: A balancing act of stem cells in the skin.* Nat Rev Mol Cell Biol, 2009. **10**: p. 207-217.
2.   Schneider, M.R. and R. Paus, *Deciphering the functions of the hair follicle infundibulum in skin physiology and disease.* Cell Tissue Res, 2014. **358**: p. 697-704.
3.   Biggs, L.C. and M.L. Mikkola, *Early inductive events in ectodermal appendage morphogenesis.* Semin Cell Dev Biol, 2014. **25-26**: p. 11-21.
4.   Enshell-Seijffers, D., et al., *Beta-catenin activity in the dermal papilla regulates morphogenesis and regeneration of hair.* Dev Cell, 2010. **18**: p. 633-642.
5.   Woo, W.M., H.H. Zhen, and A.E. Oro, *Shh maintains dermal papilla identity and hair morphogenesis via a noggin-shh regulatory loop.* Genes Dev, 2012. **26**: p. 1235-1246.
6.   Rompolas, P., et al., *Live imaging of stem cell and progeny behaviour in physiological hair-follicle regeneration.* Nature, 2012. **487**: p. 496-499.
7.   Schmidt-Ullrich, R. and R. Paus, *Molecular principles of hair follicle induction and morphogenesis.* Bioessays, 2005. **27**: p. 247-261.
8.   Panteleyev, A.A., C.A. Jahoda, and A.M. Christiano, *Hair follicle predetermination.* J Cell Sci, 2001. **114**: p. 3419-3431.
9.   Rompolas, P., K.R. Mesa, and V. Greco, *Spatial organization within a niche as a determinant of stem-cell fate.* Nature, 2013. **502**: p. 513-518.
10.   Zhang, Y.V., et al., *Distinct self-renewal and differentiation phases in the niche of infrequently dividing hair follicle stem cells.* Cell Stem Cell, 2009. **5**: p. 1-12.
11.   Greco, V., et al., *A two-step mechanism for stem cell activation during hair regeneration.* Cell Stem Cell, 2009. **4**: p. 155-169.
12.   Sequeira, I. and J.F. Nicolas, *Redefining the structure of the hair follicle by 3d clonal analysis.* Development, 2012. **139**: p. 3741-3751.
13.   Legue, E. and J.F. Nicolas, *Hair follicle renewal: Organization of stem cells in the matrix and the role of stereotyped lineages and behaviors.* Development, 2005. **132**: p. 4143-4154.
14.   Langbein, L., et al., *A novel epithelial keratin, hk6irs1, is expressed differentially in all layers of the inner root sheath, including specialized huxley cells (flugelzellen) of the human hair follicle.* J Invest Dermatol, 2002. **118**: p. 789-799.
15.   Muller-Rover, S., et al., *A comprehensive guide for the accurate classification of murine hair follicles in distinct hair cycle stages.* J Invest Dermatol, 2001. **117**: p. 3-15.
16.   Paus, R., et al., *A comprehensive guide for the recognition and classification of distinct stages of hair follicle morphogenesis.* J Invest Dermatol, 1999. **113**: p. 523-32.
17.   Ellis, T., et al., *The transcriptional repressor cdp (cutl1) is essential for epithelial cell differentiation of the lung and the hair follicle.* Genes Dev, 2001. **15**: p. 2307-2319.
18.   Rothnagel, J.A. and D.R. Roop, *The hair follicle companion layer: Reacquainting an old friend.* J Invest Dermatol, 1995. **104**: p. 42S-43S.

19. Morioka, K., *Outer rooth sheath and companion layer*, in *Hair follicle*, K. Morioka, Editor. 2005, Springer Tokyo: Tokyo. p. 89-106.

20. Gu, L.H. and P.A. Coulombe, *Keratin expression provides novel insight into the morphogenesis and function of the companion layer in hair follicles.* J. Invest. Dermatol., 2007. **127**: p. 1061-1073.

21. Winter, H., et al., *A novel human type ii cytokeratin, k6hf, specifically expressed in the companion layer of the hair follicle.* J Invest Dermatol, 1998. **111**: p. 955-962.

22. Chapman, R.E., *Cell migration in wool follicles of sheep.* J Cell Sci, 1971. **9**: p. 791-803.

23. Orwin, D.F.G., *Cell differentiation in the lower outer sheath of the romney wool follicle: A companion cell layer.* Aust J Biol Sci, 1971. **24**: p. 989-999.

24. Veniaminova, N.A., et al., *Keratin 79 identifies a novel population of migratory epithelial cells that initiates hair canal morphogenesis and regeneration.* Development, 2013. **140**: p. 4870-4880.

25. Harfe, B.D., et al., *Evidence for an expansion-based temporal shh gradient in specifying vertebrate digit identities.* Cell, 2004. **118**: p. 517-528.

26. Yuhki, M., et al., *Bmpr1a signaling is necessary for hair follicle cycling and hair shaft differentiation in mice.* Development, 2004. **131**: p. 1825-1833.

27. Srinivas, S., et al., *Cre reporter strains produced by targeted insertion of eyfp and ecfp into the rosa26 locus.* BMC Dev Biol, 2001. **1**: p. 4.

28. Peterson, S.C., et al., *Basal cell carcinoma preferentially arises from stem cells within hair follicle and mechanosensory niches.* Cell Stem Cell, 2015. **16**: p. 400-412.

29. Paus, R., et al., *A murine model for inducing and manipulating hair follicle regression (catagen): Effects of dexamethasone and cyclosporin a.* J Invest Dermatol, 1994. **103**: p. 143-147.

30. Kaufman, C.K., et al., *Gata3: An unexpected regulator of cell lineage determination in skin.* Genes Dev, 2003. **17**: p. 2108-2122.

31. Wojcik, S.M., M.A. Longley, and D.R. Roop, *Discovery of a novel murine keratin 6 (k6) isoform explains the absence of hair and nail defects in mice deficient for k6a and k6b.* J Cell Biol, 2001. **154**: p. 619-630.

32. Rothnagel, J.A., et al., *The mouse keratin 6 isoforms are differentially expressed in the hair follicle, footpad, tongue and activated epidermis.* Differentiation, 1999. **65**: p. 119-130.

33. Smyth, I., et al., *Krt6a-cre transgenic mice direct loxp-mediated recombination to the companion cell layer of the hair follicle and following induction by retinoic acid to the interfollicular epidermis.* J. Invest. Dermatol., 2004. **122**: p. 232-234.

34. Quigley, D.A., et al., *Gene expression architecture of mouse dorsal and tail skin reveals functional differences in inflammation and cancer.* Cell Rep, 2016. **16**: p. 1153-1165.

35. Chiang, C., et al., *Essential role for sonic hedgehog during hair follicle morphogenesis.* Dev Biol, 1999. **205**: p. 1-9.

36. St-Jacques, B., et al., *Sonic hedgehog signaling is essential for hair development.* Curr Biol, 1998. **8**: p. 1058-1068.

37. Oro, A.E. and K. Higgins, *Hair cycle regulation of hedgehog signal reception.* Dev Biol, 2003. **255**: p. 238-248.

38. Levy, V., et al., *Distinct stem cell populations regenerate the follicle and interfollicular epidermis.* Dev Cell, 2005. **9**: p. 855-861.

39. Ouspenskaia, T., et al., *Wnt-shh antagonism specifies and expands stem cells prior to niche formation.* Cell, 2016. **164**: p. 156-169.

40. Nowak, J.A., et al., *Hair follicle stem cells are specified and function in early skin morphogenesis.* Cell Stem Cell, 2008. **3**: p. 33-43.

41. Santegoets, L.A., et al., *Hpv related vin: Highly proliferative and diminished responsiveness to extracellular signals.* Int J Cancer, 2007. **121**: p. 759-66.

42. Rezza, A., et al., *Signaling networks among stem cell precursors, transit-amplifying progenitors, and their niche in developing hair follicles.* Cell Rep, 2016. **14**: p. 3001-3018.

43. Page, M.E., et al., *The epidermis comprises autonomous compartments maintained by distinct stem cell populations.* Cell Stem Cell, 2013. **13**: p. 1-12.

44. Jensen, K.B., et al., *Lrig1 expression defines a distinct multipotent stem cell population in mammalian epidermis.* Cell Stem Cell, 2009. **4**: p. 427-439.

45. Andl, T., et al., *Epithelial bmpr1a regulates differentiation and proliferation in postnatal hair follicles and is essential for tooth development.* Development, 2004. **131**: p. 2257-2268.

46. Genander, M., et al., *Bmp signaling and its psmad1/5 target genes differentially regulate hair follicle stem cell lineages.* Cell Stem Cell, 2014. **15**: p. 619-633.

47. Kobielak, K., et al., *Defining bmp functions in the hair follicle by conditional ablation of bmp receptor 1a.* J Cell Biol, 2003. **163**: p. 609-623.

48. Wang, L.C., et al., *Conditional disruption of hedgehog signaling pathway defines its critical role in hair development and regeneration.* J Invest Dermatol, 2000. **114**: p. 901-8.

49. Stenn, K.S. and R. Paus, *Controls of hair follicle cycling.* Physiol Rev, 2001. **81**: p. 449-494.

50. Mesa, K.R., et al., *Niche-induced cell death and epithelial phagocytosis regulate hair follicle stem cell pool.* Nature, 2015. **522**: p. 94-97.

51. Hsu, Y.C., H.A. Pasolli, and E. Fuchs, *Dynamics between stem cells, niche, and progeny in the hair follicle.* Cell, 2011. **144**: p. 92-105.

52. Joost, S., et al., *Single-cell transcriptomics reveals that differentiation and spatial signatures shape epidermal and hair follicle heterogeneity.* Cell Syst, 2016. **3**: p. 1-17.

53. Veniaminova, N.A., et al., *Keratin 79 identifies a novel population of migratory epithelial cells that initiates hair canal morphogenesis and regeneration.* Development, 2013. **140**(24): p. 4870-80.

54. Botchkarev, V.A., et al., *Noggin is a mesenchymally derived stimulator of hair-follicle induction.* Nat Cell Biol, 1999. **1**: p. 158-164.

55. Oshimori, N. and E. Fuchs, *Paracrine tgf-beta signaling counterbalances bmp-mediated repression in hair follicle stem cell activation.* Cell Stem Cell, 2012. **10**: p. 63-75.

56.   Rosenquist, T.A. and G.R. Martin, *Fibroblast growth factor signalling in the hair growth cycle: Expression of the fibroblast growth factor receptor and ligand genes in the murine hair follicle.* Dev Dyn, 1996. **205**: p. 379-386.

57.   Hwang, J., et al., *Dlx3 is a crucial regulator of hair follicle differentiation and cycling.* Development, 2008. **135**: p. 3149-3159.

58.   Cai, J., et al., *Genetic interplays between msx2 and foxn1 are required for notch1 expression and hair shaft differentiation.* Dev Biol, 2009. **326**: p. 420-430.

59.   Zhang, Y.V., et al., *Stem cell dynamics in mouse hair follicles: A story from cell division counting and single cell lineage tracing.* Cell Cycle, 2010. **9**: p. 1504-1510.

60.   Hanakawa, Y., et al., *Desmogleins 1 and 3 in the companion layer anchor mouse anagen hair to the follicle.* J. Invest. Dermatol., 2004. **123**: p. 817-822.

61.   Seldin, L., A. Muroyama, and T. Lechler, *Numa-microtubule interactions are critical for spindle orientation and the morphogenesis of diverse epidermal structures.* eLife, 2016. **5**: p. e12504.

Chapter III: Characterization of Keratin 79 Positive Cells in Hair Canal Formation

3.1 Summary

The epidermis acts as a barrier to protect our bodies from external damage and dehydration. The acquisition of barrier function occurs in conjunction with hair follicle morphogenesis, with the hair shaft extending out of an opening called the hair canal. The mechanisms underlying hair canal formation are poorly understood, although the process likely involves complex cellular rearrangements. Previous findings from our lab identified a novel population of hair follicle-derived cells marked by the expression of keratin 79 (K79). These cells appear early in follicle development, extend out into the surrounding epidermis, and disappear a few days after birth, suggesting that they may be involved in hair canal formation. Here, I characterize the behavior of K79+ cells during canal formation. K79+ cells in the epidermis initially express cellular junction and early differentiation markers, appearing similar to the neighboring epidermal cells. At later stages the adjacent epidermal cells reorient themselves, bending down around the distal K79+ cells which are lost to cell death at the same time as initial canal formation. The timing of these events strongly suggests that K79+ cells are involved in hair canal formation. The early entry of K79+ cells into the epidermis sets the stage for canal formation and circumvents the complications associated with breaching a complete epidermal barrier.

3.2 Introduction

The epidermis acts as an important protective barrier to shield our bodies from external damage, while also regulating water loss (reviewed in [2]). The epidermis can

perform this feat due to its specialized architecture consisting of 4 distinct cellular layers connected by an extensive adhesive network made up primarily of desmosomal and tight junctions **(Figure 3.1A)** (reviewed in [222, 327, 328]). As epidermal cells move towards the skin surface, they undergo a unique form of terminal differentiation termed cornification. Terminally differentiated cells in the outer layer (stratum corneum) are called corneocytes and together with an extensive lipid network form the epidermal barrier **(Figure 3.1A)** (reviewed in [232, 233]). Hair follicles are interspersed throughout the epidermis and contain hairs which emerge through an opening or canal **(Figure 3.1B & 3.1C)**. The hair canal serves as the interface between hair follicles and the epidermis and is frequently affected in human pathologies including acne, hair loss (alopecia areata, androgenetic alopecia), hidradenitis suppurativa, and the rare barrier disease harlequin ichthyosis [16-19, 251, 255] (reviewed in [20]). Despite the physiologic and pathogenic importance of the hair canal, the mechanisms underlying its formation during development are not well understood.

Hair follicle development occurs around the same time as the formation of the epidermal barrier. As the follicle matures and generates the differentiated cell types like the hair shaft, the overlying epidermis undergoes a differentiation process to confer barrier function. Notch signaling is a critical regulator of both follicular and epidermal terminal differentiation (reviewed in [178]) [173, 181, 204, 223]. Epidermal terminal differentiation requires a multitude of different proteins, each expressed in precise regions and tasked with specific functions **(Figure 3.1A)** (reviewed in [233, 328]). Desmosomes and adherens junctions provide mechanical strength by linking adjacent epidermal cells together, while tight junctions act as a seal to confer barrier function [229-231, 328,

329]. The generation of flattened, terminally differentiated corneocytes of the outer layer of the epidermis requires the coordinated expression of several differentiation markers **(Figure 3.1A)**. These include involucrin, loricrin, and filaggrin, which form an insoluble protein mass (cornified envelope) that replaces the plasma membrane in corneocytes, and acts as a scaffold for surrounding lipids. The epidermis completes this differentiation process by embryonic day (E) E18.5 to generate a multi-layered functional barrier [330]. At this time, hair follicles located directly below the epidermis are still developing, and most follicles lack a mature hair canal [58, 64].

Evidence from mouse models and human patients suggests that these processes may be linked. Mice deficient for the serine protease, matriptase 1 (MT-SP1) exhibit impaired barrier function and die shortly after birth [331]. These mice also display abnormal hair canals, with ingrown hair shafts, suggesting MT-SP1 has dual roles in barrier, and hair follicle development. Additonally, mutations in MT-SP1 underlie autosomal recessive ichthyosis with hypotrichosis (ARIH), a condition with both barrier and hair follicle abornomalities [332]. Harlequin Ichthyosis, the most severe form of ichthyosis, is characterized by a massive expansion of the outer layer of the epidermis [251, 255]. Interestingly, these patients sometimes exhibit hair canal abnormalities prior to the epidermal phenotype [255]. Further work is needed to understand whether hair canal abnormalities in these instances are a separate phenotype or simply an indirect result of disrupted epidermal barrier function. I explore the link between hair follicle development and harlequin ichthyosis disease pathogenesis in Chapter IV.

Descriptive studies from the early 1900's outlined 2 potential models for hair canal formation **(Figure 3.2A & 3.2B)**. Model 1 suggests that cells within the follicle

move out into the epidermis, displacing resident epidermal cells to generate a small

canal which keratinizes **(Figure 3.2A)** [66, 67]. These follicle-derived cells are attached

to the sebaceous gland, which is located near the top of the follicle and produces a

waxy substance (sebum) that lubricates the skin and hair. Sebaceous glands form late

in hair follicle morphogenesis; therefore, according to this model, the outward

movement of hair follicle-derived cells also must occur late in development. Model 1

originated from work in sheep and opossum, and subsequent studies using a mouse

explant *in vitro* culture system failed to find a link between sebaceous gland

development and hair canal formation [68]. In this system, the first signs of hair canal

formation occurred prior to the generation of differentiated sebocytes [68]. These

discrepancies may be due to differences between *in vitro* and animal model systems.

They may also reflect variances between species (mouse vs. sheep/opossum). Model 2

outlines the proposed mechanism for canal formation in mice and humans, which

begins with reorientation of epidermal cells above the follicle **(Figure 3.2B)** [69, 70]. In

mice, cells in the spinous layer turn 90 degrees during stage 3 of follicle development.

The subsequent events involved in generating the mature canal are not clear.

Both models fail to explain how the timing of the hair canal relates to epidermal

barrier formation. Model 1 suggests that the initiation of hair canal formation occurs very

late in development, at a time after the epidermal barrier has formed **(Figure 3.2A)**.

While Model 2 supports that this process begins slightly earlier, it does not outline the

details of canal formation **(Figure 3.2B)**.

A recent study by Veniaminova et al. identified a novel population of cells marked

by the expression of keratin 79 (K79) that may play a role in hair canal formation

(Figure 3.2C) [21]. This population of cells was initially identified as a marker of the inner hair canal in mature follicles **(Figure 3.2D)**. In development, K79+ cells are specified at E16.5 and are located within the center of the follicle **(Figure 3.2C)** [21]. Shortly after specification, a stream of K79+ cells extends into the epidermis [21]. K79+ cells within the epidermis are follicle-derived as evident from lineage tracing studies [21]. Importantly, the K79+ cells in the epidermis are lost around postnatal day (P) P3.5, a time when most hair canals appear in mice [21]. These findings raised the question of whether K79+ cells may be involved in hair canal formation.

In this chapter, I evaluated the role of K79+ cells in hair canal formation by characterizing their behavior throughout follicle development. Distinct stages of K79+ cell-streams appear during hair canal formation. These stages differ based on the distal cell shape, relationship to the surrounding epidermal cells, and co-localization with cellular junction and differentiation markers. Further, I find that K79+ cells in the epidermis are lost via cell-death concurrent with canal formation. I also provide preliminary evidence that the canonical Notch signaling cascade is not required for the specification of K79+ cells during development. Finally, I show that K79 expression is not required for canal formation or the maintenance of K79+ cells. Together these data provide new insights into the mechanisms governing hair canal formation and implicate K79+ cells, but not K79 expression in this process.

3.3 Experimental Procedures

3.31 Mice

Most experiments were performed on E16.5-P4.5 wild-type C57BL/6 mice. In addition, the following strains were used: *Shh^{tm1(EGFP/cre)Cjt}/J* (*Shh-EGFP-Cre*) [291], *Rbpj^{tm1Hon}* (Rbp-j^{flox})

[204], and *Keratin-5-Cre.* To generate *K79^{tm2a}* mice, embryonic stem cells from clone

EPD0179-4-A12 were purchased from KOMP and microinjected into blastocysts. Resulting

K79^{tm2a} mice were inter-crossed to generate *K79*-null mice. These mice still contain the

neomycin cassette from the original construct. All studies were performed in accordance with

regulations established by the University of Michigan Unit for Laboratory Animal Medicine.

3.32 Tissue Staining

Skin biopsies were fixed in 3.7% formalin overnight for paraffin embedding. For frozen

sections, samples were fixed in 3.7% paraformaldehyde at 4°C for 1 hour, rinsed in

PBS, sunk in 30% sucrose overnight and embedded into OCT. Antibodies are listed

below. Cell-death was assessed on frozen sections using the ApopTag Red In Situ

Apoptosis Detection Kit (Millipore, S7165).

3.33 Antibodies

Table 3.1: Antibodies used in Chapter III

Antibody	Species/Clonality	Clone #/Product #	Source	Dilution	Notes
Keratin 79	Goat	Y-17	Santa Cruz	1:500	Lot #J2412
Keratin 79	Rabbit	Ab7195	Abcam	1:500	This antibody, originally generated against mouse Gli2, is known to cross-react with K79 [33]
Keratin 14	Goat	C-14	Santa Cruz	1:1000	
Keratin 5	Guinea Pig	03-GP-CK5	American Research Products	1:1000	
Desmoglein 1/2	Mouse	03-61002	American Research Products	1:500	
Desmoplakin 1/2	Mouse	03-651109	American Research Products	1:500	
Zona Occluin 1	Rabbit	61-7300	Invitrogen	1:1000	
Notch 1 Intracellular Domain	Rabbit	4147	Cell Signaling	1:500	
E-Cadherin	Rabbit	24E10	Cell Signaling	1:500	
Loricrin	Rabbit	PRB-145P	Covance	1:500	
Filaggrin	Rabbit	PRB-417P	Covance	1:500	
Involucrin	Rabbit	PRB-140C	Covance	1:500	
RBPJ (RBPSUH)	Rabbit	5313	Cell Signaling	1:300	

3.34 Quantitation

For quantitation of both K79 stream stage **(Figure 3.3C)** and K79/TUNEL **(Figure 3.6B)**, 3-4 non-consecutive sections were used per sample, and 4 fields were imaged per section. Follicles were counted if K79+ cells were clearly present at the follicle-epidermal interface. For K79 stream stage quantitation, over 100 follicles were scored for all timepoints besides E19.5 where 44 follicles were scored. Criteria for K79+ stream staging is in Table 1. For K79/TUNEL quantitation, a follicle was considered double positive if at least 1 K79+ cell at the follicle-epidermal interface was also TUNEL positive. Over 50 hair follicles were scored for P0.5 and P3.5 timepoints, while 15 follicles were scored at E16.5.

3.4 Results

3.41 Characterization of K79+ Cells Throughout Hair Canal Formation

The timing of K79 cell specification, as well as their extension into the epidermis, suggested that they may be involved in hair canal formation. To clarify the behavior of K79+ cells during this process, we stained wild-type skin samples from E19.5-P4.5, a timeframe when the hair canal is generated. Given that we were interested in understanding canal formation, we focused our analysis on the distal K79+ cells present in the epidermis. We noticed differences in the shape of distal K79+ cells, as well as their co-localization, or lack thereof, with the epithelial marker, E-cadherin (ECAD) throughout development **(Figure 3.3A)**. We defined 3 distinct stages (cuboidal, pointed, mature) of K79+ cell streams **(Figure 3.3B)**. Cuboidal K79+ streams strongly colocalized with ECAD in the epidermis. Follicles with cuboidal K79+ streams showed

no signs of a putative canal or changes in the orientation of the surrounding epidermal cells **(Figure 3.3A).** Pointed K79+ streams represent a transient state where the distal K79+ cells have lost association with ECAD **(Figure 3.3A).** At this stage, the surrounding epidermal cells bend down around the pointed distal K79+ cells, and a small gap in the epidermis is present **(Figure 3.3A)**. Finally, the mature stage defines follicles where the K79+ cells are no longer in the epidermis and instead localize to the inner layer of the hair canal. These samples contain a clear opening or hair canal **(Figure 3.3A)**.

To understand the sequential relationship between these stages we performed quantitation of K79+ stream type across development **(Figure 3.3C)**. At E19.5 most follicles contained cuboidal K79+ streams, reflecting their early stage of development. By P0.5, there was a shift, and the pointed stage was most prominent, although greater than 30% were still cuboidal. K79+ cells were confined to the inner layers of the mature hair canal in approximately 15% of cases at P4.5. This distribution implies that during development K79+ streams transition from cuboidal to pointed and finally to a mature stage. During this K79+ stream maturation process, the hair canal also forms.

3.42 Differences in the Expression of Cellular Junction Proteins in Cuboidal and Pointed K79+ Streams

Our initial studies utilized ECAD as a marker for all epithelial cells. ECAD is also a component of adherens junctions (AJ), a type of cellular junction found in the follicle and epidermis. AJ and another type of cellular junction, desmosomes, provide strong

cell-adhesion via connections with actin bundles and keratin filaments, respectively

[328]. Tight junctions which are present in the granular layer of the epidermis act to seal

neighboring cells together and are required for the barrier function of the epidermis

[229-231].

To understand the relationship between hair follicle-derived K79+ cells and the

surrounding epidermal cells, we performed immunofluorescence for the desmosome

markers, desmoglein 1/2 (DG1/2), and desmoplakin 1/2 (DP1/2), and the tight junction

marker, zona occludin 1 (ZO1). We focused our analysis on the cuboidal and pointed

K79 streams as most of the changes occurred between these two stages. We found

that cuboidal K79+ cells in the epidermis strongly co-localized with DP1/2 and ZO1 but

showed a weaker association with DG 1/2 (**Figure 3.4A)**. In contrast, at the pointed

stage, distal K79+ cells displayed reduced expression of all 3 markers (**Figure 3.4B)**.

These findings suggest that early in follicle development K79+ cells express some

cellular junction markers, like the surrounding epidermis. As development proceeds,

K79+ cells located in the epidermis lose the expression of these markers as the initial

gap forms in the epidermal layers.

3.43 Distal K79+ Cells Do Not Express Late Epidermal Differentiation Markers

The formation of the epidermal barrier involves the coordinated expression of a

variety of proteins, including the differentiation markers involucrin (INVL), loricrin (LOR),

and filaggrin (FIL) [236]. These markers are expressed in the upper layers of the

epidermis and are important constituents of the cornified envelope, a mix of insoluble

proteins that replaces the plasma membrane in cells of the stratum corneum **(Figure**

3.1A). Our initial report noted that distal K79+ cells disappeared around P3.5 [21]. One explanation for this result is that K79+ cells in the epidermis undergo cornification, like the neighboring epidermal cells, resulting in their loss late in development. If they do undergo cornification, distal K79+ cells in the epidermis should express late differentiation markers. To evaluate this possibility, we performed immunofluorescence for K79 and differentiation markers and again focused on the cuboidal and pointed K79+ stages. Cuboidal K79+ streams show overlap with INVL, but not LOR and FIL (**Figure 3.5A)**. Remarkably, K79+ cells showed almost a mutual exclusion with LOR and FIL and rarely extended above these layers (**Figure 3.5A)**. INVL is expressed in the upper spinous layers, while LOR/FIL are not expressed until the granular layer (**Figure 3.1A)**. Thus, it is possible that cuboidal K79+ cells express INVL because it represents a slightly earlier differentiation marker than LOR and FIL. Similar to the cellular junction markers, all 3 differentiation markers were absent from the distal cells of pointed K79+ cell streams **(Figure 3.5B)**. These data suggest that the loss of K79+ cells is likely not due to the classical-cornification process.

3.44 Distal K79+ Cell Apoptosis Occurs at the Same Time as Putative Canal Generation

Our initial report showed the disappearance of the distal tip of K79 streams around the same time as initial canal formation [21]. To understand how the timing of K79+ cell loss related to canal formation we stained for the cell-death marker, TUNEL (terminal deoxynucleotidyl-transferase-mediated deoxyuridine triphosphate nick-end labeling). Cells containing fragmented DNA, a hallmark of cell-death, are TUNEL+. Cuboidal K79+ streams did not exhibit TUNEL positivity **(Figure 3.6A)**. However, both

106

pointed and mature K79 streams contained TUNEL+ cells in their distal-most region **(Figure 3.6A).** We quantitated the percentage of TUNEL/K79 double positive cells throughout development. At E16.5, no K79+ cells undergo cell-death. In contrast, at P0.5 at least 50% of K79+ streams contain at least 1 TUNEL+ cell **(Figure 3.6B).** By P3.5, over 70% of K79+ streams show TUNEL positivity **(Figure 3.6B)**. At both P0.5 and P3.5 most follicles contain the transient pointed K79+ stream stage **(Figure 3.3C).** These findings indicate that K79+ cells undergo cell-death late in development, around the same time as canal formation and prior to hair shaft emergence.

3.45 Canonical Notch Signaling is Not Required for The Specification of K79+ Cells

Next, we were interested in understanding potential regulators of K79 cell specification. The Notch pathway is active in differentiated cells in the center of the developing follicle, the same area that K79+ cells occupy during early development [181]. Given this and the importance of Notch signaling in driving differentiation (reviewed in [178]) [173, 181, 204, 223], we took a closer look at this pathway. First, we tested whether K79+ cells exhibited activated Notch signaling. To address this question, we performed immunofluorescence for cleaved Notch 1 intracellular domain (NICD), an indicator of upstream pathway activity. We found that early K79+ cells were often NICD positive **(Figure 3.7A)**. However, at a slightly later timepoint, the precise co-localization of K79 and NICD was less definitive, and NICD+ cells were often found adjacent to K79+ cells **(Figure 3.7A)**. As K79+ cells seem to have activated Notch signaling at early stages, we probed the importance of this pathway in their specification. We blocked Notch signaling by knocking out a critical mediator of the pathway, *Rbpj,* throughout the

epidermis (*Keratin-5-Cre;Rbpj^{fl/fl}*) **(Figure 3.7B)** and specifically within the hair follicle (*Shh-Cre; Rbpj^{fl/fl}*) **(Figure 3.7C)**. Our preliminary analysis indicates that K79+ cells are present in these mutants, suggesting that the classical Notch pathway is not required for their specification **(Figure 3.7B & 3.7C).**

3.46 K79-Knockout Mice Do Not Display Hair Canal Abnormalities

Finally, we tested the requirement for K79 during development and canal formation. We generated *K79^{tm2a/tm2a}* (*K79-KO*) mice, where both alleles of *K79* are disrupted by a gene-trap cassette **(Figure 3.8A).** We first confirmed the loss of K79 using 2 independent antibodies (**Figure 3.8B**). *K79-KO* mice are indistinguishable from littermates at birth and display no overt skin or hair follicle phenotype **(Figure 3.8C).** Further, early signs of canal formation, as evident by gaps in epidermal differentiation marker expression, were observed in K79-KOs **(Figure 3.9A & 3.9B)**. These findings indicate that K79 itself is not required for hair canal formation.

3.5 Discussion

Hair shafts emerge from openings or canals located at the top of hair follicles. The mechanisms governing hair canal generation are unclear, although the process likely requires complex cellular rearrangements of follicular and epidermal cells [66-70]. These rearrangements may involve cells moving out of the follicle into the epidermis, or epidermal cells reorienting themselves to prepare for canal formation [66-70]. Hair canal generation is not complete until late in follicular development after the epidermal barrier has formed. This observation raises an important question: how is the brick-like epidermal barrier breached to generate an opening to allow for hair shaft emergence?

We previously identified a population of cells marked by the expression of K79+ that may be involved in canal formation [21]. Here we characterize this new population of K79+ cells throughout development. We define distinct stages (cuboidal, pointed, mature) of K79+ cell streams, based on the morphology of the distal cells, as well as their relationship to the surrounding epidermal cells. Not surprisingly, at E19.5, over 85% of follicles contain cuboidal K79+ streams. By P0.5, the majority of K79+ streams were pointed, and initial signs of canal formation were evident. There was a mix of K79+ stream types in follicles at P0.5, with 65% being pointed, and 35% being cuboidal. This heterogeneity may reflect the different times of follicle specification. Hair follicle development begins at E14.5 with the specification of guard hairs [57, 58]. Subsequent waves at E16.5 and E18.5 specify the remaining hair types (awl, auchene, and zig-zag) [57, 58]. At P0.5, follicles from all three waves are present and are at various stages of development. It is also conceivable that K79+ streams differ slightly across the hair types, although we did not notice any evidence of this assertion.

Our data suggest that cuboidal K79+ streams found at early timepoints transition into pointed streams later in development. The morphology changes that occur between these stages are likely influenced by both intrinsic and extrinsic factors. Indeed, this transition involves cellular remodeling within K79+ cells to prepare for cell death, as well as reorientations in the adjacent epidermal cells to generate a putative canal. Both of these factors contribute to the morphology shift that occurs in distal K79+ cells.

We noticed that most changes with respect to canal generation occurred between the cuboidal and pointed stages. The surrounding epidermis of cuboidal K79+ streams showed no signs of canal formation; the cells were still parallel to the basement

membrane, and no discernable gap was present. These cuboidal K79+ streams most often co-localized with cellular junction markers, like DP1/2 (desmosomes) and ZO-1 (tight junctions). Interestingly, while they expressed the early differentiation marker, INVL, they did not express the late differentiation markers, LOR or FIL. INVL is expressed in the upper spinous layer, while LOR and FIL are restricted to the granular layers and above. Thus, cuboidal K79+ streams may adopt an early differentiation status by expression of markers like INVL, but not later differentiation markers like LOR and FIL. At the pointed K79+ stage, the surrounding epidermal cells bent down around the distal K79+ cells, and a clear gap was present in the epidermis. The distal K79+ cells in the epidermis did not co-localize with any of the cellular junction or differentiation markers we tested. In our first report, we noted that distal K79+ cells express the matrix metalloproteinase, MMP9 late in development [21]. *Mmp9*-knockout mice display delayed hair emergence with thinner hair canals, implicating this proteolytic enzyme in canal formation [333]. MMP9 may serve to degrade cellular junctions between epidermal and K79+ cells to prepare for the generation of the putative canal.

At later stages in development, distal K79+ cells often appeared frayed and disordered, suggesting they may be undergoing cell death. Distal K79+ cells were frequently TUNEL+, marking fragmented DNA at P0.5 and P3.5. TUNEL positivity is most commonly associated with apoptosis. However, distal K79+ cells were negative for the apoptosis marker, cleaved caspase 3 (data not shown), suggesting they may undergo an alternative method of cell-death. Non-apoptotic cell death has been implicated in other contexts, including palate formation and mammary gland involution following lactation (reviewed in [334]) [335, 336]. Cornification or terminal differentiation

epidermal cells is another form of non-apoptotic cell death that results in TUNEL positivity [337, 338]. Indeed, we often noticed evidence of epidermal cells that were TUNEL+ in the upper epidermal layers. During cornification, epidermal cells undergo extensive remodeling, losing their intracellular organelles and forming the cornified envelope in place of their plasma membrane [232-234]. This process also results in DNA degradation which may explain the presence of TUNEL+ epidermal cells [232]. While we cannot rule out cornification as the cause of K79+ cell death, our data indicate that it is unlikely. K79+ cells do not express late differentiation markers like LOR and FIL, which are important contributors to the process of terminal differentiation. Although the precise mechanism is unclear, distal K79+ cells are lost via cell death concurrently with the formation of a gap in the epidermal layers.

We were also interested in understanding the signaling pathways that regulate K79+ cells. Given the importance of Notch signaling in differentiation we tested whether this pathway was required for K79+ cell specification. Knockout of the Notch effector, *Rbpj* throughout the epidermis and hair follicles (*Keratin-5-Cre)*, or specifically within hair follicles (*Shh-Cre)* did not block K79+ cell specification, suggesting Notch is not required for K79+ cell specification. Similar findings in the adult setting support this notion. Blocking Notch in the *Lrig1+* stem cells that replenish the K79+ cells of the hair canal did not alter K79+ expression [21]. No canal defects were noted in either *Keratin-5-Cre* or *Shh-Cre* mice, although the analysis was performed at P0.5, and therefore defects may arise later in development.

Finally, we found that K79 itself is not required for hair canal formation. Whole-body *K79*-knockout (*K79^{tm2a/tm2a}*) mice did not display defects in canal formation. This

111

result may be due to functional redundancy with related keratin family members. In mice, the keratin family includes over 50 members [339]. Type I and type II keratins bind together in pairs. K79 is a type II keratin; therefore in a *K79*-deficient setting, another type II keratin may compensate for its loss.

Our findings suggest a model wherein, K79+ cells extend into the epidermis early in development, prior to the formation of the barrier. These initial K79+ cells act as a placeholder for the future hair canal. As this process proceeds, epidermal cells bend down around the K79+ cells. At later stages, the distal K79+ cells are lost to cell-death, and a clear gap in the epidermis is present. This gap matures into the hair canal where hairs exit during development and adult homeostasis **(Figure 3.10)**. Our data support aspects of earlier models proposed from descriptive studies in the early 1900s. Indeed, we describe both the outward extension of hair-follicle derived cells into the epidermis **(Model 1, Figure 3.2A)** and reorientation of epidermal cells above the follicle **(Model 2, Figure 3.2B).** One difference is the timing of the initiating events. For example, in model 1, the follicle-derived cells did not move into the epidermis until very late in development after the epidermal barrier is complete. Our model suggests this process initiates much earlier, overcoming the need for penetration of a complete barrier, making the generation of the canal much easier.

Future work should focus on the functional manipulation of K79+ cells to determine whether they are required for hair canal formation. This could be accomplished by genetically ablating K79+ cells in early development and looking at the resultant effects on canal formation. Another area of focus should be identifying which signaling pathways (e.g., WNT, SHH, BMP) are required for K79+ cell specification.
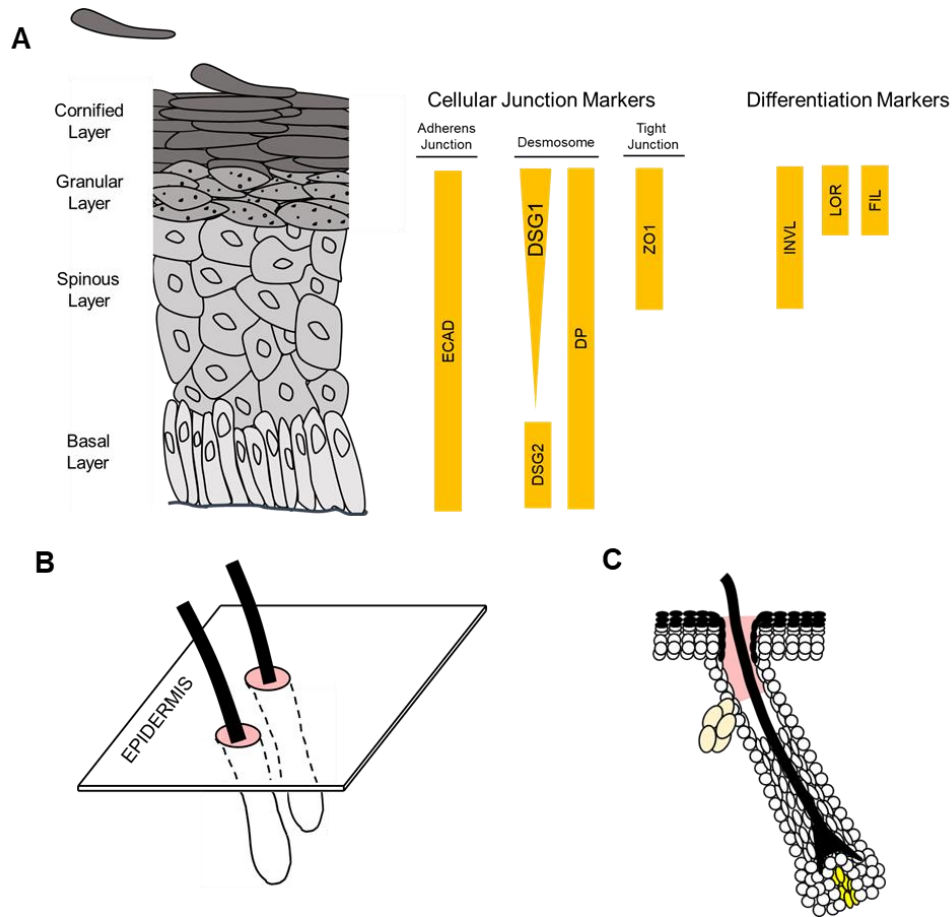
3.6 Acknowledgements

3.7 Figures

Figure 3.1. Schematic Depiction of the Epidermal Barrier and Hair Follicles. A. Architecture of the Epidermal Barrier. The epidermis contains 4 distinct cellular layers which go through a specialized differentiation process to generate a complete barrier. Cells within the epidermis are linked by cellular junctions, including adherens junctions, desmosomes, and tight junctions. Proliferative basal cells are connected to the basement membrane via specialized desmosomes (hemidesmosomes). The suprabasal layers are linked together tightly by adherens junctions and desmosomes. Tight junctions are critical for conferring barrier function and are located in the granular layer. Specialized desmosomes (corneodesmosomes) link cells of the outer cornified layer together. Each layer of the epidermis represents a distinct differentiation state. Cells of the cornified layer are terminally differentiated and have replaced their plasma membrane with an insoluble protein mass (cornified envelope) that serves as a scaffold for lipid attachment. The formation of the cornified envelope involves the coordinated expression of several proteins including INVL, LOR, and FIL. The expression patterns of cellular junction and differentiation markers discussed in this chapter are highlighted in yellow boxes. Abbreviations: ECAD: E-cadherin, DSG1: Desmoglein 1, DSG2: Desmoglein 2, DP: Desmoplakin, ZO1: Zona Occludin 1, INVL: Involucrin, LOR: Loricrin, FIL, Filaggrin. Adapted from [2,3]. **B. Top-down View of the Epidermis.** The epidermis represents a brick-like barrier for our bodies. Interspersed throughout the epidermis are hair follicles. These hair follicles house the hair shaft which emerges out of the hair canal (red) and through the epidermis. **C. Side View of a Hair Follicle.** Hair follicles contain an opening or canal (red) at the junction with the epidermis. The specific mechanisms responsible for generating this hole are poorly understood. Light Yellow: sebaceous glands sit adjacent to the hair canal and produce substances that lubricate the canal and epidermis. Dark yellow: dermal papilla, a mesenchymal cell population critical for development and homeostasis of the hair follicle.
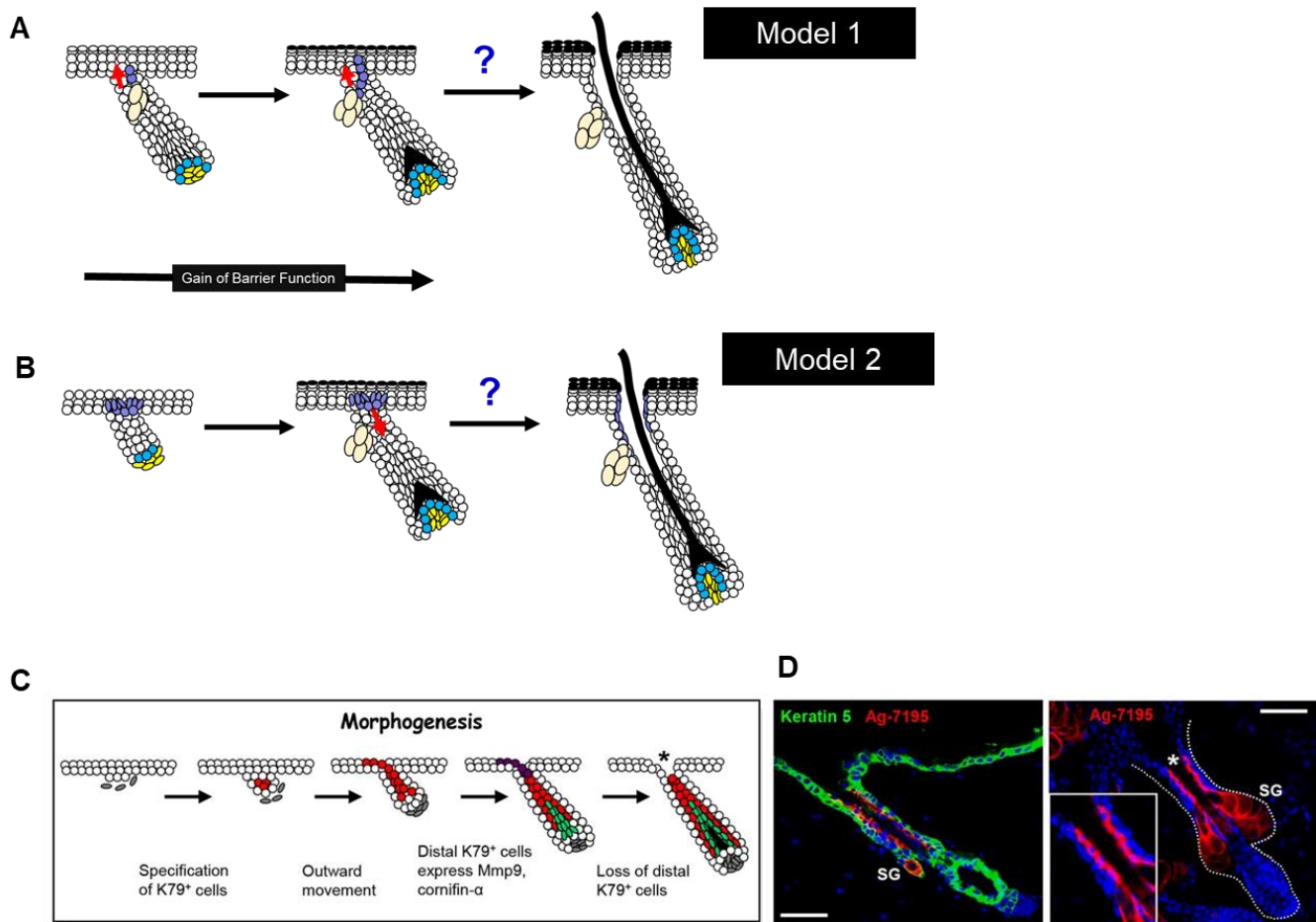
Figure 3.2. Models for Hair Canal Formation. A. Model 1. Cells (purple) attached to developing sebocytes (light yellow) move out of the hair follicle, keratinize, ultimately resulting in canal formation. **B. Model 2**. During stage 3 of follicle development spinous epidermal cells (purple) above the follicle reorient themselves to initiate canal specification. In contrast to the model in (A), this model is thought to proceed from the epidermis down into the follicle. Note that the epidermal barrier is forming concurrently with canal generation and that in both models the canal is formed after acquisition of barrier function. Blue cells represent hair follicle progenitor cells. Yellow cells represent the dermal papilla, a mesenchymal cell population required for development. **C. Schematic of Keratin 79+ cells During Hair Follicle Development** [33]**.** K79+ cells (red) originate in the developing hair follicle and extend into the epidermis. At later stages, these K79+ cells are lost, leaving behind a gap above the future site of the hair canal. Purple cells signify distal K79+ cells in the epidermis that express MMP9 and Cornifin-α and disappear around hair canal formation. The behavior of K79+ cells indicates they may be involved in hair canal formation, although this possibility needs to be evaluated further. Green cells represent differentiated inner root sheath cells. Grey cells represent the dermal papilla, a mesenchymal signaling hub required for development. **D. Keratin 79+ Cells Line the Hair Canal in Mature Follicles.** Immunofluorescence image from [33] showing K79+ cells (red) in the inner layer of the hair canal in an adult follicle. Ag-7195 detects K79. Abbreviations: K79: Keratin 79, MMP-9: Matrix Metalloproteinase 9, SG: Sebaceous Gland.

A

| | Cuboidal | Pointed | Mature |

Merge / E-cad K79 / E-cad rows

E19.5 | P3.5 | P4.5

B

Criteria	Cuboidal	Pointed	Mature
Shape of distal K79+ cells in epidermis	Cuboidal	Pointed	N/A
Reorientation of adjacent epidermal cells	No	Yes	Yes
Putative canal present	No	Yes	Yes

C
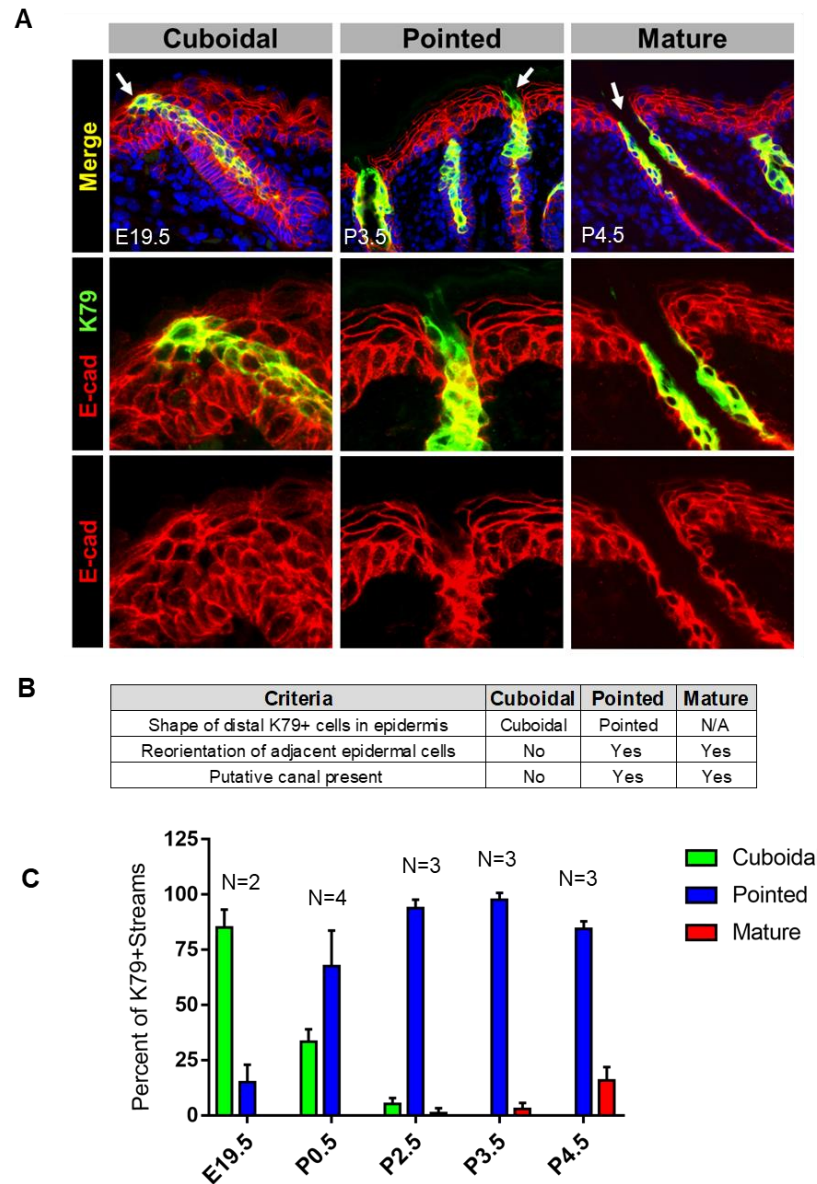
Figure 3.3. Characterization of K79+ Cells Throughout Development. A. Stages of K79+ Cell Streams. Immunofluorescence on E19.5-P4.5 wild-type dorsal skin samples for K79 (green) and the epithelial marker, ECAD (red). Arrows in top row indicate zoomed in area shown in lower panels. 3 distinct stages of K79+ streams were identified based on criteria described in **B.** No signs of canal formation are present in follicles with cuboidal K79+ streams. In contrast, follicles with pointed K79+ cells show changes in the surrounding epidermis and a gap in the epidermal layers. At the mature stage, the hair canal has fully formed and K79+ cells are no longer present within the epidermis. **B. Criteria for 3 Different K79+ Stream Stage. C. Quantitation of K79+ Stream Stage.** At early timepoints follicles contain mainly cuboidal K79+ streams. As development proceeds, most follicles have pointed K79+ streams. By P4.5, 15% of follicles have completed hair canal formation (mature). Quantitation details are described in the methods section. Abbreviations: ECAD: E-Cadherin, K79: Keratin 79.

116
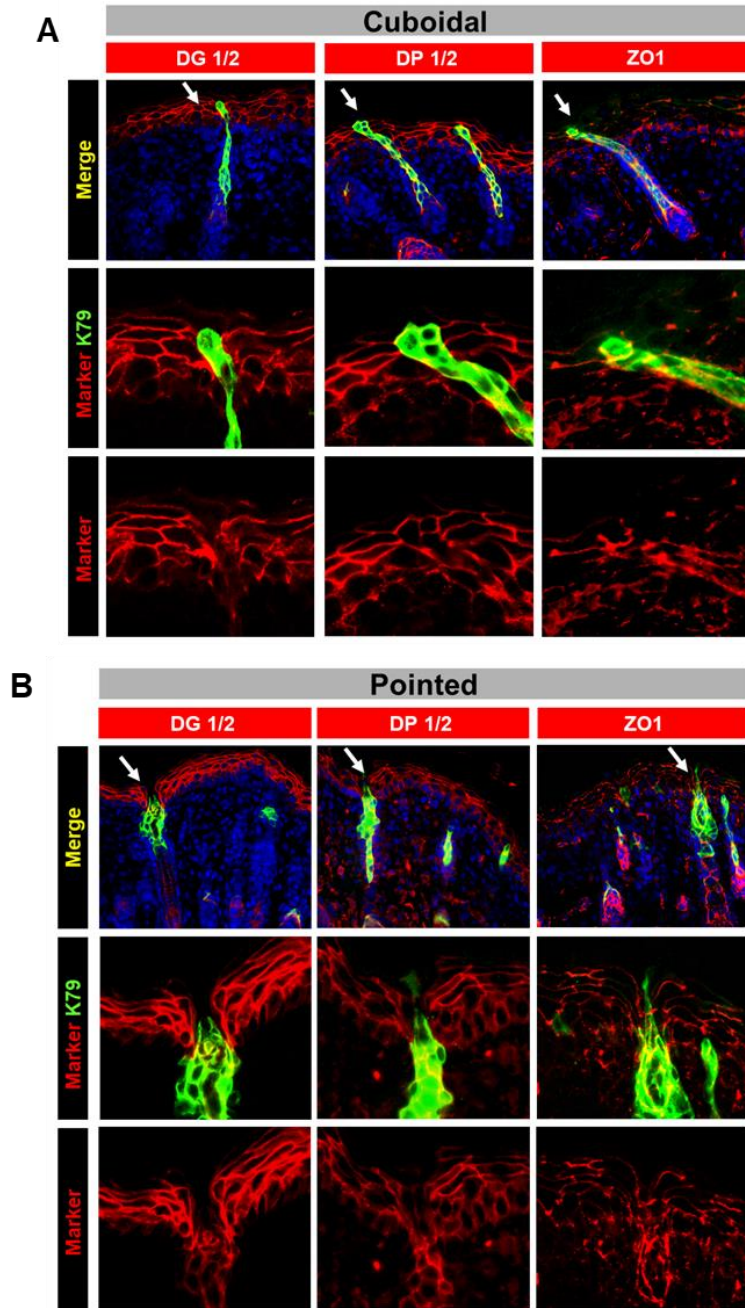
Figure 3.4. Distal K79+ Cells Express Cellular Junction Markers Early But Lose This Association at Later Stages.
Immunofluorescence on wild-type dorsal skin samples for K79 (green) and desmosome and tight junction markers (red). Arrows in top row indicates zoomed in area shown in lower panels. Cuboidal and pointed images were taken on E19.5-P0.5 and P3.5 samples, respectively. **A. Co-Localization of Cellular Junction Markers and Cuboidal K79+ streams. A.** Both DP1/2 (desmosomes) and ZO1 (tight junctions) are expressed in the distal cells of cuboidal K79+ cell streams. The desmosome maker DG1/2 is not expressed strongly by distal K79+ cells at this stage. **B. Characterization of Cellular Junction Markers and Pointed K79+ streams.** Distal cells of pointed K79+ streams lack the expression of all 3 cellular junction markers. Abbreviations: DG1/2: Desmoglein 1/2, DP1/2: Desmoplakin 1/2, ZO1: Zona Occludin 1, K79: Keratin 79.

117
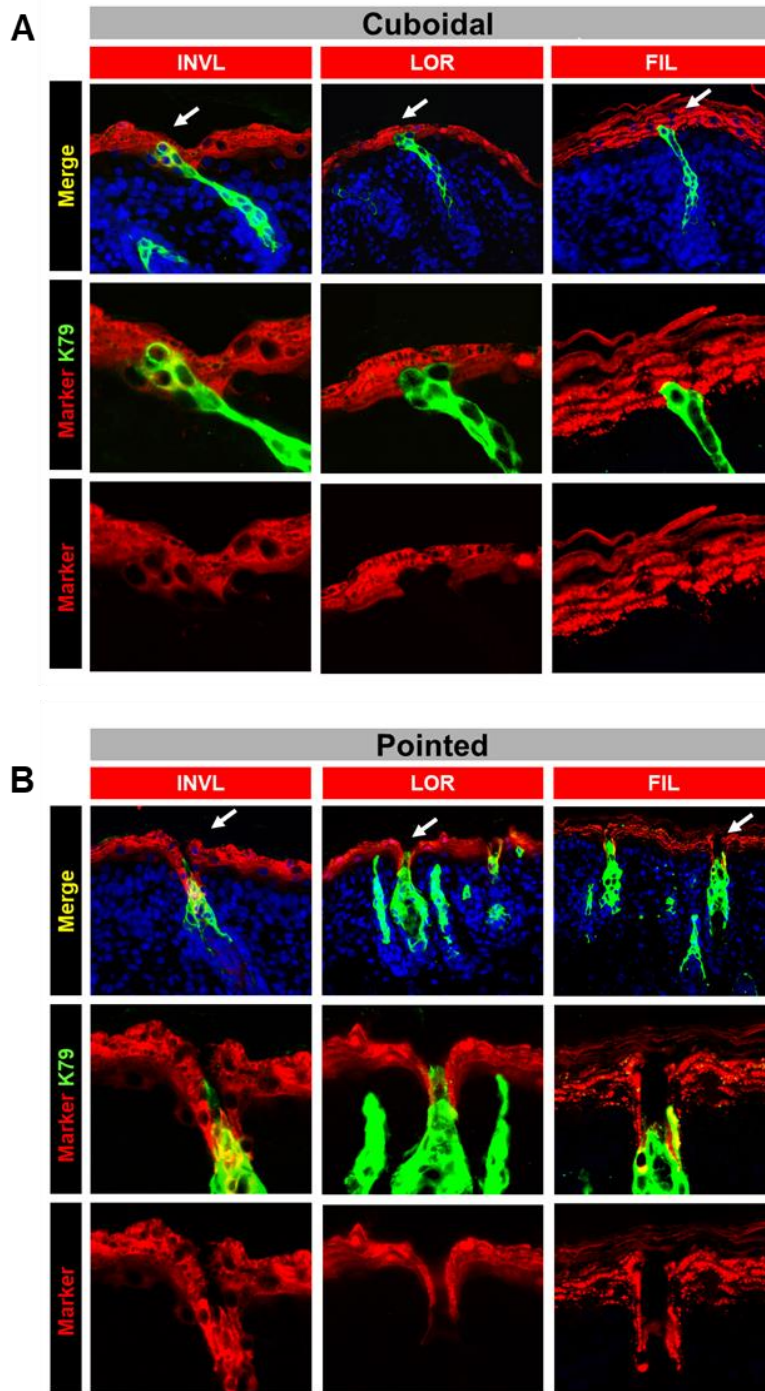
Figure 3.5. Distal K79+ Cells Express Early, but Not Late Differentiation Markers. Immunofluorescence on wild-type dorsal skin samples for K79 (green) and differentiation markers (red). Arrows in top row indicates zoomed in area shown in lower panels. Cuboidal and pointed images were taken on E19.5-P0.5 and P3.5 samples, respectively. **A. Characterization of Cuboidal K79+ Streams and Differentiation Markers.** Distal cells in cuboidal K79+ streams express INVL, but not LOR or FIL. **B. Characterization of Pointed K79+ Streams and Differentiation Markers.** Distal K79+ cells do not express any of these markers at this stage. Abbreviations: INVL: Involucrin, LOR: Loricrin, FIL: Filaggrin, K79: Keratin 79.

118
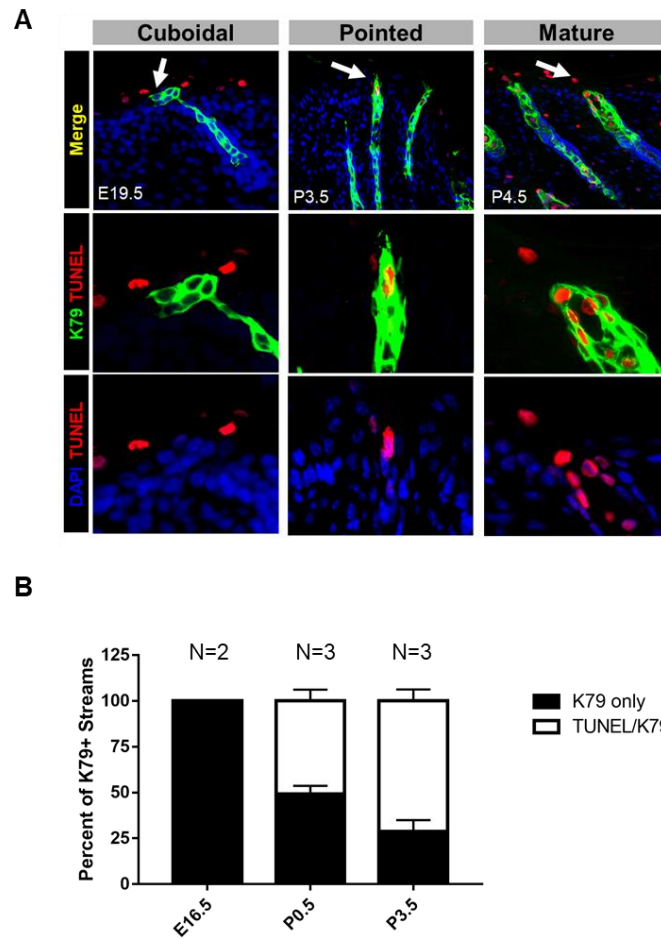
Figure 3.6. **Distal K79+ Cells Are Lost to Cell-Death During Hair Canal Formation. A. Immunofluorescence of wild-type dorsal skin stained for K79 (green) and the cell-death marker, TUNEL (red).** Note the presence of K79/TUNEL double positive cells in the distal tips of the later stages (e.g., pointed and mature). This co-localization is markedly absent in earlier streams (e.g., cuboidal). Arrow in the top panel refers to zoomed in region in lower panels. **B. Quantitation of K79+ Cell Death.** No cell death is observed at E16.5 when most K79+ streams are in the cuboidal stage. In contrast, at P0.5, 50% of K79+ streams contain at least 1 TUNEL+ cell. By P3.5 over 70% K79+ streams show signs of cell death. Quantitation details are described in the methods section. Abbreviations: TUNEL: terminal deoxynucleotidyl-transferase-mediated deoxyuridine triphosphate nick-end labeling, K79: Keratin 79.
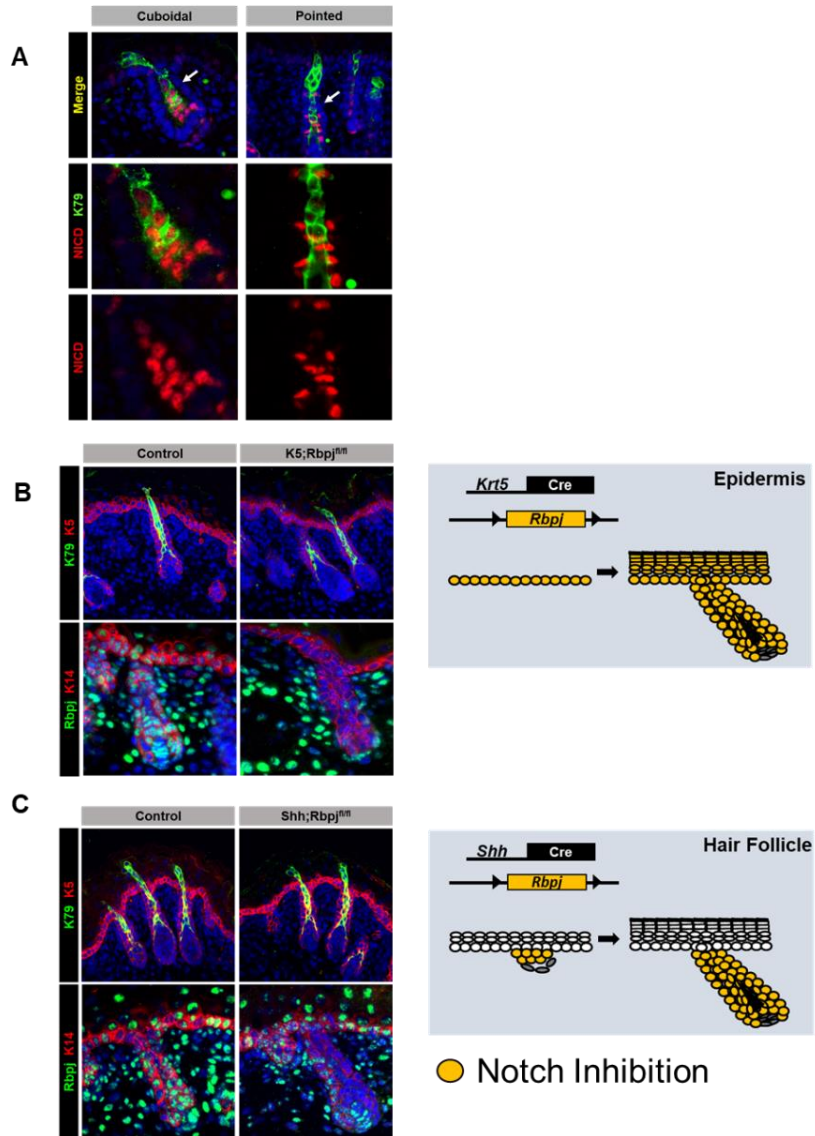
Figure 3.7. Notch Signaling is Not Required for K79+ Cell Specification. A. The Notch Pathway is Active in K79+ Cells. Immunofluorescence on wild-type dorsal skin for K79 (green) and the activated intracellular fragment of Notch1 receptor (NICD, red). Arrows in top row indicates zoomed in area shown in lower panels. At early stages K79+ cells are often NICD+. This association is strongest in the proximal K79+ cells. At later stages the co-localization between K79 and NICD is less clear. NICD+ cells are often located directly outside of the K79+ stream. **B & C. Blocking Notch Signaling Does Not Affect K79+ Cell Specification.** Top panels: *Rbpj*-knockout throughout the entire epidermis (*Krt5-Cre,* **B***),* or just within the hair follicle *(Shh-Cre,* **C**) does not block K79+ cell specification. Analysis was performed at P0.5 and stained for K5 (red) and K79 (green). Bottom: Confirmation of *Rbpj*-knockout. RBPJ is largely absent in the epidermis and hair follicles of *Krt5-Cre; Rbpj*^fl/fl^ skin and hair follicles of *Shh-Cre; Rbpj*^fl/fl^ skin. Schematics depicting cells with Notch inhibition in yellow. Abbreviations: NICD: Notch 1 Intracellular Domain, K79: Keratin 79, K5: Keratin 5, K14: Keratin 14.
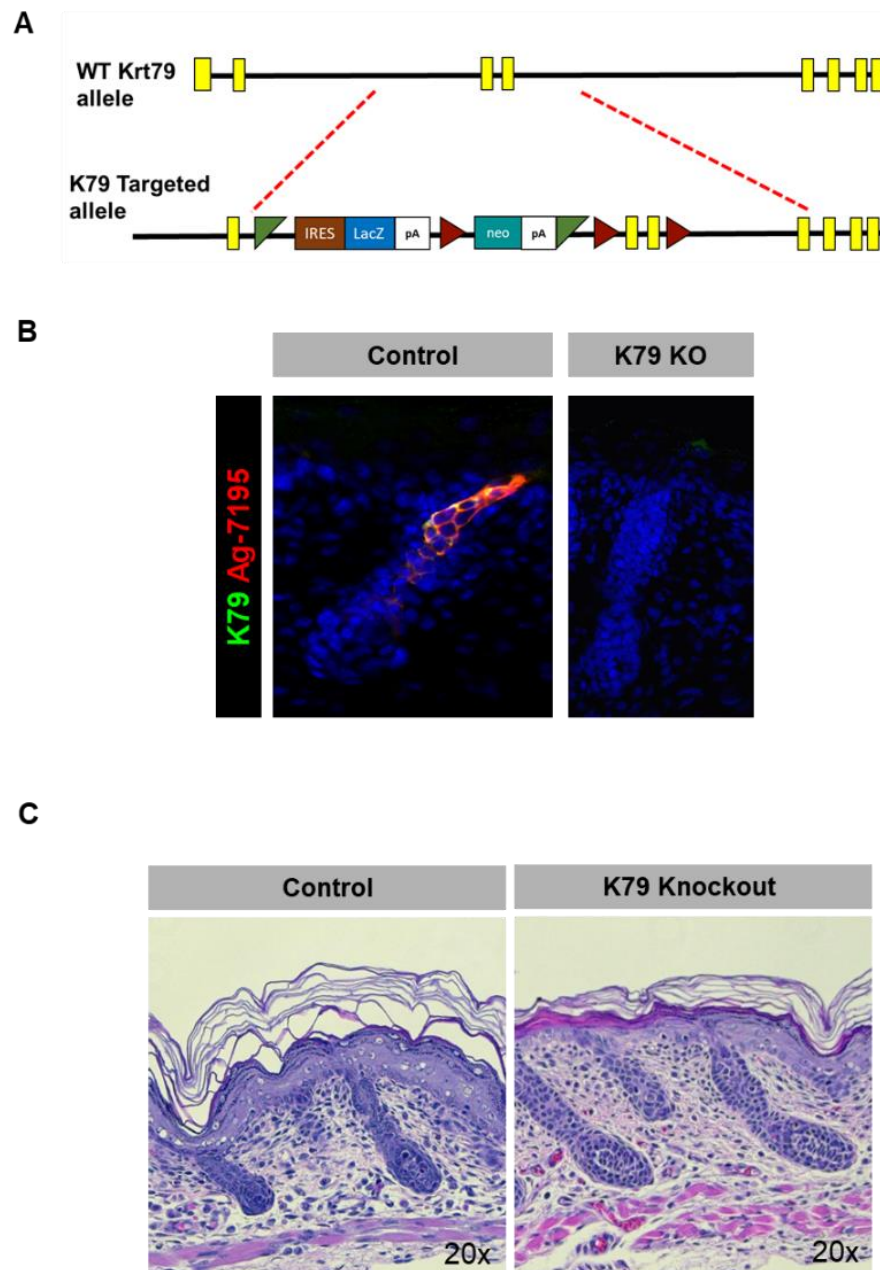
Figure 3.8. Loss of K79 Does Not Affect Hair Follicle Development. A. Schematic of the *K79^{tm2a}* Targeted Allele. K79 gene function is disrupted by the insertion of an IRES:*lacZ* trapping cassette and a floxed promoter-driven *neo* cassette. **B. Verification of K79 loss.** Immunofluorescence of P0.5 samples stained for 2 different K79 antibodies. *K79^{tm2a/tm2a}* sample clearly lacks staining for either antibody, confirming effective knockout. **C. Histology of P0.5 *K79^{tm2a/tm2a}* samples.** Analysis at P0.5 does not reveal any overt histological differences between *K79^{tm2a/tm2a}* and control samples.
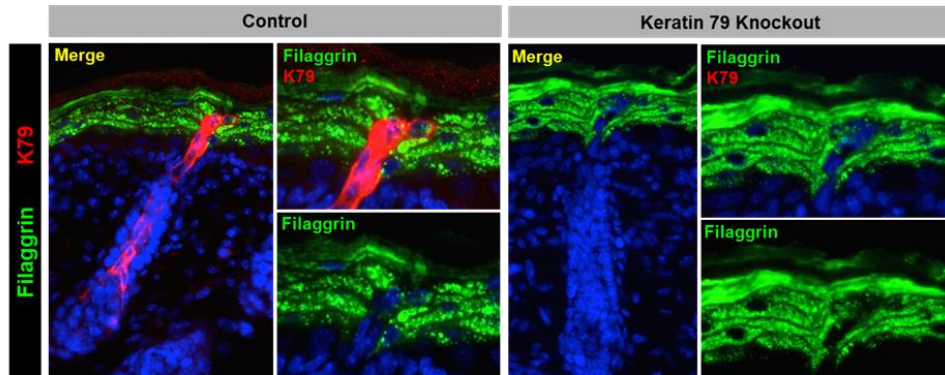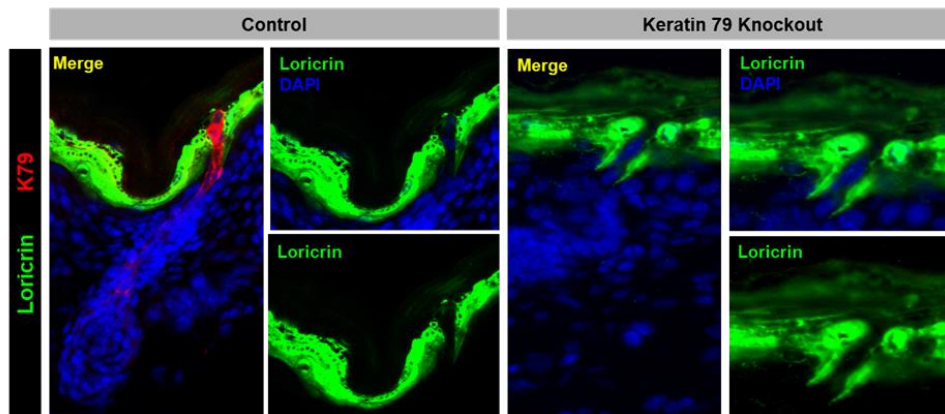
Figure 3.9. Loss of K79 Does Not Affect Early Canal Formation. A & B. Analysis of Differentiation Markers in *K79*$^{tm2a/tm2a}$ **samples.** Immunofluorescence of P0.5 samples stained for K79 (red) and the differentiation markers filaggrin **(A)** and loricrin **(B).** *K79*$^{tm2a/tm2a}$ knockout samples do not display differences in the pattern of these differentiation markers. Note that the gap (putative canal) in both markers is still present in *K79*$^{tm2a/tm2a}$ samples.

No gap in epidermal layers

Distal K79+ cells:
Cell Junction markers **+**
Early Differentiation marker **+**

Cuboidal

(incomplete barrier)

Putative canal present
(epidermal cells bend down)

Distal K79+ cells:
TUNEL **+**

Pointed

(complete barrier)

Hair canal formation complete

K79+ cells present on inner
hair canal (not in epidermis)

Mature
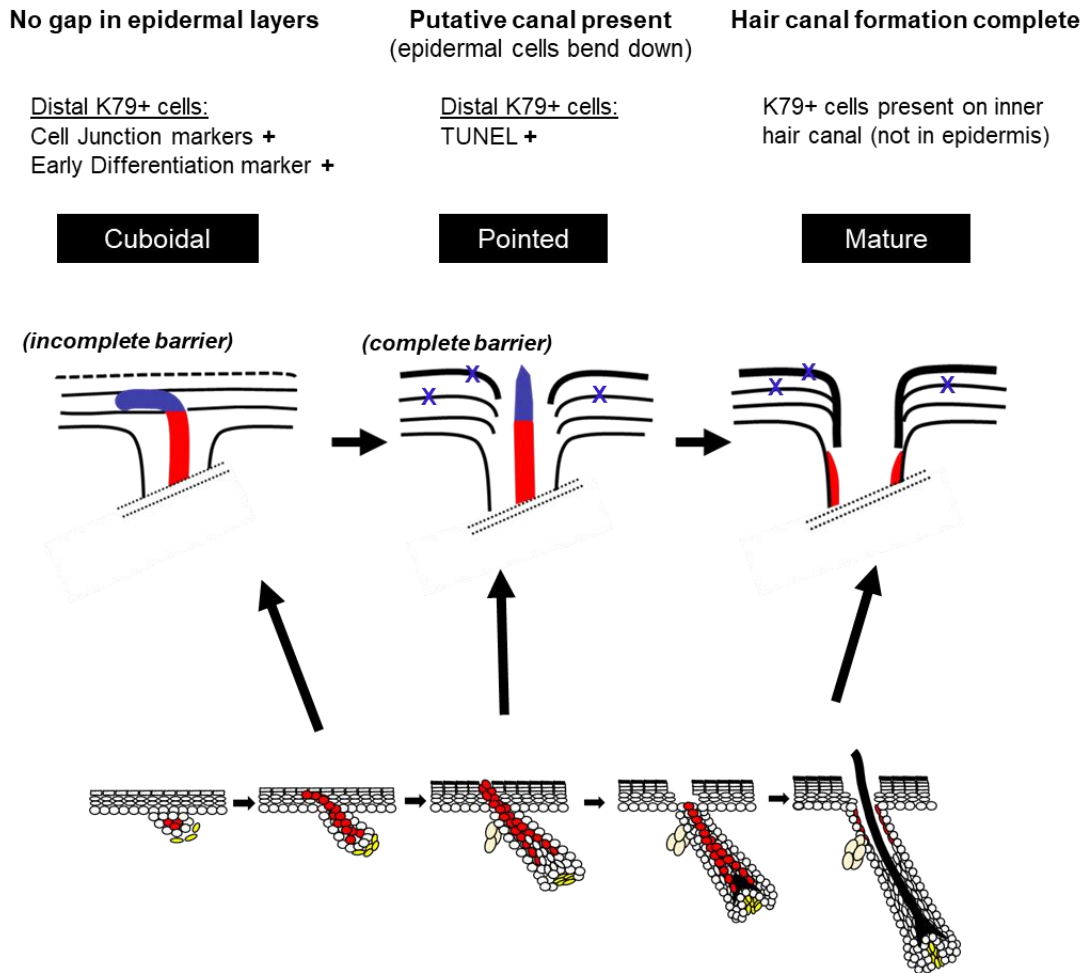
Figure 3.10. Schematic of K79+ Cell Behavior During Hair Canal Formation. Bottom: Diagram of K79+ cell behavior as described previously [33]. K79 cells are highlighted in red. **Top:** Close-view of the hair follicle-epidermal interface at 3 distinct stages of canal formation. K79+ streams are depicted in red, with the distal tip colored blue. Initially, K79+ cells appear cuboidal in shape and express similar markers (cell junction, early differentiation) as their neighboring epidermal cells. At this stage, the epidermal layers show no signs of disruption. Later in development, distal K79+ cells appear more pointed and are often TUNEL+ indicating they are undergoing cell-death. The surrounding epidermal cells undergoing cornification are also TUNEL + (blue X). A clear gap in the epidermis is present and the epidermal cells bend down around the distal K79+ cells (blue). This gap likely represents the putative canal. Shortly after birth hair canal formation is complete. At this point, K79+ cells are absent from the epidermis, and instead localize to the inner hair canal. Key: Light Yellow cells represent sebaceous glands which produce substances that lubricate the canal and epidermis. Dark Yellow cells in bottom schematic represent the dermal papilla, a mesenchymal cell population.

123

3.8 Reference List

1.   Adolphe, C. and B. Wainwright, *pathways to improving skin regeneration.* Expert Reviews in Molecular Medicine, 2005. **7**(20): p. 1-14.
2.   Kirschner, N. and J.M. Brandner, *Barriers and more: functions of tight junction proteins in the skin.* Ann N Y Acad Sci, 2012. **1257**: p. 158-66.
3.   Brandner, J., M. Haftek, and C. Niessen, *Adherens Junctions, Desmosomes and Tight Junctions in Epidermal Barrier Function.* Vol. 4. 2010. 14-20.
4.   Simpson, C.L., D.M. Patel, and K.J. Green, *Deconstructing the skin: cytoarchitectural determinants of epidermal morphogenesis.* Nat Rev Mol Cell Biol, 2011. **12**(9): p. 565-80.
5.   Eckhart, L., et al., *Cell death by cornification.* Biochim Biophys Acta, 2013. **1833**(12): p. 3471-80.
6.   Candi, E., R.A. Knight, and G. Melino, *Cornification of the Skin: A Non-apoptotic Cell Death Mechanism.* 2009.
7.   Nirmal, B., et al., *Evaluation of Perifollicular Inflammation of Donor Area during Hair Transplantation in Androgenetic Alopecia and its Comparison with Controls.* International Journal of Trichology, 2013. **5**(2): p. 73-76.
8.   Zhang, B., et al., *Early stage alopecia areata is associated with inflammation in the upper dermis and damage to the hair follicle infundibulum.* Australasian Journal of Dermatology, 2013. **54**(3): p. 184-191.
9.   Bellew, S., D. Thiboutot, and J.Q. Del Rosso, *Pathogenesis of Acne Vulgaris: What's New, What's Interesting and What May Be Clinically Relevant.* Journal of Drugs in Dermatology, 2011. **10**(6): p. 582-585.
10.   van der Zee, H.H., et al., *Hidradenitis suppurativa: viewpoint on clinical phenotyping, pathogenesis and novel treatments.* Exp Dermatol, 2012. **21**(10): p. 735-9.
11.   Richard, G. *Autosomal Recessive Congenital Ichthyosis* Gene Reviews [Internet] 2001 May 18, 2017; Available from: https://www.ncbi.nlm.nih.gov/books/NBK1420/.
12.   Akiyama, M., Dale, B. A., Smith, L. T. , Shimuzu, S., and Holbrook, K. A. , *Regional differene in expression of characterstic abnormality of Harlequin Ichthyosis in affected fetuses* Prenatal Diagnosis 1998. **18**: p. 425-436.
13.   Schneider, M.R. and R. Paus, *Deciphering the functions of the hair follicle infundibulum in skin physiology and disease.* Cell Tissue Res, 2014.
14.   Watt, F.M., S. Estrach, and C.A. Ambler, *Epidermal Notch signalling: differentiation, cancer and adhesion.* Curr Opin Cell Biol, 2008. **20**(2): p. 171-9.
15.   Blanpain, C., et al., *Canonical notch signaling functions as a commitment switch in the epidermal lineage.* Genes Dev, 2006. **20**(21): p. 3022-35.
16.   Moriyama, M., et al., *Multiple Roles of Notch Signaling in the Regulation of Epidermal Development.* Developmental Cell. **14**(4): p. 594-604.
17.   Pan, Y., et al., *gamma-secretase functions through Notch signaling to maintain skin appendages but is not required for their patterning or initial morphogenesis.* Dev Cell, 2004. **7**(5): p. 731-43.

18.   Yamamoto, N., et al., *Notch/RBP-J Signaling Regulates Epidermis/Hair Fate Determination of Hair Follicular Stem Cells.* Curr Biol, 2003. **13**: p. 333-338.

19.   Morita, K., et al., *Subcellular Distribution of Tight Junction-Associated Proteins (Occludin, ZO-1, ZO-2) in Rodent Skin.* Journal of Investigative Dermatology, 1998. **110**(6): p. 862-866.

20.   Schlüter, H., et al., *Sealing the live part of the skin: The integrated meshwork of desmosomes, tight junctions and curvilinear ridge structures in the cells of the uppermost granular layer of the human epidermis.* European Journal of Cell Biology, 2004. **83**(11): p. 655-665.

21.   Furuse, M., et al., *Claudin-based tight junctions are crucial for the mammalian epidermal barrier: a lesson from claudin-1-deficient mice.* J Cell Biol, 2002. **156**(6): p. 1099-111.

22.   Delva, E., D.K. Tucker, and A.P. Kowalczyk, *The Desmosome.* Cold Spring Harbor Perspectives in Biology, 2009. **1**(2): p. a002543.

23.   Hardman, M.J., D.N. Banbury, and C. Byrne, *Patterned acquisition of skin barrier function during development.* Development, 1998. **125**: p. 1541-1552.

24.   Paus, R., et al., *A Comprehensive Guide for the Recognition and Classification of Distinct Stages of Hair Follicle Morphogenesis.* J Invest Dermatol, 1999. **113**(4): p. 523-534.

25.   Duverger, O. and M.I. Morasso, *Epidermal patterning and induction of different hair types during mouse embryonic development.* Birth Defects Res C Embryo Today, 2009. **87**(3): p. 263-72.

26.   List, K., et al., *Matriptase/MT-SP1 is required for postnatal survival, epidermal barrier function, hair follicle development, and thymic homeostasis.* Oncogene, 2002. **21**: p. 3765.

27.   Basel-Vanagaite, L., et al., *Autosomal Recessive Ichthyosis with Hypotrichosis Caused by a Mutation in ST14, Encoding Type II Transmembrane Serine Protease Matriptase.* American Journal of Human Genetics, 2007. **80**(3): p. 467-477.

28.   Gibbs, H.F., *A Study of the development of the skin and hair of the Australian Opossum, Trichosurus vulpecula.* Proc. Zool. Soc. Lond., 1938. **108B**: p. 611-648.

29.   Wildman, A.B., *Coat and fibre development in some British Sheep.* Proc. Zool. Soc. Lond., 1932. **102**: p. 257-285.

30.   Hardy, M.H., *The development of mouse hair in vitro with some observations on pigmentation.* J. Anat., 1949. **83**(3): p. 364-384.

31.   Pinkus, H., *Embryology of Hair.* 1958, New York, NY: Academic Press.

32.   Maximow, A.A. and W. Bloom, *A Textbook of Histology*, ed. W.B. Saunders. 1934, Philadelphia, PA.

33.   Veniaminova, N.A., et al., *Keratin 79 identifies a novel population of migratory epithelial cells that initiates hair canal morphogenesis and regeneration.* Development, 2013. **140**(24): p. 4870-80.

34.   Harfe, B.D., et al., *Evidence for an expansion-based temporal Shh gradient in specifying vertebrate digit identities.* Cell, 2004. **118**: p. 517-528.

35.   Kypriotou, M., M. Huber, and D. Hohl, *The human epidermal differentiation complex: cornified envelope precursors, S100 proteins and the 'fused genes' family.* Exp Dermatol, 2012. **21**(9): p. 643-9.

36.   Sunberg, J.P., *Handbook of mouse mutations with skin and hair abnormalities: animal models and biomedical tools.* 1994, Boca Raton, FL: CRC Press.

37.   Sharov, A.A., et al., *Matrix metalloproteinase-9 is involved in the regulation of hair canal formation.* J Invest Dermatol, 2011. **131**(1): p. 257-60.

38.   Kutscher, L.M. and S. Shaham, *Non-apoptotic cell death in animal development.* Cell Death And Differentiation, 2017. **24**: p. 1326.

39.   Schweichel JU, M.H., *The morphology of various types of cell death in prenatal tissues* Teratology, 1973. **7**(3): p. 253-266.

40.   Kreuzaler, P.A., et al., *Stat3 controls lysosomal-mediated cell death in vivo.* Nature Cell Biology, 2011. **13**: p. 303.

41.   Gandarillas, A., et al., *Evidence that apoptosis and terminal differentiation of epidermal keratinocytes are distinct processes* Experimental Dermatology, 1999. **8**: p. 71-79.

42.   Vanden Berghe, T., et al., *Determination of apoptotic and necrotic cell death in vitro and in vivo.* Methods, 2013. **61**(2): p. 117-29.

43.   Candi, E., R. Schmidt, and G. Melino, *The cornified envelope: a model of cell death in the skin.* Nat Rev Mol Cell Biol, 2005. **6**(4): p. 328-40.

44.   Pan, X., R.P. Hobbs, and P.A. Coulombe, *The expanding significance of keratin intermediate filaments in normal and diseased epithelia.* Current Opinion in Cell Biology, 2013. **25**(1): p. 47-56.

Chapter IV: Generation of a Conditional *Abca12*-Deficient Mouse Model for Studying the Pathogenesis of the Human Barrier Disease Harlequin Ichthyosis

4.1 Summary

The development of mammalian skin involves a series of differentiation events to generate a multi-layered, "brick-like" epithelium that acts as a barrier to protect our bodies from external damage and dehydration. Barrier function is compromised in several human pathologies, including the severe congenital disease, harlequin ichthyosis (HI). HI patients are born with a thick plate-like outer skin layer due to mutations in the lipid transporter gene *ABCA12* and frequently die shortly after birth. Interestingly, case studies indicate that the HI phenotype appears in utero in the hair canal, prior to the epidermal phenotype. These observations raise the possibility of a potential link between a barrier disease and hair follicle formation. In support of this association, the acquisition of our barrier occurs in conjunction with hair follicle morphogenesis, with the hair shaft ultimately extending through the hair canal and skin surface. While other groups have generated *Abca12*-knockout mice (whole body), they have focused on barrier analysis at the skin surface, largely ignoring any involvement of the hair follicle. In addition, the perinatal lethality of these models has precluded further studies in adult mice. This limitation is significant as patient survival rates have increased to roughly 50% and a dramatic phenotypic improvement is seen in those that survive into adulthood. Here we evaluate the potential link between hair follicle development and HI. We find that *Abca12* is expressed in the forming hair canal as well

as differentiated layers of the follicle. To address the role of *Abca12* in specific cell populations, we have generated a conditional *Abca12*-knockout mouse model which will enable spatial and temporal deletion of *Abca12*. This genetic tool can be leveraged to understand the role of Abca12 in normal hair follicle development. It will also facilitate analysis of the involvement of the hair follicle in the pathogenesis of HI and barrier function.

4.2 Introduction

Harlequin ichthyosis (HI) is a severe congenital skin disease caused by mutations in the lipid transporter, <u>A</u>TP <u>b</u>inding <u>c</u>assette subfamily <u>A</u> member 12 (*ABCA12*) [259, 261]. This disease is characterized by the massive expansion of the outer epidermal layer resulting in the formation of armor-like plaques that cover the body [251]. The protective barrier function of the epidermis is compromised in HI patients, rendering them susceptible to infection and excessive dehydration as well as impairing thermoregulation [253-255] (reviewed in [251]). Case studies reveal dilated, clogged hair canals in some HI patients [255]. These abnormal hair canals are present in utero, prior to the epidermal phenotype [255]. Hair follicle development occurs at the same time as epidermal barrier formation, and the hair canal forms in concert with acquisition of barrier function **(Figure 4.1A)** [64, 340]. Given these observations, it is conceivable that ABCA12 may play a role in hair follicle development, or conversely, that hair follicles are involved in the development of HI, or serve a barrier function. Neither of these possibilities has been rigorously evaluated as the severity of the epidermal barrier defects have garnered most attention.

The outer layer (stratum corneum) of the epidermis confers barrier function. This layer is comprised of dead, flattened cells (corneocytes), immersed in an intercellular lipid matrix **(Figure 4.1B)**. Barrier formation initiates when proliferative cells in the basal layer exit the cell cycle and move up towards the skin surface. These cells undergo cornification, a form of terminal differentiation, which ultimately results in their death and the formation of the stratum corneum **(Figure 4.1A)**. Cornification involves the loss of intracellular organelles and the replacement of the plasma membrane with a cornified envelope, an insoluble protein mass that serves as a scaffold for lipid attachment (reviewed in [232, 233]). The granular layer, situated just underneath the stratum corneum, possesses abundant secretory organelles called lamellar granules. These granules are loaded with lipid precursors (e.g., glucosylceramides) and proteolytic enzymes by transporter proteins, including ABCA12 **(Figure 4.1C)** [259, 341]. In the stratum corneum lamellar granules secrete their cargo into the inter-corneocyte space **(Figure 4.1C)**. These lipids help restrict water loss, while also blocking absorption of toxins, pathogens, and allergens [342]. HI patients display reduced inter-corneocyte lipids, as well as abnormal or absent lamellar granules [259].

The thickness of the epidermis is normally maintained by a balance of cells differentiating up, and dead cells sloughed off at the skin surface. This process requires proteases like cathepsins and kallikreins, which are transported in lamellar granules along with the lipids. Once at the stratum corneum, they are activated and break the cellular junctions linking corneocytes together [244, 245]. The trafficking of these proteolytic enzymes is decreased in HI patients, contributing to the massive thickening of the stratum corneum [265].

Several groups have generated whole-body *Abca12*-knockout mouse models to study HI [250, 267-269, 271]. These mice all display a phenotype reminiscent of HI patients with rigid tight skin and a massive expansion of the stratum corneum [250, 267-269, 271]. Analysis using whole-body *Abca12*-knockout mice has focused at the skin surface with little attention paid to the hair follicle. Further, *Abca12*-knockout mice die shortly after birth, limiting their utility in adult studies. While HI was once considered invariably fatal, survival rates have increased to nearly 50% [254]. This improvement can be attributed to advancements in neonatal care which decrease chances of severe infection and respiratory distress, leading causes of early death in HI patients. The likelihood of surviving past infancy is also linked to *ABCA12* mutation type. Rajpopat et al. surveyed 50 HI cases and found that all patients who died at infancy harbored homozygous mutations, or the same mutation on both alleles of *ABCA12* [254]. Amongst the survivors, 48% carried homozygous mutations, and 52% compound heterozygous mutations (different mutations on each allele) [254]. Remarkably, surviving patients exhibit dramatic phenotypic improvements, resembling non-bullous congenital ichthyosis erythroderma, a less severe related disease [254, 256, 343, 344]. Uncovering the mechanisms resulting in the phenotypic rescue may provide valuable information about the pathogenesis of HI. Current *Abca12*-knockout mouse models are not well positioned to study the consequence of *Abca12* loss in a long-term setting.

Here we develop a genetic mouse model that facilitates the spatial and temporal targeting of *Abca12*. We confirmed the efficacy of this targeting strategy by generating mice which lack *Abca12* throughout the epidermis. These mice exhibit shiny skin and an expanded stratum corneum layer, although the phenotype is milder than our whole-body

Abca12-knockout model. We show that *Abca12* is expressed in the forming hair canal as well as the differentiating layers of hair follicles. Preliminary analysis of hair follicle-specific *Abca12*-knockout revealed no overt abnormalities although further characterization is needed. We also find that *Abca12* expression is induced upon wounding suggesting that it may play a role in wound healing and re-establishment of barrier function.

4.3 Experimental Procedures

4.31 Mice

To generate *Abca12^{tm1a}* mice, embryonic stem cells from clone HEPD0708-3-F11 were purchased from EUCOMM and microinjected into blastocysts. Resulting *Abca12$^{tm1a/+}$* mice were intercrossed to generate whole body *Abca12*-null mice (Abca12$^{tm1a/tm1a}$) See Figure 4.2. *Abca12$^{tm1a/+}$* mice were crossed to *R26:FLPo* mice to generate conditional ready *Abca12$^{tm1c/+}$* mice which harbor a floxed exon 4. Additional mouse strains used include *Shh$^{tm1(EGFP/cre)Cjt}$/J* (*Shh-EGFP-Cre*) [291], and *Keratin-5-Cre.* For wounding experiments, full thickness wounds (0.5cm x 0.5cm) were created on the dorsal skin of mice as described previously [345]. Biopsies spanning the wound site as well as matched contralateral intact skin were harvested 6 days after wounding. All studies were performed in accordance with regulations established by the University of Michigan Unit for Laboratory Animal Medicine.

4.32 PCR Screening of Whole Body Knockout (Abca12$^{tm1a/tm1a}$) and Conditional Knockout Mice (Abca12$^{tm1c/tm1c}$)

Genotypes were determined by PCR analysis of DNA derived from ear tissue. For tm1a and tm1c: WT1F (5'-GCTCTCTCTCTCTCTTCCTCTTC-3'), CSD-F (5'-CACACCTCCCCCTGAACCTGAAAC-3'), 3R (5'-

GCCTGCAATGCTTTATTCAAGTAAGTTC-3') primers were used together with an annealing temperature of 56ºC. Expected sizes: WT: 530bp, Tm1a: 450bp, Tm1c: 600bp. To detect the recombined allele (tm1d) after Cre-recombinase excision of exon 4, the following primers were used: WT-2F (5'- GGGCATCGGTCCCACTGTGTTCC-3'), 2R (5'-TCAGGACTTCACCTGCAAAA-3'), with an annealing temperature of 60ºC. Expected sizes: WT: 986bp, Tm1c: 1086bp, Tm1d: 325bp.

4.33 Tissue Staining

Skin biopsies were fixed in 3.7% formalin overnight for paraffin embedding. For frozen sections, samples were fixed in 3.7% paraformaldehyde at 4°C for 1 hour, rinsed in PBS, sunk in 30% sucrose overnight and embedded into OCT. Antibodies are listed below. For onslide β-Gal staining, skin biopsies were directly embedded into OCT. Frozen sections were fixed in 0.5% glutaraldehyde for 5 min, then stained with X-Gal (Roche, 10 651 745 001) for 24-48 hrs, before counterstaining with Nuclear Fast Red Solution (Sigma-Aldrich).

4.34 Skin Permeability Assay

This assay depends on the barrier-dependent access of X-gal to untreated skin. At low pH skin possesses abundant endogenous β-galactosidase activity, which cleaves X-gal to produce a blue precipitate [330]. Mice were sacrificed at P0.5, partially submerged in standard X-gal solution (adjusted to pH 4.5) and incubated at 37ºC for 24hrs.

Table 4.1: Antibodies used in Chapter IV

Antibody	Species/Clonality	Clone #/Product #	Source	Dilution	Notes
Abca12	Goat	NB100-93466	Novus Biologics	1:500	
Keratin 79	Rabbit	Ab7195	Abcam	1:500	This antibody, originally generated against mouse Gli2, is known to cross-react with K79 [35]
Keratin 14	Goat	C-14	Santa Cruz	1:1000	
Keratin 5	Guinea Pig	03-GP-CK5	American Research Products	1:1000	
Loricrin	Rabbit	PRB-145P	Covance	1:500	
Filaggrin	Rabbit	PRB-417P	Covance	1:500	

4.4 Results

4.41 Generation of a Novel Abca12 Whole-Body Knockout Mouse Model

To generate a conditional *Abca12*-knockout mouse model we utilized a multi-step targeting strategy. First, we generated *Abca12^{tm1a}* mice which possess a gene trap *lacZ* cassette as well as a promoter-driven *neomycin* cassette knocked into an intron of *Abca12* **(Figure 4.2A)**. Further downstream, exon 4 is flanked by loxP sites **(Figure 4.2A)**. *Abca12^{tm1a}* mice are not conditional-ready as the *lacZ* gene trap cassette upstream of the floxed exon disrupts gene function in all cells. *Abca12^{tm1a}* mice were crossed to *FLP* recombinase mouse to generate mice expressing a conditional-ready allele **(Figure 4.2A)**. Expression of *FLP* recombinase results in the removal of the *lacZ* and *neomycin* cassettes, leaving behind the floxed critical exon **(Figure 4.2A)**. *Abca12^{tm1c}* mice can be crossed to the Cre-recombinase mouse of choice to knockout *Abca12* function in the desired cell population **(Figure 4.2A).** We confirmed each allele by PCR genotyping **(Figure 4.2B)** and confirmed the loss of *lacZ* cassette in *Abca12^{tm1c}* mice **(Figure 4.2C).**

We began our analysis on *Abca12^{tm1a}* mice. Importantly, the *lacZ* cassette disrupts gene function, such that *Abca12$^{tm1a/tm1a}$* mice lack *Abca12* throughout the entire

body. *Abca12^{tm1a/tm1a}* mice are smaller than control littermates at birth and possess a thick, rigid layer of skin encasing their bodies **(Figure 4.3A)**. Histological analysis reveals an expansion of the outer layer of the skin (stratum corneum) **(Figure 4.3B)**. These expanded layers are also compacted, lacking the traditional basket-weave appearance of the stratum corneum seen in controls **(Figure 4.3B)**. The gross and histological phenotype in these mice is reminiscent of HI patients and previously described *Abca12*-knockout mouse models [250, 259, 267-269, 271]. To confirm the loss of ABCA12, we performed immunofluorescence staining on *Abca12^{tm1a/tm1a}* and control samples using an anti-ABCA12 antibody that recognized an epitope near the C-terminus of the protein. Control mice express ABCA12 in the granular layer as evident by co-staining with the granular marker, loricrin **(Figure 4.3C)**. In contrast, *Abca12^{tm1a/tm1a}* mice lack ABCA12 throughout the epidermis **(Figure 4.3C)**. The levels of loricrin staining were similar between the control and *Abca12^{tm1a/tm1a}* samples. We also confirmed that early differentiation within the hair follicle was not disrupted as keratin 79 was expressed in *Abca12^{tm1a/tm1a}* samples **(Figure 4.3D)**. Together these data are consistent with a whole-body *Abca12*-knockout mouse model.

4.42 Abca12 Expression in Developing Epidermis and Hair Follicles

In addition to disrupting gene function, the *lacZ* cassette encodes β-galactosidase (β-gal) and can be used as a readout of *Abca12* promoter activity in Abca12^{tm1a/+} mice **(Figure 4.2A)**. This capability is significant as the antibody is capable of detecting ABCA12 in the epidermis, but high background signal precludes its use for mapping ABCA12 expression within the hair follicle. At P0.5, β-gal activity is detected in

134

the upper epidermis, matching previous reports as well as our immunofluorescence analysis **(Figure 4.4A)** [268, 271]. Interestingly, the putative hair canal and differentiated cells lower in the follicle also display β-gal activity **(Figure 4.4A)**. *Abca12tm1a/tm1a* samples possess much higher β-gal activity than do *Abca12tm1a/+* samples **(Figure 4.4B)**. This result likely reflects the fact that *Abca12tm1a/tm1a* samples have the *lacZ* cassette knocked into both alleles of *Abca12,* while *Abca12tm1a/+* samples only possess 1 copy. Alternatively, it is possible that the *Abca12* gene is more active in the whole-body knockout. Together, these data highlight the known role of Abca12 in epidermal barrier function and reveal a previously unreported expression pattern within specific regions of the developing hair follicle.

4.43 Abca12 Expression in Adult Epidermis and Hair Follicle

We were also interested in evaluating *Abca12* expression in adult samples using our *Abca12tm1a/+* mice. Our analysis revealed β-gal activity in the epidermis of dorsal skin as well as the tail and ear **(Figures 4.5A & 4.6)**. We often observed β-gal activity in the hair canal of follicles in all 3 body sites **(Figures 4.5A & 4.6)**. Detailed analysis of β-gal activity in hair follicles in dorsal skin revealed *Abca12* promoter activity in the differentiated cell layers, matching our observations in development **(Figure 4.5B)**. Our initial analysis suggests these cells may represent the inner root sheath, a differentiated cell layer that surrounds the hair shaft and supports its movement up the follicle. Most of the lower hair follicle was negative, with the exception of cells near the differentiating hair shaft, potentially representing nascent inner root sheath cells **(Figure 4.5B)**. ABCA12's role as a lipid transporter led us to question whether it was expressed in the

lipid-secreting sebaceous glands, located just below the hair canal. While we often observe strong β-gal activity near the top of the sebaceous gland, we also occasionally observe a weak signal in control samples **(Figure 4.6B)**. Further analysis is needed to confirm whether *Abca12* is expressed in the sebaceous gland as well as to confirm the identity of ABCA12 positive cells in the hair follicle.

4.44 Abca12 Expression is Induced Upon Wounding

Given that ABCA12 is required for barrier function, we were curious whether it might be induced in situations when the skin was challenged. To address this possibility, we wounded *Abca12$^{tm1a/+}$* mice and followed β-gal activity, reflecting *Abca12* promoter expression. Prior to wounding, β-gal activity was detected in the upper epidermis at normal levels **(Figure 4.7A)**. β-gal activity was significantly higher in wound-adjacent skin 6 days following wounding **(Figure 4.7B)**. The strongest β-gal activity was observed in epidermis and hair follicles directly bordering the wounded skin **(Figure 4.7B)**. β-gal activity was also present in the region undergoing re-epithelization, a process similar to epidermal differentiation during development **(Figure 4.7B)**. These findings show that *Abca12* expression is induced upon wound healing and may point to a critical role for Abca12 during re-estabishment of the epidermal barrier.

4.45 Epithelial Abca12-Knockout Confirms Targeting Strategy

To generate a conditional *Abca12*-knockout mouse model we bred Abca12^{tm1a} mice to mice ubiquitously expressing a *FLP* recombinase. This cross resulted in the

removal of the *lacZ* and *neomycin* cassettes **(Figure 4.2A)** and generated *Abca12^{tm1c}* (*Abca12$^{c/c}$*) animals containing a floxed exon 4. To confirm the efficacy of this targeting strategy we crossed *Abca12$^{c/c}$* mice to mice expressing a constitutive *Keratin5-Cre* which recombines early in epidermal development, resulting in *Abca12*-deficiency throughout the epidermis and hair follicles **(Figure 4.8A)**. At P0.5, *Keratin5-Cre; Abca12$^{c/c}$* mice possess shiny skin covering their body **(Figure 4.8B)**. This phenotype is milder than whole-body *Abca12*-knockout (*Abca12$^{tm1a/tm1a}$*) **(Figure 4.2A)**, but clearly abnormal compared to the controls. To examine if these samples lacked a functioning barrier, we performed a dye exclusion assay. While the control effectively excluded the dye, the *Keratin5-Cre; Abca12$^{c/c}$* sample turned blue indicating the barrier was defective **(Figure 4.8C).** Histological analysis revealed the characteristic expansion of the stratum corneum **(Figure 4.8D).** To confirm the loss of ABCA12, we performed immunofluorescence analysis using an anti-ABCA12 antibody. We found that ABCA12 protein expression was mostly absent in *Keratin5-Cre; Abca12$^{c/c}$* mice, although patchy regions of ABCA12 expression were occasionally observed **(Figure 4.9A)**. The residual ABCA12 signal may reflect cells that did not undergo recombination and therefore still possess a wild-type protein. Both loricrin and filaggrin were expressed in the epithelial-specific knockout, suggesting that late epidermal differentiation was not severely impaired **(Figure 4.9B)**. However, the filaggrin expression pattern appeared more compacted than control samples **(Figure 4.9B)**. Together these data confirm the efficacy of our targeting strategy for *Abca12* loss.

Next, we were interested in determining the consequence of hair follicle-specific deletion of *Abca12*. This was motivated by the expression of *Abca12* in the hair follicle

(Figure 4.4A) as well as hair canal defects observed in some HI patients [255]. To achieve hair follicle-specific knockout, we crossed mice expressing a constitutive *Shh-Cre* with *Abca12$^{c/c}$* mice **(Figure 4.10A).** Preliminary analysis of *Shh-Cre; Abca12$^{c/c}$* mice revealed no overt gross or histological defects **(Figure 4.10B).** However, this analysis was performed at P0.5, a time before hair emergence in the dorsal skin. Future experiments should focus on analysis at later timepoints to determine if defects arise in mature follicles.

4.5 Discussion

Harlequin Ichthyosis is a severe skin condition caused by loss of function mutations in the lipid transporter *ABCA12*. Once considered invariably fatal, survival rates for HI have increased dramatically in recent years due to improved standard of care as well, as the introduction of retinoids (vitamin A derivatives) in some cases [253, 254, 256, 257]. Intriguingly, patients who survive infancy show a dramatic phenotypic improvement and can live into adulthood. Previous studies using whole-body *Abca12*-knockout mouse models have facilitated closer interrogation of many aspects of HI, including the characterization of differentiation, desquamation, and lamellar granule defects [250, 267-269, 271]. However, the perinatal lethality of these models restricts their utility to development. To circumvent the early lethality and probe potential mechanisms of compensation, Yanagi et al. grafted *Abca12*-knockout skin onto severe combined immunodeficient (SCID) mice and studied the morphological and biochemical alterations in the skin following grafting [271]. Like HI patients, *Abca12*-grafted skin showed phenotypic improvements and rescue of differentiation defects found prior to grafting, although the driving events behind the phenotypic rescue are still unclear. Hair

canal abnormalities are also noted in some patients, raising the question of whether the hair follicle is involved in HI [255]. Little is known about the appearance of hair follicles in whole-body *Abca12*-knockout mouse models as most research efforts have focused at the skin surface. Here we generate new genetic tools that can be leveraged to address the above questions and improve our understanding of ABCA12 function in both developmental and disease contexts.

We first generated a novel whole-body *Abca12*-knockout (*Abca12^tm1a^*) model that recapitulates classical features of HI patients and displays a similar phenotype to previously described *Abca12*-knockout models [250, 259, 267-269, 271]. *Abca12^tm1a/tm1a^* mutants are smaller than littermate controls and are encased in a thick armor-like skin with an expanded stratum corneum. Like other models, these mice die shortly after birth. It is notable that distinct targeting strategies were used to generate all 4 previously described mouse models as well as our *Abca12^tm1a/tm1a^* mice [250, 267-269, 271].

Over 60 distinct mutations across the *ABCA12* gene have been reported in HI patients [259, 260, 346]. Interestingly, *ABCA12* mutations are also linked to 2 less severe forms of ichthyosis, lamellar ichthyosis type 2 (LI) and non-bullous congenital ichthyosiform erythroderma (NBCIE) [347, 348]. These milder skin conditions are caused by missense mutations in *ABCA12,* and are found restricted to the ATP-binding domain of the protein [260, 349] . In contrast, HI is caused by truncation and deletion mutations that can occur all along the *ABCA12* gene and severely impair protein function [254, 261]. Thus, *ABCA12* may possess critical functions independent of its ATP-binding domain, explaining the severity of HI relative to LI and NBCIE. This

observation is particularly interesting given that HI patients that survive into adulthood display a NBCIE-like phenotype.

Previous work in human and mice links ABCA12 expression to the granular layer of the epidermis where it localizes to lamellar granules and transports lipids and lipid precursors into them [259, 268]. We confirmed this result, showing co-localization of ABCA12 and the granular layer marker, loricrin. To map out *Abca12* expression in more detail we utilized *Abca12tm1a/+* reporter mice, which contain β-galactosidase (β-gal) knocked into the endogenous *Abca12* locus. We analyzed β-gal activity in developing and adult epidermis of skin. We find that higher β-gal activity was detected in the developing skin, which may reflect a development-specific role for *Abca12,* or may be due to differences in the thickness of the epidermis. Indeed, the skin is much thicker during development versus in adult homeostasis. β-gal activity was also present in the upper epidermis of ear and tail skin, highlighting a potential universal role for ABCA12 in barrier function across distinct body sites.

While ABCA12 expression in the epidermis is well characterized, its expression in the hair follicle remains unclear. One report in studying human scalp follicles suggested that ABCA12 may be expressed at low levels throughout hair follicles [350]. Understanding ABCA12's expression pattern in the follicle is important as some HI patients exhibit hair canal abnormalities prior to expansion of the outer layer of the epidermis [255]. Using *Abca12tm1a/+* mice, we find β-gal activity in the hair canal and differentiated cell layers of developing and adult samples. The hair canal represents the junction between the epidermis and the follicle. This opening serves as a channel for the hair shaft as well as sebum, a waxy substance that lubricates and moisturizes the

skin surface. Some evidence suggests that the hair canal may possess a barrier function analogous to the overlying epidermis. First, the hair canal must prevent sebum, produced by sebaceous glands connected to the upper follicle, from leaking into the dermis, where it can lead to a detrimental inflammatory response [351]. Thus, the hair canal must be equipped to prevent the movement of sebum laterally into the dermis. Second, late epidermal differentiation markers are expressed in the hair canal of mature follicles [21]. These include loricrin and filaggrin, which are expressed in the granular layer of the epidermis, where ABCA12 is also found [21]. Given that hair shafts emerge through breaks in the strong brick-like epidermis and the above evidence, it is logical that the hair canal may possess barrier function.

We also noted the expression of *Abca12* within differentiated cells within the hair follicle in both development and regeneration. The location of these cells leads us to believe that they are inner root sheath cells, a terminally differentiated cell layer that sits directly outside the hair shaft. The inner root sheath supports the movement of the nascent hair shaft up the follicle before disintegrating near the sebaceous gland allowing the hair shaft to exit out of the canal. The role of ABCA12 in this cell population is unclear, although it may be involved in generating the lipid layer which coats the surface of the hair shaft [352]. The composition of this lipid layer is distinct from sebaceous gland and epidermal lipids [353], suggesting that it is derived from a distinct source like cells within the follicle. Ultrastructural analysis reveal the lipid layer is localized to the outmost layer of the hair shaft as well as the keratinized portion of the inner root sheath, a region abundant with lamellar granules [354]. Given the role of ABCA12 on lamellar granules in the epidermis, it is attractive to consider that ABCA12

may play a similar role within the follicle. Further work is needed to evaluate this possibility in more detail.

The role of ABCA12 in barrier function prompted us to consider whether it may also be involved in wound healing. Preliminary experiments reveal the induction of *Abca12* expression in wound-adjacent skin, including epidermis and hair follicles. The signal was highest in the skin directly adjacent to the wound. We also observed *Abca12* expression within the region of the wound undergoing re-epithelization. The process of re-epithelialization involves reversion to a developmental phenotype, wherein the different layers of the epidermis form to reestablish barrier function in the wound. These observations suggest that ABCA12 may play a role in wound healing. Studying wound healing in an adult *Abca12*-deficient context is critical to determine the precise requirement of ABCA12 in this process.

Finally, we generated a conditional *Abca12*-knockout (*Abca12$^{c/c}$*) mouse model that will allow for the interrogation of previously unstudied aspects of HI. To confirm the efficacy of our targeted allele, we crossed *Abca12$^{c/c}$* mice with *Keratin-5-Cre* mice to knockout *Abca12* throughout the epidermis and hair follicle. Given the extent of deletion, we predicted that *Keratin-5-Cre; Abca12$^{c/c}$* mice would exhibit a severe phenotype like that of the whole-body knockouts. These mice are shiny at birth and are clearly distinguishable from control littermates. However, this phenotype appears milder than the whole-body knockout (Abca12$^{tm1a/tm1a}$). The mild phenotype may reflect inefficient recombination. Indeed, we found patchy areas with residual wild-type ABCA12 protein expression in the epidermis. The initial mice were harvested at P0.5 to confirm the efficacy of our targeting strategy. As *Keratin5-Cre; Abca12$^{c/c}$* mice display a mild

phenotype they may survive and be useful for examining the long-term consequence of Abca12 loss to uncover compensatory mechanisms that occur in human HI patients.

Hair canal abnormalities seen in human patients prompted us to consider whether Abca12 played a role in hair follicle development. This question became particularly interesting to us after noting that Abca12 is expressed in the hair canal, the site first affected in some HI patients [255]. Preliminary analysis of P0.5 samples revealed no overt phenotype in *Shh-Cre; Abca12^{c/c}* mice, although we have not confirmed the degree of *Abca12* deletion in the follicle. It is also conceivable that defects may arise later in development around the time of hair emergence. To evaluate this possibility, we will graft P0.5 *Shh-Cre; Abca12^{c/c}* skin onto immunocompromised mice and analyze hair emergence. This system will circumvent any potential perinatal lethality that may preclude analysis of hair emergence which occurs later in development.

Here we have created a new genetic tool to facilitate spatial and temporal knockout of the lipid transporter *Abca12*. This tool will prove useful in follow up studies in the skin and hair follicle as we seek to determine whether a barrier gene Abca12 plays a role in hair follicle homeostasis. Conversely, it will also facilitate closer interrogation of new aspects of HI pathogenesis, including any involvement of the hair follicle. This tool can be used in other organs as well to understand the role *Abca12* in development and homeostasis. One organ of interest is the lung which serves as a barrier to the external environment, like the skin. One *Abca12*-knockout model reported alveolar collapse leading to perinatal lethality in their model, while a second group failed to confirm this finding [268, 269]. Experiments utilizing our conditional *Abca12*-knockout

may enable experiments which clarify the true role of Abca12 in the lung and other organs.
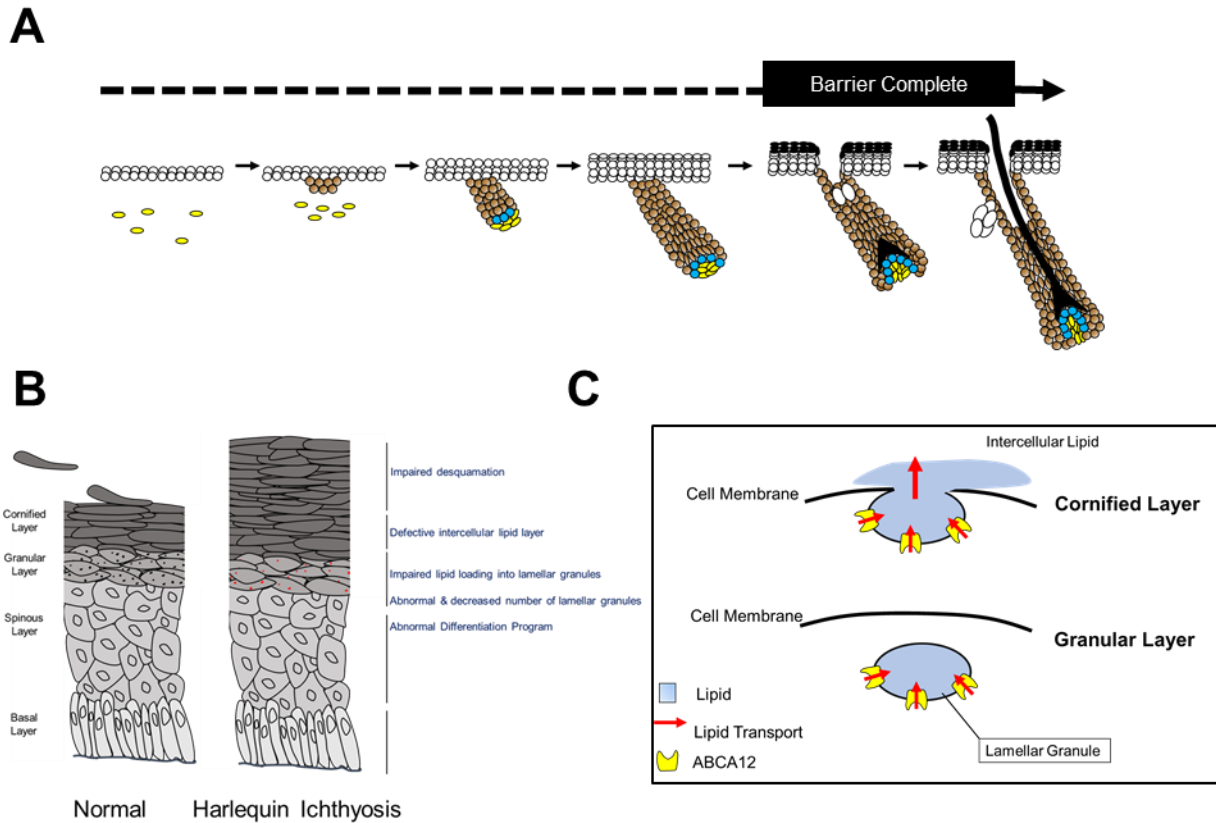
4.6 Acknowledgements

4.7 Figures

Figure 4.1. Graphical Depiction of Epidermal and Hair Follicle Development and Defects in Harlequin Ichthyosis Patients. Hair follicle development occurs at the same time as epidermal barrier formation. This process begins with induction as the follicle (brown) placode forms below the epidermis. As morphogenesis continues, the follicle grows down and progenitor cells (blue) wrap around the dermal papilla (yellow). Hair canal formation occurs around the same time as epidermal barrier completion. Shortly following birth, the hair shaft emerges from the canal. Dotted line indicates incomplete barrier, while solid line indicates complete barrier. **B. Left, Normal Epidermis.** Barrier formation occurs when proliferative cells in the basal layer detach from the basement membrane, move into the spinous layer and stop proliferating. Differentiation continues as the cells move towards the skin surface. The granular layer contains secretory organelles (lamellar granules) which are loaded with lipids and proteins by transporter proteins, including ABCA12. At the transition from the granular to cornified layer the content of the lamellar granules is extruded into the intercellular space. This intercellular lipid matrix combined with terminally differentiated cells form the epidermal barrier. The thickness of the epidermis is maintained by differentiating cells moving towards the skin surface, and dead cells sloughed off at the top. **Right, Harlequin Ichthyosis (HI)** patients exhibit expansion of cornified layer due to mutations in *ABCA12.* The cornified layer has decreased levels of lipids between the corneocytes, which combined with the massive expansion of this layer contributes to barrier dysfunction. Impaired desquamation also contributes to epidermal thickness. Lamellar granules (red) are abnormal or completely absent from the granular layer. Normal epidermis diagram adapted from [9,10]. **C. Function of the Lipid Transporter ABCA12.** ABCA12 (yellow) loads lipids into lamellar granules (secretory organelles) in the granular layer of the epidermis. These lipids are extruded into the intercellular space of the outer cornified layer and are critical for barrier function.
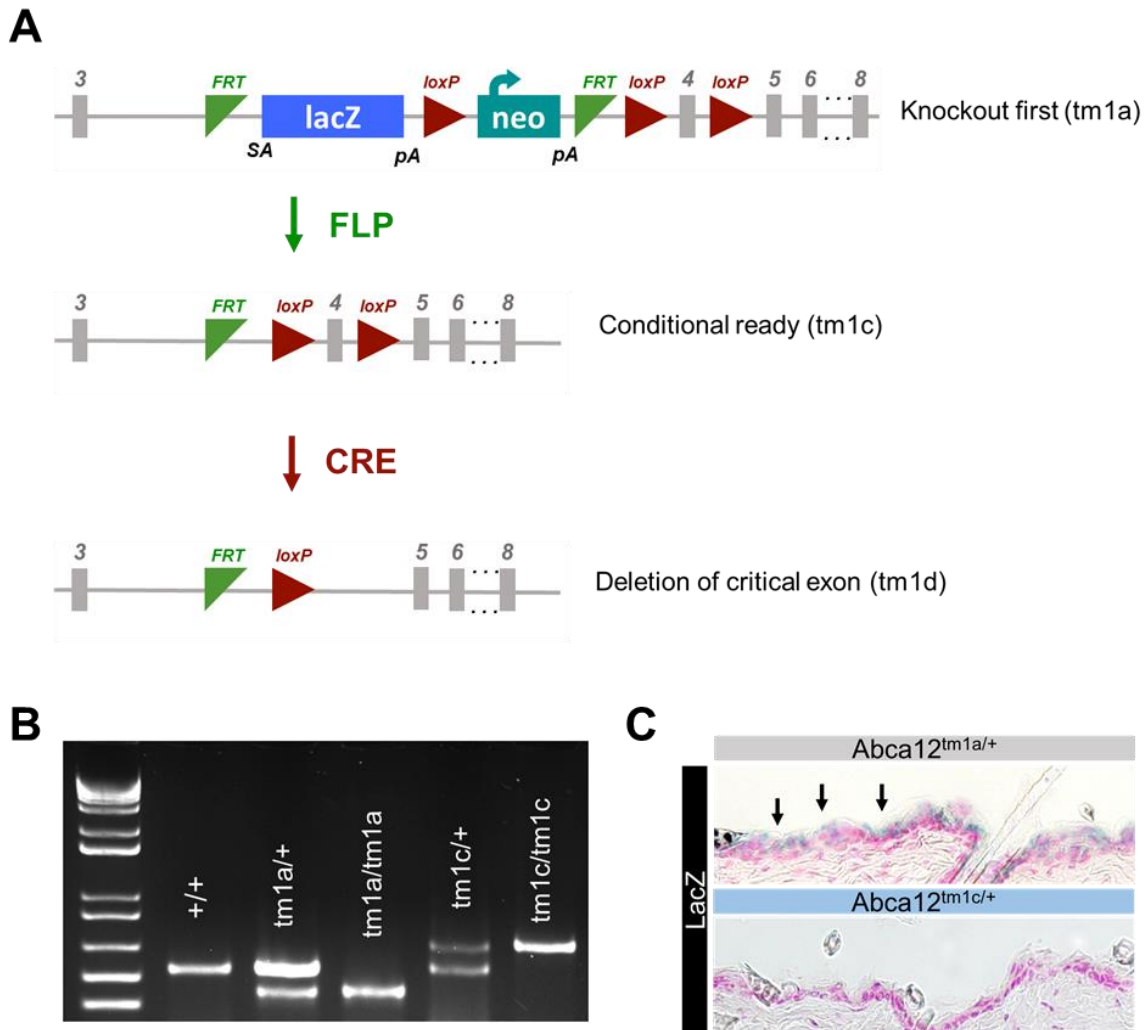
145

Figure 4.2. Generation of *Abca12^tm1a* and *Abca12^tm1c* Mice. A. Schematic of Targeted Alleles. The knockout-first tm1a allele contains a gene trap *lacZ* cassette and promoter-driven *neomycin* cassette upstream of a floxed exon 4. Crossing with a *FLP* recombinase mouse removes the *lacZ* and *neomycin* cassettes generating the functional conditional (tm1c) allele. Subsequent crossing to a *CRE* recombinase mouse facilitates deletion of exon 4. **B. Confirmation of Different Alleles by DNA Genotyping.** PCR reactions showing different band sizes of tm1a and tm1c mice. Ladder on left is 1Kb. Expected band sizes listed in experimental procedures. **C. Confirmation of *lacZ* Loss in *Abca12^tm1c/+* mice**. Crossing Tm1a mice with mice expressing a FLP recombinase should remove the *lacZ* cassette. β-galactosidase (β-gal) activity is detected in *Abca12^tm1a/+*, but not *Abca12^tm1c/+* mice. Arrows point to β-gal activity.
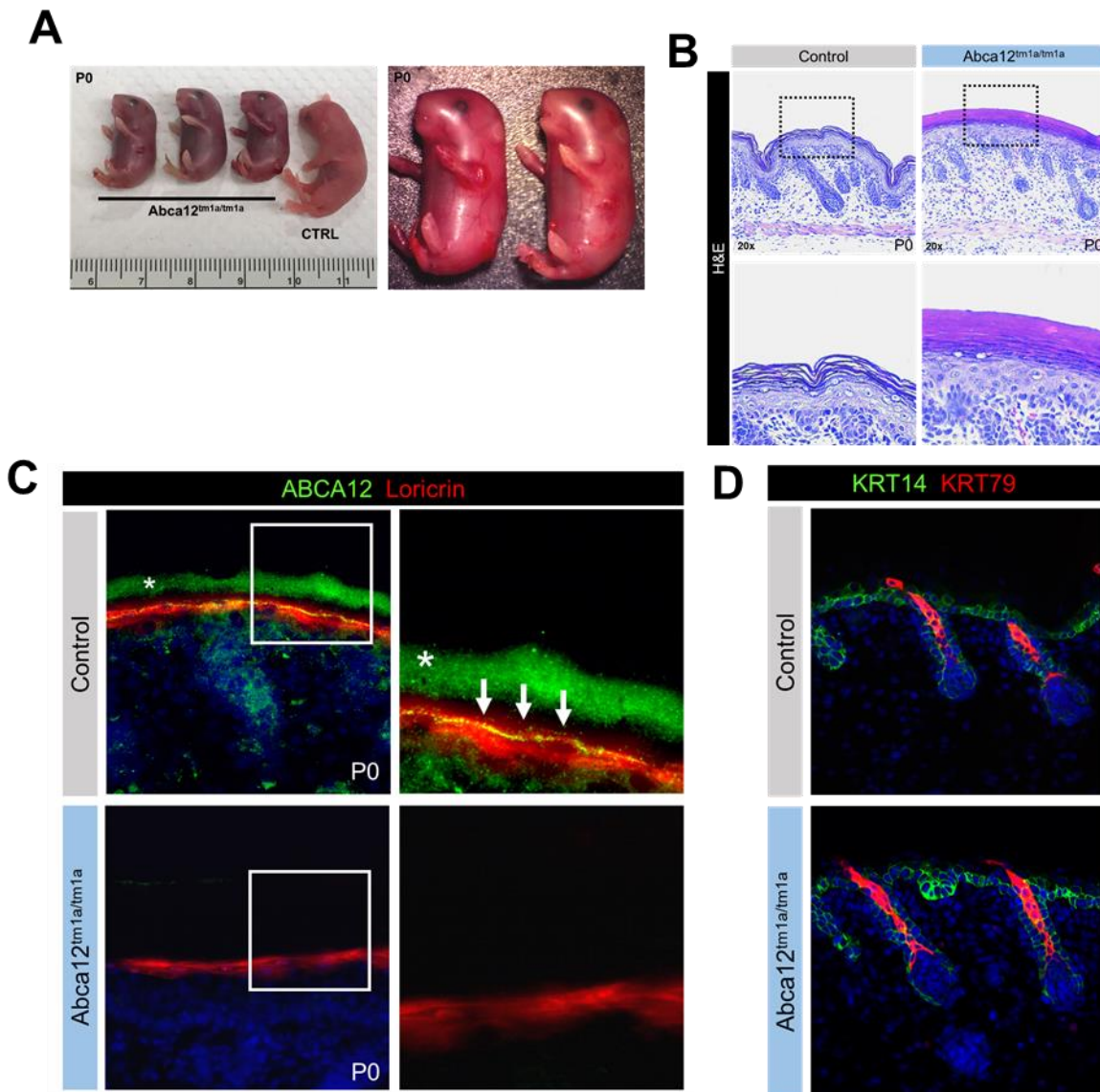
Figure 4.3. *Abca12^{tm1a/tm1a}* **Mice Recapitulate the Human HI Phenotype. A. Gross Analysis of *Abca12^{tm1a/tm1a}* Whole Body Knockouts**. Left, *Abca12*^{tm1a/tm1a} mice are born with smaller bodies than control littermates. Right, *Abca12*^{tm1a/tm1a} mice have rigid tight skin covering their bodies. **B. Histological Analysis of *Abca12^{tm1a/tm1a}* mice.** Control mice show normal basket-weave appearance of the outer stratum corneum (left). *Abca12*^{tm1a/tm1a} samples show a thick, compact stratum corneum. Boxed region is shown at higher magnification below. **C. Confirmation of ABCA12 loss in *Abca12^{tm1a/tm1a}* mice.** Immunofluorescence analysis for ABCA12 (green) and the granular layer marker loricrin (red). Note in the control ABCA12 expression co-localizes with loricrin. This signal is absent in knockout mice. Asterisk indicates background, non-specific staining. White boxed area indicates region shown on right. **D. Early Hair Follicle Differentiation is Not Affected in *Abca12^{tm1a/tm1a}* mice.** Immunofluorescence analysis of the early hair follicle differentiation marker keratin 79 (red) and the basal marker, keratin 14 (Green). Note that K79 is present in both control and knockout samples.
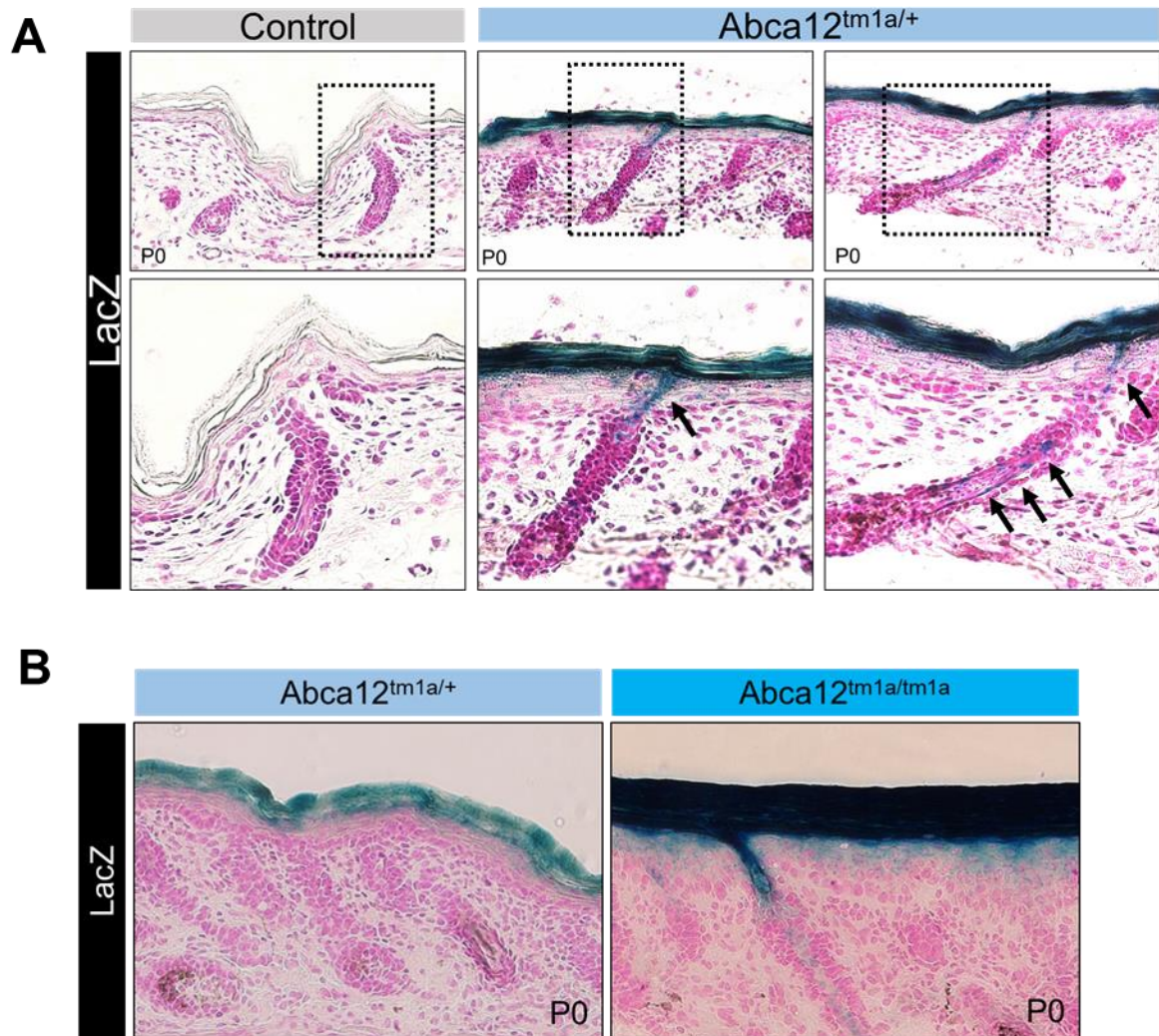
Figure 4.4. Analysis of *Abca12* Expression in Developing Samples. Analysis performed on P0 samples from *Abca12^tm1a/+^* mice in which a *lacZ* cassette, encoding β-galactosidase (β-gal), was inserted into the endogenous *Abca12* locus, thereby inactivating the allele but also serving as a reporter for *Abca12* promoter activity. **A. Abca12 Expression in the Epidermis and Hair Follicle.** β-gal activity in *Abca12^tm1a/+^* is detected strongly in the upper epidermis as well as the hair canal and differentiated cells in the most progressed follicles. Higher magnification of the boxed area in the top is shown below. Arrows point to signal in the hair follicle. No signal is detected in the control sample (left). **B. Comparison of *Abca12^tm1a/tm1a^* and *Abca12^tm1a/+^* samples.** β-gal activity in *Abca12^tm1a/tm1a^* (knockout) samples which contain *lacZ* cassette in both alleles of *Abca12* show much stronger signal than corresponding *Abca12tm1a/+* which only contain a *lacZ* cassette in 1 allele.
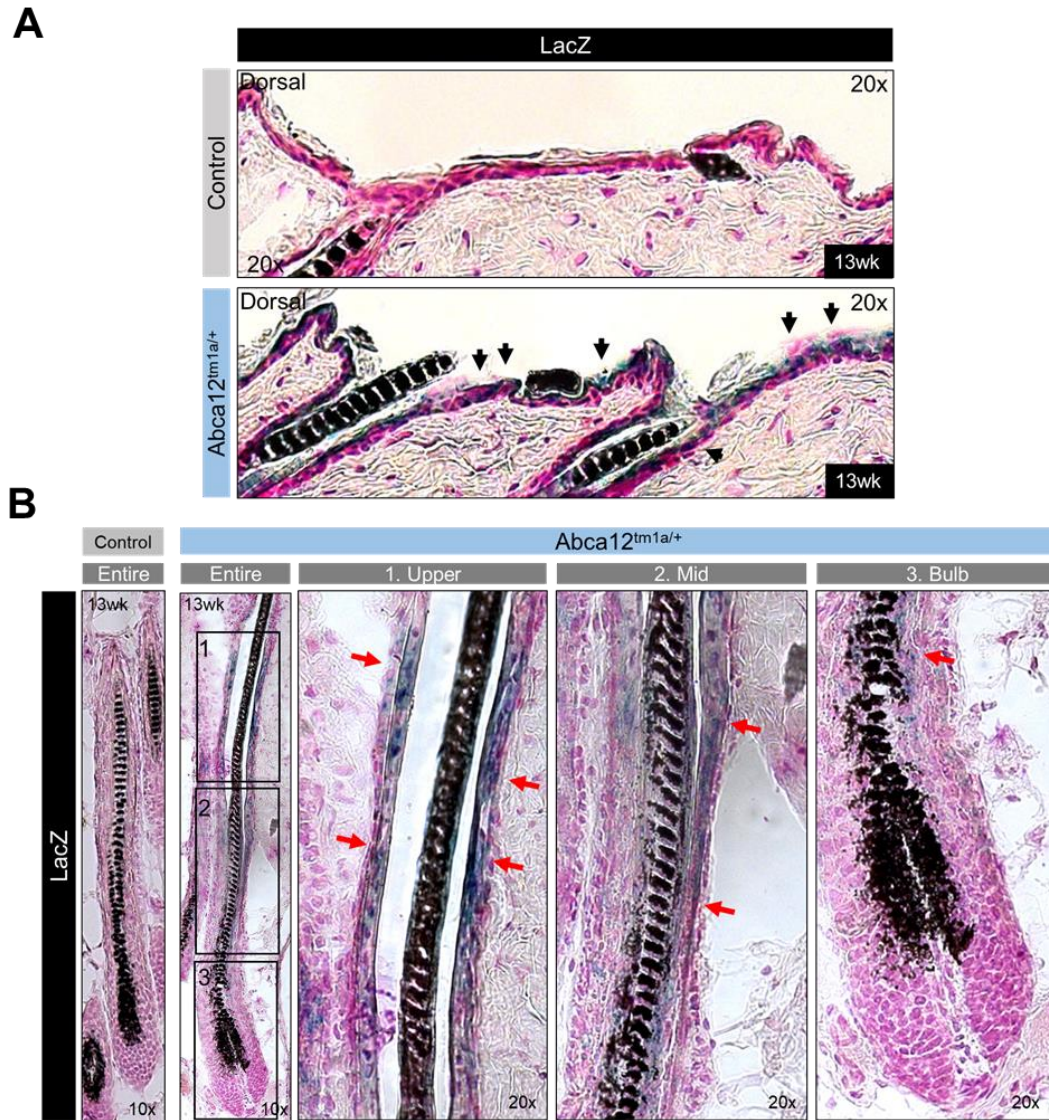
148

Figure 4.5. Analysis of *Abca12* Expression in Dorsal Skin of Adult Samples. Analysis performed on 13-week-old samples from *Abca12tm1a/+* mice in which a *lacZ* cassette, encoding β-galactosidase (β-gal), was inserted into the endogenous *Abca12* locus, thereby inactivating the allele but also serving as a reporter for *Abca12* promoter activity. **A. *Abca12* Expression in Adult Dorsal Skin.** β-gal activity in *Abca12tm1a/+* is detected in the epidermis of adult mice. This signal appears weaker than in developing samples shown in Figure 4. β-gal activity is also detected in the hair canal. Black arrows denote signal in the epidermis and hair canal. No signal is detected in the control sample (top). **B. *Abca12* Expression in Adult Anagen Hair Follicles.** *Abca12tm1a/+* mature anagen hair follicle is separated into 3 regions (black boxes) with each shown at higher magnification on the right. β-gal activity in *Abca12tm1a/+* is detected in the clear differentiated cells surrounding the hair shaft in the upper and middle regions of the hair follicle. Most of the hair bulb is negative although some positive signaling can be seen in the area representing nascent differentiating cells. Red arrows denote β-gal signal. No signal is seen in the control (left).

149
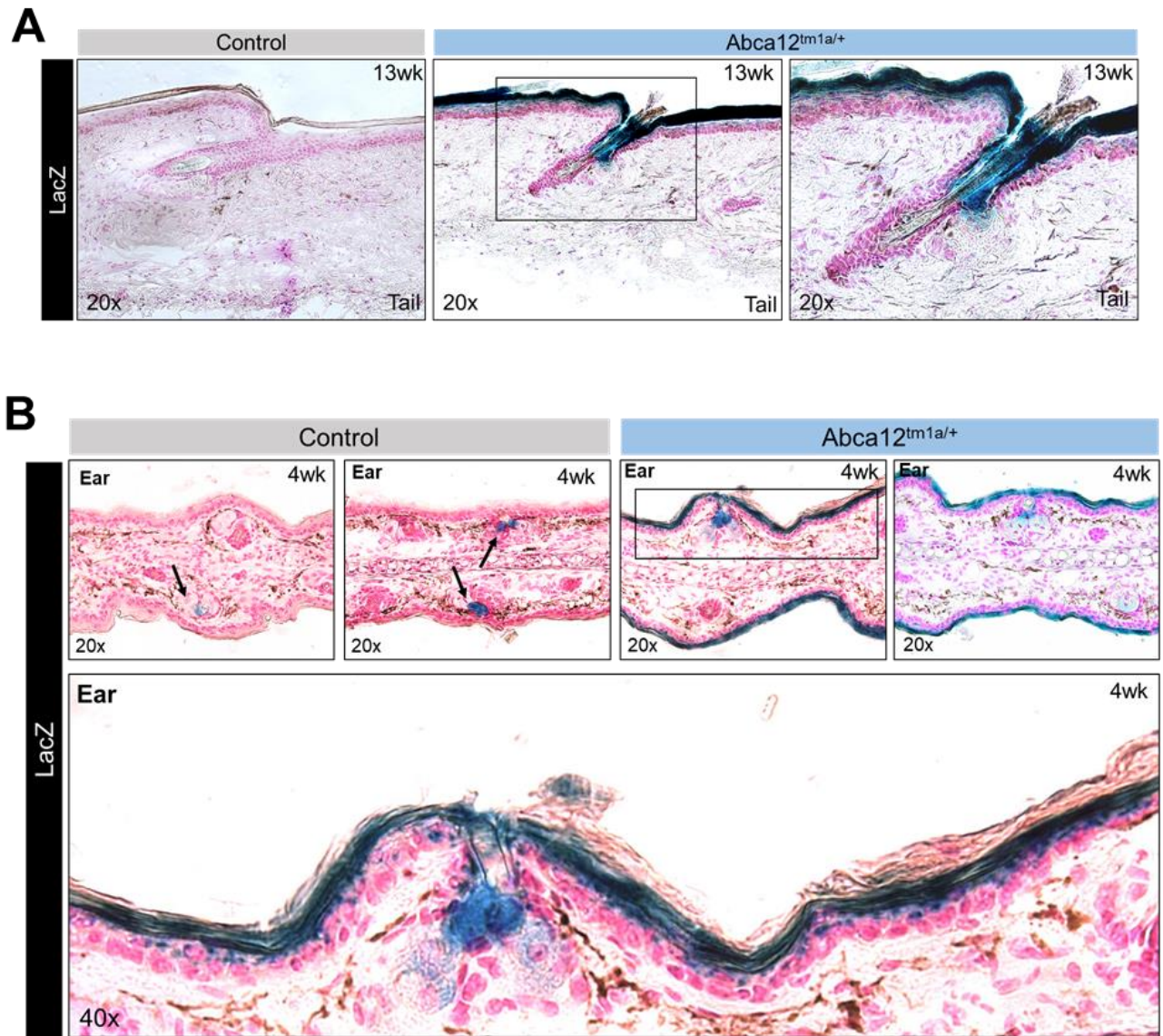
Figure 4.6. Analysis of *Abca12* Expression Adult Tail and Ear Skin. Analysis performed on 4-week (ear) or 13-week (tail) samples from *Abca12*tm1a/+ mice in which a *lacZ* cassette, encoding β-galactosidase (β-gal), was inserted into the endogenous *Abca12* locus, thereby inactivating the allele but also serving as a reporter for *Abca12* promoter activity. **A. *Abca12* Expression in Adult Tail Skin.** Like the dorsal skin (Figure 5), β-gal activity in *Abca12*tm1a/+ is detected in the upper epidermis and hair canal. Image on far right is zoomed in version of boxed area in middle image. Control (left) shows no signal. **B. *Abca12* Expression in Adult Ear Skin.**, β-gal activity in *Abca12*tm1a/+ is detected in the upper epidermis and hair canal of ear skin. Signal is also detected in the sebaceous glands, however control samples (black arrows) also show signal in this region so it may represent a non-specific signal. 2 independent samples are shown for control (left) and *Abca12*tm1a/+ (right) mice. Boxed area in *Abca12*tm1a/+ sample on top is shown at higher magnification in the bottom image.
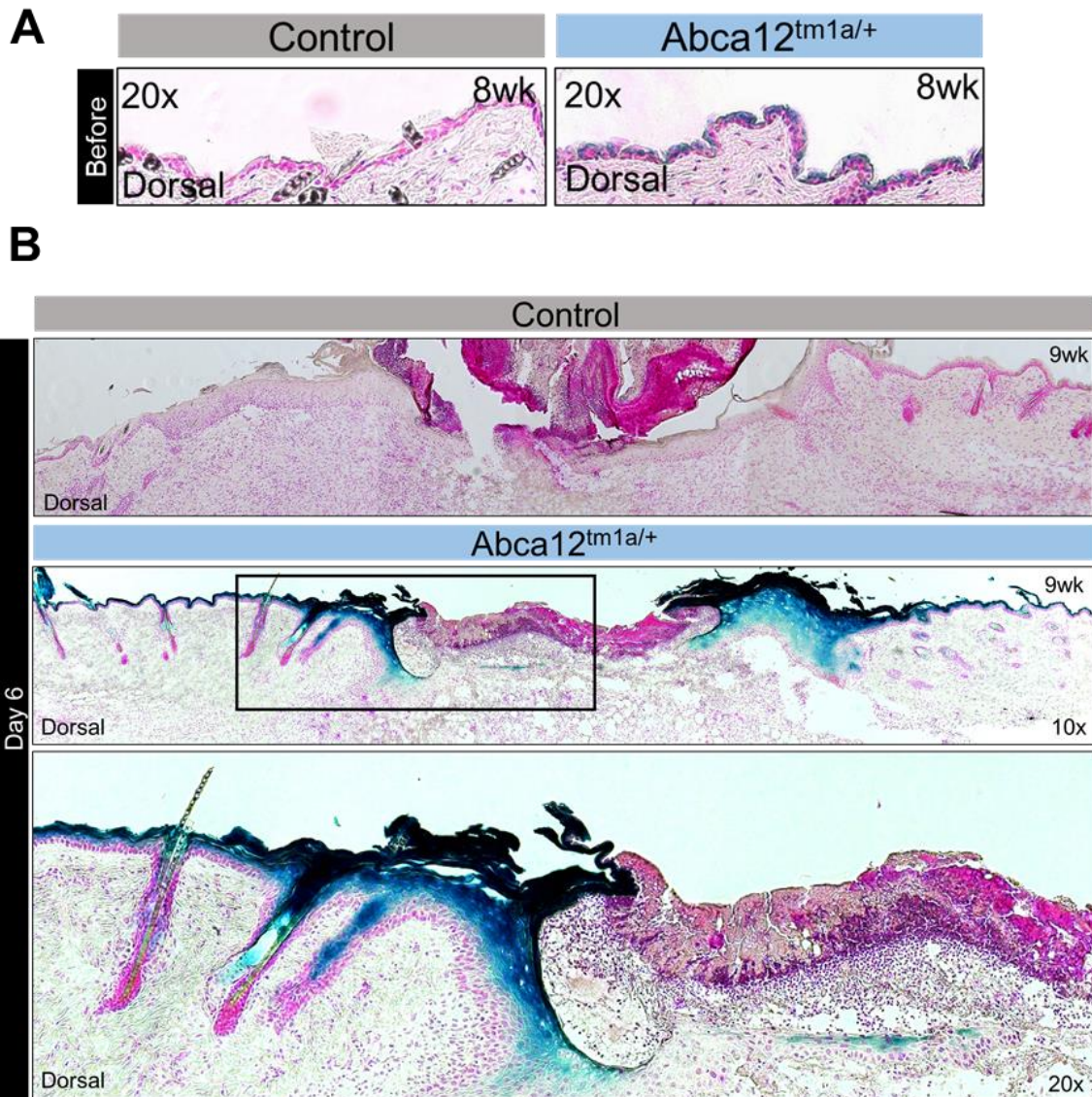
Figure 4.7. Analysis of *Abca12* Expression in Wounded Skin. Analysis performed on samples from *Abca12*[tm1a/+] mice in which a *lacZ* cassette, encoding β-galactosidase (β-gal), was inserted into the endogenous *Abca12* locus, thereby inactivating the allele but also serving as a reporter for *Abca12* promoter activity. Full thickness wounds were created in the dorsal skin and biopsies were taken before wounding and day 6 after wounding. **A. *Abca12* Expression in Adult Dorsal Skin Before Wounding.** At day 0, β-gal activity in *Abca12*[tm1a/+] is detected in the upper epidermis. No signal is observed in the control (left). **B. *Abca12* Expression in Wounded Dorsal Skin.** At day 6 after wounding, β-gal activity in *Abca12*[tm1a/+] is detected in the wound-adjacent skin. Note that the signal is much higher than the corresponding signal in D0 samples. Signal is strongest in the epidermis and hair follicles closest to the wound. Boxed area in the top is shown at higher magnification in the bottom. No signal is detected in the control sample (top).

151
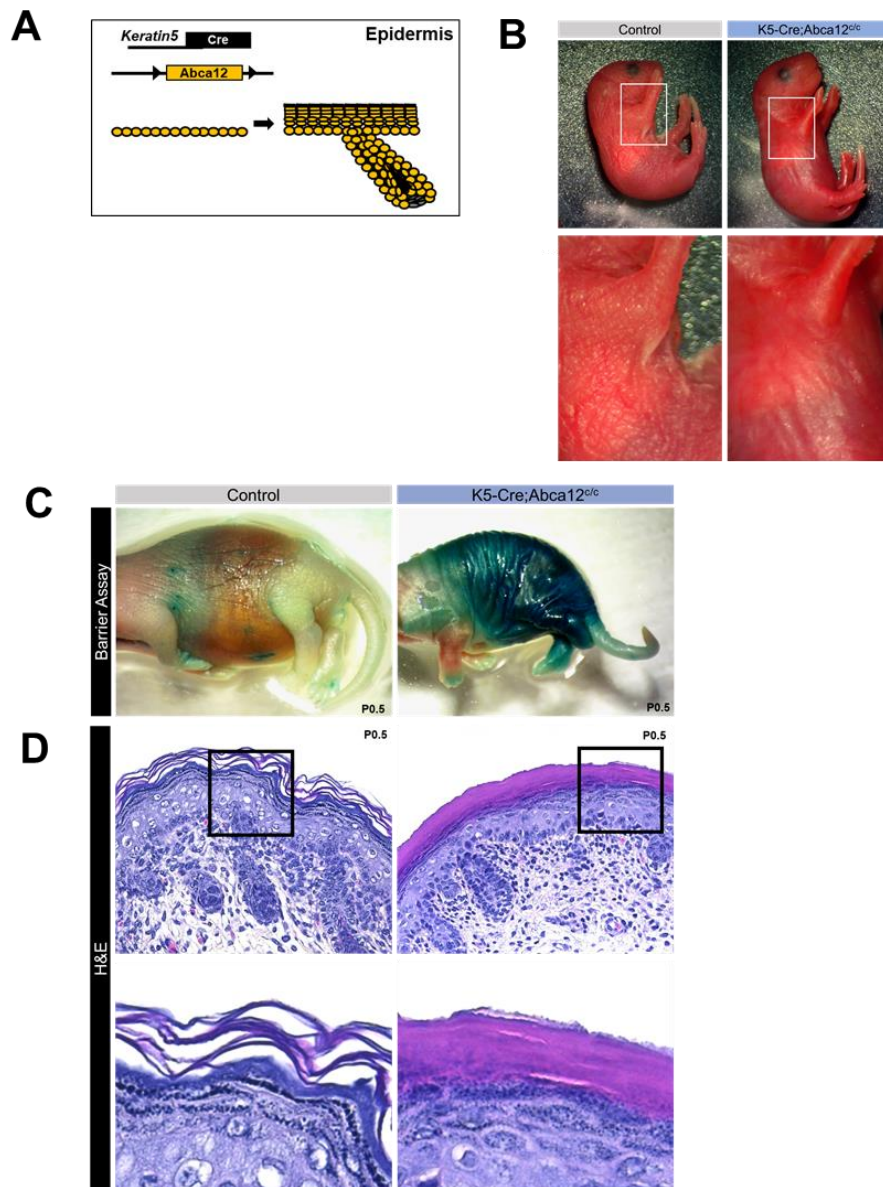
Figure 4.8. Epidermal-Specific *Abca12 Targeting.* A. Schematic Depicting Targeting Strategy. To achieve *Abca12*-knockout throughout the epidermis and hair follicles, *Keratin5-Cre* mice were crossed to *Abca12^c/c^* mice. Yellow circles indicate cells with loss of Abca12 expression in this scheme. **B. Gross Analysis of *Keratin5-Cre;* Abca12^c/c^ samples.** Note the shiny appearance of *Kertain5-Cre; Abca12^c/c^* mouse compared to control. Area in white box is shown close-up on the right to highlight the different textures of the skin. This phenotype appears milder than *Abca12^tm1a/tm1a^* whole body knockout mice (Figure 2). **C. Barrier Analysis of *Keratin5-Cre;* Abca12^c/c^ samples.** Dye exclusion assay performed on P0.5 mice. This assay depends on barrier-dependent access of X-gal to untreated skin. Control (left) possess a complete epidermal barrier and does not turn blue. *Keratin5-Cre; Abca12^c/c^* sample (right) turns blue due to a defective barrier. **D. Histological Analysis of *Keratin5-Cre;* Abca12^c/c^ samples.** Control mice show normal basket-weave appearance of the outer stratum corneum (left). *Kertain5-Cre; Abca12^c/c^* samples show a thick, compact stratum corneum. Area in box of top panel shown in close up view below. Abbreviations: K5: Keratin 5.
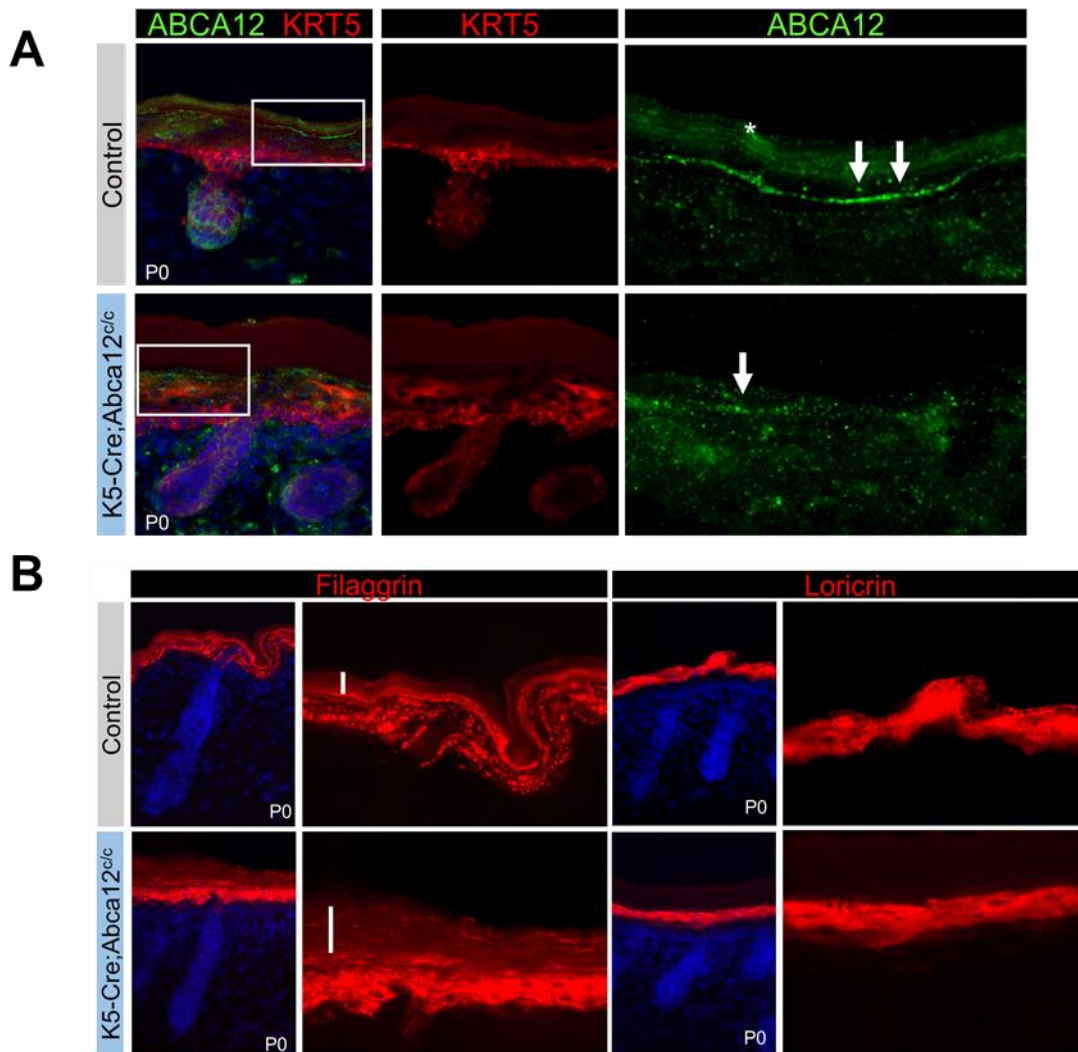
Figure 4.9. Analysis of Epidermal-Specific *Abca12* Targeting*. A. Confirmation of ABCA12 loss in *Keratin5-Cre; Abca12^{c/c}* samples. Immunofluorescence analysis for ABCA12 (green) and the basal cell marker keratin 5 (red). Note the presence of thin line of ABCA12 in the control. In the *Keratin5-Cre;* Abca12^{c/c} samples most of this signal is gone, however some ABCA12 signal is still detected (white arrow). Also note that the basal marker, keratin 5 (red), is expressed in the suprabasal layers (*) in the *Keratin5-Cre;* Abca12^{c/c} samples. **B. Analysis of Late Differentiation Markers in *Keratin5-Cre; Abca12^{c/c}* samples.** Immunofluorescence analysis for filaggrin (left) and loricrin (right). Both markers are expressed in *Keratin5-Cre;* Abca12^{c/c} samples. Filaggrin expression appears more compacted than in the control. Further analysis is needed to determine if there are any abnormalities. White bars indicate thickness of the stratum corneum. Abbreviations: K5: Keratin 5.
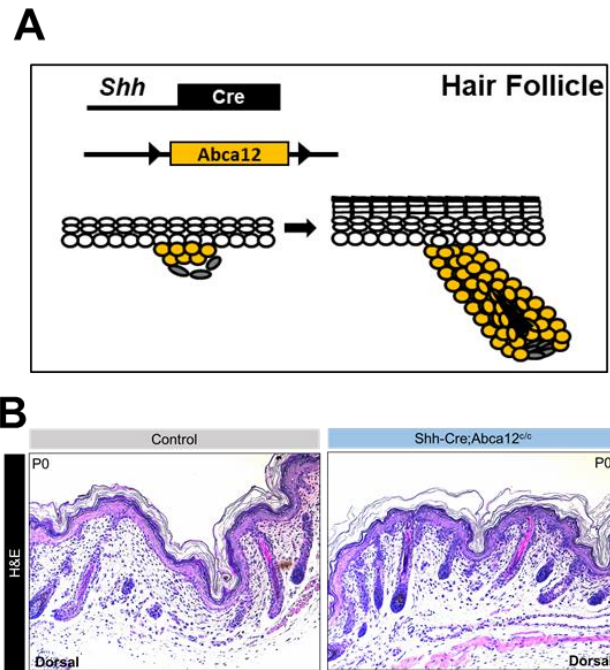
Figure 4.10. Hair Follicle-Specific *Abca12* Targeting. A. Schematic Depicting Targeting Strategy. To achieve *Abca12*-knockout specifically in hair follicles, *Shh-Cre* mice were crossed to *Abca12^{c/c}* mice. Yellow circles indicate cells with loss of Abca12 expression in this scheme. **B. Histological Analysis of *Shh-Cre;* Abca12^{c/c} samples.** No obvious defects were detected in hair follicle-specific *Abca12* knockout samples at P0.

4.8 Reference List

1. Thomas, A.C., et al., *Abca12 is the major harlequin ichthyosis gene.* J Invest Dermatol, 2006. **126**(11): p. 2408-13.
2. Akiyama, M., et al., *Mutations in lipid transporter abca12 in harlequin ichthyosis and functional recovery by corrective gene transfer.* J Clin Invest, 2005. **115**(7): p. 1777-84.
3. Richard, G. *Autosomal recessive congenital ichthyosis* Gene Reviews [Internet] 2001 May 18, 2017; Available from: https://www.ncbi.nlm.nih.gov/books/NBK1420/.
4. Kun-Darbois, J.D., et al., *Facial features in harlequin ichthyosis: Clinical findings about 4 cases.* Rev Stomatol Chir Maxillofac Chir Orale, 2016. **117**(1): p. 51-3.
5. Rajpopat, S., et al., *Harlequin ichthyosis: A review of clinical and molecular findings in 45 cases.* Arch Dermatol, 2011. **147**(6): p. 681-6.
6. Akiyama, M., Dale, B. A., Smith, L. T. , Shimuzu, S., and Holbrook, K. A. , *Regional difference in expression of characterstic abnormality of harlequin ichthyosis in affected fetuses* Prenatal Diagnosis 1998. **18**: p. 425-436.
7. Paus, R., et al., *A comprehensive guide for the recognition and classification of distinct stages of hair follicle morphogenesis.* J Invest Dermatol, 1999. **113**(4): p. 523-534.
8. Hardman, M.J., et al., *Patterned acquisition of skin barrier function during development.* Development, 1998. **125**(8): p. 1541-52.
9. Eckhart, L., et al., *Cell death by cornification.* Biochim Biophys Acta, 2013. **1833**(12): p. 3471-80.
10. Candi, E., R.A. Knight, and G. Melino, *Cornification of the skin: A non-apoptotic cell death mechanism.* 2009.
11. Ishida-Yamamoto, A., et al., *Epidermal lamellar granules transport different cargoes as distinct aggregates.* Journal of Investigative Dermatology, 2004. **122**(5): p. 1137-1144.
12. Prausnitz, M.R., P.M. Elias, and T.J. Franz, *Skin barrier and transdermal drug delivery.* Dermatology, 2012: p. 2065-2073.
13. Borgoño, C.A., et al., *A potential role for multiple tissue kallikrein serine proteases in epidermal desquamation.* Journal of Biological Chemistry, 2007. **282**(6): p. 3640-3652.
14. Hachem, J.-P., et al., *Acute acidification of stratum corneum membrane domains using polyhydroxyl acids improves lipid processing and inhibits degradation of corneodesmosomes.* The Journal of investigative dermatology, 2010. **130**(2): p. 500-510.
15. Thomas, A.C., et al., *Premature terminal differentiation and a reduction in specific proteases associated with loss of abca12 in harlequin ichthyosis.* Am J Pathol, 2009. **174**(3): p. 970-8.
16. Yanagi, T., et al., *Harlequin ichthyosis model mouse reveals alveolar collapse and severe fetal skin barrier defects.* Hum Mol Genet, 2008. **17**(19): p. 3075-83.
17. Yanagi, T., et al., *Self-improvement of keratinocyte differentiation defects during skin maturation in abca12-deficient harlequin ichthyosis model mice.* Am J Pathol, 2010. **177**(1): p. 106-18.

18. Zuo, Y., et al., *Abca12 maintains the epidermal lipid permeability barrier by facilitating formation of ceramide linoleic esters.* J Biol Chem, 2008. **283**(52): p. 36624-35.

19. Zhang, L., et al., *Defects in stratum corneum desquamation are the predominant effect of impaired abca12 function in a novel mouse model of harlequin ichthyosis.* PLoS One, 2016. **11**(8): p. e0161465.

20. Smyth, I., et al., *A mouse model of harlequin ichthyosis delineates a key role for abca12 in lipid homeostasis.* PLoS Genet, 2008. **4**(9): p. e1000192.

21. Washio, K., et al., *Case of harlequin ichthyosis with a favorable outcome: Early treatment and novel, differentially expressed, alternatively spliced transcripts of the atp-binding cassette subfamily a member 12 gene.* J Dermatol, 2017. **44**(8): p. 950-953.

22. Mithwani, A.A., et al., *Harlequin ichthyosis: A case report of prolonged survival.* BMJ Case Rep, 2014. **2014**.

23. Glick, J.B., et al., *Improved management of harlequin ichthyosis with advances in neonatal intensive care.* Pediatrics, 2016.

24. Harfe, B.D., et al., *Evidence for an expansion-based temporal shh gradient in specifying vertebrate digit identities.* Cell, 2004. **118**: p. 517-528.

25. Wong, S.Y. and J.F. Reiter, *Wounding mobilizes hair follicle stem cells to form tumors.* Proceedings of the National Academy of Sciences of the United States of America, 2011. **108**(10): p. 4093-4098.

26. Hardman, M.J., D.N. Banbury, and C. Byrne, *Patterned acquisition of skin barrier function during development.* Development, 1998. **125**: p. 1541-1552.

27. Haftek, M., et al., *A longitudinal study of a harlequin infant presenting clinically as non-bullous congenital ichthyosiform erythroderma.* Brit J of Derm, 1996. **135**(3): p. 448-453.

28. Shibata, A. and M. Akiyama, *Epidemiology, medical genetics, diagnosis and treatment of harlequin ichthyosis in japan.* Pediatrics International, 2015. **57**(4): p. 516-522.

29. Kelsell, D.P., et al., *Mutations in abca12 underlie the severe congenital skin disease harlequin ichthyosis.* Am J Hum Genet, 2005. **76**(5): p. 794-803.

30. Lefevre, C., et al., *Mutations in the transporter abca12 are associated with lamellar ichthyosis type 2.* Hum Mol Genet, 2003. **12**(18): p. 2369-78.

31. Sakai K Fau - Akiyama, M., et al., *Abca12 is a major causative gene for non-bullous congenital ichthyosiform erythroderma.* 2009(1523-1747 (Electronic)).

32. Walsh, D.M., et al., *A novel abca12 mutation in two families with congenital ichthyosis.* Scientifica, 2012. **2012**: p. 6.

33. Haslam, I.S., et al., *Differential expression and functionality of atp-binding cassette transporters in the human hair follicle.* British Journal of Dermatology, 2014. **172**(6): p. 1562-1572.

34. Strauss, J.S. and A.M. Kligman, *The pathogenic dynamics of acne vulgaris.* Arch Dermatol, 1960. **82**: p. 779-790.

35. Veniaminova, N.A., et al., *Keratin 79 identifies a novel population of migratory epithelial cells that initiates hair canal morphogenesis and regeneration.* Development, 2013. **140**(24): p. 4870-80.

36.   Allen, D.E., *Lipids.* Laboratory histopathology: A complete reference section 6, ed. A.E. Woods and R.C. Ellis. 1994.

37.   Wertz, P.W. and D.T. Downing, *Integral lipids of human hair.* Lipids, 1988. **23**(9): p. 878-881.

38.   Lee, W.-S., et al., *Integral lipid in human hair follicle.* Journal of Investigative Dermatology Symposium Proceedings, 2005. **10**(3): p. 234-237.

Chapter V: Summary and Perspectives

5.1 Summary

My thesis examined poorly understood aspects of hair follicle biology, including hair canal formation, and terminal differentiation within the follicle. I also generated a conditional *Abca12*-knockout mouse model, which will facilitate the analysis of ABCA12 function in development and disease states across different organ systems. Here I discuss the main findings of my dissertation, identify remaining questions, and discuss experiments that will address them.

5.2 Matrix Progenitors in the Hair Follicle

5.21 The Relationship Between Early and Late Matrix Progenitor Cells

In chapter II, I examine how matrix progenitor cells housed at the bottom of the follicle make cell fate decisions to produce the suite of differentiated cell types. During morphogenesis and anagen, the matrix population expands as the follicular epithelium wraps around the dermal papilla (DP) (**Figure 5.1A**). Previously it was thought that terminal differentiation of matrix progenitors occurred only after engulfment of the DP, presumably due to signals provided by this mesenchymal signaling hub [9, 285]. However, we found that primitive matrix cells give rise to differentiated companion layer cells prior to DP engulfment in both development and regeneration. Our data support a model wherein the matrix population can be separated into 'early' and 'late' phases, based on distinct temporal (anagen stage), morphological (relationship to the DP), and

158

molecular status. Early matrix cells differentiate into companion layer cells and can do so in the absence of bone morphogenetic protein (BMP) signaling, sonic hedgehog (SHH) expression, or a mature DP. In contrast, later matrix cells, which produce the inner root sheath and hair shaft, require these pathways and only differentiate following DP engulfment. While we divided the matrix progenitor population into early and late phases, it is also possible that matrix cells with varying cell fate potentials may co-exist throughout anagen. Yang et al. utilized single-cell RNA sequencing to probe whether matrix cells at anagen 2 (early) possessed multi-lineage potential [80]. Their analysis uncovered progenitors with features of both the inner root sheath and hair shaft, as well as a separate group with features of the companion layer [80]. Thus, at this point the early matrix population has already separated from the multipotent later matrix pool. This result is not surprising given that we observed the specification of the companion layer as early as anagen 2 [273].

Do early matrix cells directly give rise to later matrix cells? To address this question, I would utilize *Shh-CreERT2; R26-YFP* mice to label individual matrix cells during early anagen and follow their fate throughout regeneration. If early matrix cells give rise to late matrix cells, I would expect to detect YFP+ cells within both the companion layer and inner root sheath/hair shaft lineages. This observation would indicate that early matrix cells which produce the companion layer also contribute to later matrix cells which generate the inner root sheath and hair shaft lineages. It is also possible that early matrix cells produce later matrix cells, but that multiple cells exist in each state. For instance, later matrix cells may already exist in early anagen, but only differentiate when prompted by dermal-derived signals. This possibility cannot be

159

rigorously evaluated using *Shh-CreERT2; R26-YFP* mice, as we may be labeling both early and late matrix cells that co-exist during early anagen. Using a multi-colored reporter mouse (e.g., *R26-Confetti)* would allow for the evaluation of the potency of individual clones that exist in early anagen. In this system, the detection of a single color within the companion layer, inner root sheath and hair shaft lineages would support the existence of a tri-potent progenitor during early anagen.

5.22 Matrix Progenitor Domains

The depiction of the matrix as a single layer of cells directly abutting the DP is oversimplified. The matrix pool is complex consisting of several layers of cells, encompassing most of the anagen bulb **(Figure 5.1A)**. Lineage-tracing studies in late anagen revealed a link between the location of matrix cells and their subsequent progeny [25]. Matrix cells located more centrally form the hair shaft, whereas more peripherally-located matrix cells generate the inner root sheath and companion layer [25]. These location-specific cell fate decisions are likely driven by distinct molecular signals found throughout the anagen bulb. For example, as anagen progresses, *Shh* expression becomes restricted asymmetrically to a subset of matrix cells via poorly understood mechanisms. Interestingly, we observed that the *Shh+* domain was negative for BMP activity. In contrast, the surrounding *Shh-* matrix population displays higher BMP activation. This observation could indicate that *Shh*-responding matrix cells that outside of the *Shh+* domain activate BMP signaling. Alternatively, these expression patterns may indicate antagonism between the SHH and BMP pathways. In support of this notion, ectopic expression of noggin (NOG), the BMP inhibitor, results in expansion of the *Shh+* domain to both sides of the hair bulb [201, 209]. A comparable antagonistic

relationship between SHH and WNT pathways is observed during hair morphogenesis [198]. Interestingly, forced activation of the WNT pathway results in de novo hair formation in adult mice [184]. While these follicles resemble those formed in development, they are misaligned, with an expanded *Shh* domain in the hair bulb [184]. This observation shows that modulation of the WNT pathway activity can affect *Shh* polarization, although the precise mechanism is unclear.

These observations highlight the nuanced relationships between key signaling pathways in matrix progenitor biology. One remaining question is how the expression patterns of matrix markers change throughout development and regeneration. To date, most studies have focused in late anagen, at a point after the follicular epithelium has wrapped around the DP. By only analyzing a single timepoint, these studies may have overlooked distinct domains established in early anagen that evolve along with the matrix population. To identify putative signaling domains, I will stain samples throughout anagen for candidate markers (e.g., WNT, SHH, BMP, and Notch). By looking at each pathway individually, as well as considering how they may interact with each other, I may uncover distinct domains that may provide new insights into matrix progenitor biology.

We are specifically interested in understanding how basal matrix cells, which sit directly along the basement membrane, differ from the bulk matrix population. The basal matrix pool divides asymmetrically to give rise to inner, suprabasal matrix cells that ultimately go onto differentiate **(Figure 5.1B)** [25, 79]. Yang et al. found the existence of distinct basal matrix domains using single-cell RNA sequencing analysis of late anagen samples [80]. The molecular profile of each domain represented a different hair lineage

(e.g., companion layer, inner root sheath, hair shaft). Thus, the basal matrix is programmed to generate the intricate radial configuration of the hair lineages. Despite this data, there is a paucity of information about what makes the basal matrix distinct from the bulk matrix population. We will use a candidate approach to uncover novel markers of the entire basal matrix. Ultimately, this information can be translated to functional experiments where we genetically manipulate these markers and examine the resultant effects on hair regeneration.

5.23 The Relationship of the Matrix and the Lower Proximal Cup

Another remaining question in the field is the function of the lower proximal cup (LPC). This region comprises the outer root sheath and lower most region of the anagen bulb directly below the matrix **(Figure 5.1B)**. While the LPC is often not labeled in diagrams or considered to be part of the matrix, its molecular profile is most similar to that of hair follicle stem cells and outer root sheath cells [80]. The function of the LPC is not clear, although it is has been proposed to play a structural role in providing support to the anagen bulb [25]. Another possibility is that the LPC may contribute to the basal matrix population during homeostasis and/or during stress conditions. Indeed, it has been suggested that following chemotherapy-induced death of matrix cells, the LPC can regenerate this population [355]. Whether this same role occurs during homeostasis is not clear, although lineage tracing experiments indicate that LPC cells divide during anagen [25].

To test whether the LPC contributes to the matrix during anagen, I would perform transient lineage tracing experiments using *Lgr5-EGFP-CreERT2* mice [356]. The transient lineage tracing strategy is similar to the experiments in chapter II where I track

162

the immediate progeny of Shh+ matrix cells [273]. LGR5 is expressed in the LPC, but not the matrix of the anagen bulb [80, 357]. *Lgr5-EGFP-CreERT2* mice display highly fluorescent signal in cells that exhibit *Lgr5* promoter activity. Importantly, the immediate, *Lgr5-* progeny of these cells will also display a weak EGFP signal, likely due to the transient persistence of EGFP-Cre fusion protein. This strategy can be used to follow the direct progeny of LGR5+ LPC cells. If LPC cells give rise to matrix cells, we would expect to see EGFP-weak matrix cells directly above EGFP+ LPC cells. To confirm that the weak EGFP signal is not due to low level promoter activity in these cells, we would co-stain with an LGR5 antibody. LGR5 is also expressed within the hair follicle stem cells and outer root sheath. Given that we are focused on the LPC-matrix interface at the bottom of the follicle, I do not anticipate that LGR5 expression in other regions of the follicle will interfere with the interpretation of our experiments.

Previous work using conventional lineage tracing with *Lgr5-Cre* mice show that *Lgr5+* expressing cells can contribute to all hair lineages [41]. However, these experiments were assessing the potential of *Lgr5+* hair follicle stem cells and did not directly evaluate the LGR5+ LPC population. To corroborate our findings from the transient lineage tracing experiments, we could utilize *Lgr5-CreERT2; R26-YFP* mice and induce labeling in mid to late anagen. By analyzing biopsies shortly after labeling (e.g., 3 days) we may be able to analyze the potential of the *Lgr5+* LPC domain without the added complications of *Lgr5* activity within the stem cell compartment.

5.3 Identifying Molecular Regulators of Companion Layer Specification

The companion layer, which sits directly between the outer root sheath and inner root sheath, is the least studied internal hair lineage. This layer is initially marked by the expression of keratin 79 (K79) [21]. K79+ cells represent the first differentiated cell population in the follicle. In development, K79+ cells stream out of the follicle into the epidermis, potentially serving as a placeholder for the future hair canal (chapter III).

The signaling pathways required for K79+ cell specification remain unclear. My work in chapter II showed that K79+ cell specification does not require BMP signaling or the expression of *Shh.* Further, in chapter III I showed that the Notch pathway is also not required, despite pathway activation in K79+ cells [21]. One critical pathway we have not evaluated is the WNT signaling cascade. WNT signaling is required for hair follicle induction as well as anagen induction and hair shaft differentiation [96, 182, 183]. To examine the role of WNT signaling in K79+ cell specification, I would use *Shh-CreERT2; β-catenin^{flox/flox}* mice and induce recombination shortly after anagen induction. This experimental scheme should block WNT signaling during early anagen, the time at which the first K79+ cells are specified. One potential caveat to this strategy is that anagen onset requires WNT activation within stem cells and the secondary hair germ (future matrix population) [56, 207]. It is possible that blocking WNT signaling could prevent the follicle from entering anagen. However, as we plan to block WNT signaling after anagen induction, we do not anticipate this issue will preclude our analysis. Alternative regulators may be identified by mining existing data sets from sequencing experiments, or examining the *K79* promoter for conserved transcription factor binding sites, if we uncover that WNT is not required for companion layer specification.

5.4 The Role of ABCA12 in Development and Disease

5.41 Phenotypic Recovery in Harlequin Ichthyosis Patients

In chapter IV, I generated a novel genetic tool to assess the role of the lipid transporter *Abca12* in development and disease states. Loss-of-function mutations in *ABCA12* underlie the severe human skin disease, harlequin ichthyosis (HI). This mouse model can be utilized to understand new aspects of the pathogenesis of HI.

HI patients who survive past infancy display a dramatic phenotypic improvement, resembling non-bullous congenital ichthyosis erythroderma (NBCIE), a less severe form of ichthyosis caused by missense mutations in *ABCA12* [254, 256, 258, 348]. NBCIE presents as red skin, with small white flakes, compared to the large plate-like scales seen in HI patients [251]. The molecular mechanisms controlling the phenotypic improvement seen in HI patients are not known.

Our conditional *Abca12*-deletion mouse model can be used to study the long-term consequence of *Abca12* loss *in vivo* in adult mice. Indeed, we have already generated epithelial-specific *Abca12*-knockout mice driven by a constitutive *Keratin 5-Cre* that display a milder HI-like phenotype at birth (see chapter IV). We were initially surprised that the phenotype wasn't more severe in these mice (likely due to inefficient recombination). However, the mild phenotype may enable them to survive into adulthood, making them an ideal system to probe for compensatory mechanisms following *Abca12* loss. By comparing the histological and molecular changes between neonatal and adult samples, we can identify key differences that may drive the phenotypic improvement. Alternatively, we can utilize an inducible *Keratin 14-CreERT* line to drive *Abca12* loss in the epidermis. One benefit to this approach is that it allows

tight control of the level of *Abca12* deletion. Using this system, we can generate mice that lack *Abca12* expression in some epidermal cells, but still survive.

One possibility is that other lipid transporters are upregulated in *Abca12*-deficient adult skin. Indeed, Yanagi et al. found that 4 ATP-binding cassette transporter family genes (*Abca17, Abcb1a, Abcc5, Abcb11)* were upregulated in sub-cultured versus primary *Abca12*-knockout keratinocytes [271]. While these genes represent attractive candidates for drivers of compensation, it is not clear if they are also upregulated *in vivo* or if they play a functional role in the absence of *Abca12.* To address this question, we can employ our *Keratin 5-Cre* and *Keratin 14-CreERT* drivers to delete *Abca12* in the epidermis. These samples can be analyzed to identify mechanisms of compensation following *Abca12* loss. Alternatively, we can utilize our novel whole-body *Abca12*-knockout mouse model to answer the same question. As *Abca12*-knockout mice die perinatally, we would graft skin onto immunocompromised mice and analyze the subsequent tissue several weeks later. One advantage of this approach is that all cells would be *Abca12*-deficient, like human HI patients.

We can also use *K14-CreERT; Abca12$^{c/c}$* mice to study the importance of ABCA12 during adult skin homeostasis and stress. Interestingly, our analysis reveals much higher *Abca12* promoter activity in developing compared to adult skin. While this result may be due to differences in skin thickness between the two timepoints, it could also indicate that ABCA12 function is more critical in development than it is during adult homeostasis. We also observed high *Abca12* promoter activity in wound-adjacent skin suggesting that it may play a role during the process of wound healing. To address this possibility, we can analyze wound healing in epidermal-specific *Abca12*-deficient skin.

166

5.42 *ABCA12 and Ichthyotic Diseases*

Interestingly, *ABCA12* mutations also underlie NBCIE, as well as a related disease, lamellar ichthyosis type 2 (LI) [347, 348]. These milder skin conditions are caused by missense mutations within the ATP-binding domain, while HI is caused by truncation or deletion mutations all along the *ABCA12* gene that severely impair protein function [254, 260, 261, 349]. The ATP-binding domain is highly conserved and is required for the lipid-transport function of ABCA12 [264]. These observations raise the possibility that *ABCA12* possesses functions independent of its lipid transport function (and ATP-binding domain), explaining the severity of HI relative to NBCIE and LI. For instance, ABCA12 may function in lamellar granule biogenesis and maintenance. ABCA12 normally localizes to the membrane of lamellar granules and loads them with lipid content that will be extruded into the inter-cellular space in the upper epidermis [259]. Both HI patients and *Abca12*-knockout mouse models show defective or abnormal lamellar granules [250, 259, 267, 269, 271, 358]. This function may be independent of the ATP-binding domain of ABCA12. Alternatively, it is possible that the differences in phenotype severity are simply due to different levels of mutant ABCA12 protein activity. The missense mutations found in NBCIE and LI2 may only partially impair ABCA12 function. In contrast, the large truncation mutations associated with HI likely result in complete loss of ABCA12 function.

5.43 *ABCA12 Function in the Hair Follicle*

The hair canal bridges the epidermis and follicle, serving as a channel for the hair shaft as well as sebum, a waxy substance that moisturize the skin surface. Given the

position of the hair canal, it is conceivable that it possesses barrier function, like the epidermis. In chapter III, I discuss the coordinated timing of hair canal and epidermal barrier formation during normal conditions.

Hair canal abnormalities are also noted in some HI patient skin [255]. Histological analysis reveal that hair canals are clogged with keratin material and that this defect appears prior to the expansion of the epidermis [255]. This observation raises the question of whether there is a link between the hair follicle and the barrier disease HI. Conversely, it is possible that ABCA12 is required for normal hair canal formation, a process that occurs around the same time as epidermal barrier formation. Thus, the observed hair canal defects in HI patients may reflect an independent requirement of ABCA12 during follicle development. We observed *Abca12* promoter activity in the hair canal of newborn mouse follicles. However, analysis of our whole-body *Abca12-*deficient skin revealed largely normal hair follicles. The most progressed follicles in these samples often have a discernable hair canal, although hair shaft exit may be blocked by the expanded epidermis. These results argue against a critical role for *Abca12* function during early hair canal formation. ABCA12 function may not be required during morphogenesis, but instead may become important following hair pore generation and hair shaft emergence. To clarify the role of *Abca12* during follicle development we are generating hair follicle-specific *Abca12*-knockout (*Shh-Cre; Abca12^{c/c}*). If *Abca12* is required for hair canal formation, these samples should display abnormal canal generation or delayed hair shaft emergence. To circumvent any issues surrounding early lethality due to *Shh-Cre* activity in other organs (e.g., lung) we will graft newborn skin onto immunocompromised mice. By following hair emergence and

examining the histology of hair follicle-specific *Abca12*-knockout skin, we can determine whether any defects arise. These experiments will allow for the direct evaluation of ABCA12 function specifically within the hair follicle without the complications associated with indirect effects due to its role in the epidermis.

5.44 Beyond the Skin and Hair Follicle: ABCA12 Function in Other Organs

Our mouse model can also be used to address the function of ABCA12 in other organs. The first organ of interest is the lung, where the function of ABCA12 is contested in the field. Yanagi et al. argued that early postnatal death was caused by alveolar collapse, due to decreased pulmonary surfactant in their *Abca12*-knockout mouse model [271]. An independent group failed to find a lung defect or even the expression of ABCA12 in lung tissue in their *Abca12*-knockout model [269]. Our initial experiments in adult lung tissue reveal *Abca12* promoter activity. Next, we must confirm the expression of ABCA12 during lung development. We can then analyze *Abca12*-deficient lung tissue to clarify the role of ABCA12 during lung development. Initially, we can utilize tissue from *Keratin 5-Cre; Abca12$^{c/c}$* and *Shh-Cre; Abca12$^{c/c}$* mice, which both are active in the epithelium of developing lung [359, 360].

Both the epidermis and the lung possess barrier function. Further a related family member, ABCA3, is required for lung development in humans and mice [361, 362]. ABCA3 is localized to lamellar bodies where it functions to load pulmonary surfactant components into these secretory organelles [362]. The pulmonary surfactant is secreted into the alveolar space where it decreases surface tension and prevents alveolar collapse [362]. This function is very similar to ABCA12's role during epidermal barrier formation. Given these similarites, it is possible that ABCA12 plays an analgous role in the lung. A

leading cause of death in HI patients is respiratory distress, although these deaths have yet to be linked to specific lung defects [363]. Rather, they are thought to be caused by the extreme mechanical stress imposed by the tightness of the skin which impairs chest expansion and breathing [254]. However, it is possible that HI patients also display lung defects that have been previously overlooked.

ABCA12 may also serve critical roles in the development and homeostasis of other organs. Indeed, tissue analysis indicates that *ABCA12* is expressed in the brain, mammary gland, mouth, placenta, testis, stomach, in addition to the skin [364]. Our mouse model can be used to delinate the role of ABCA12 in these organs.
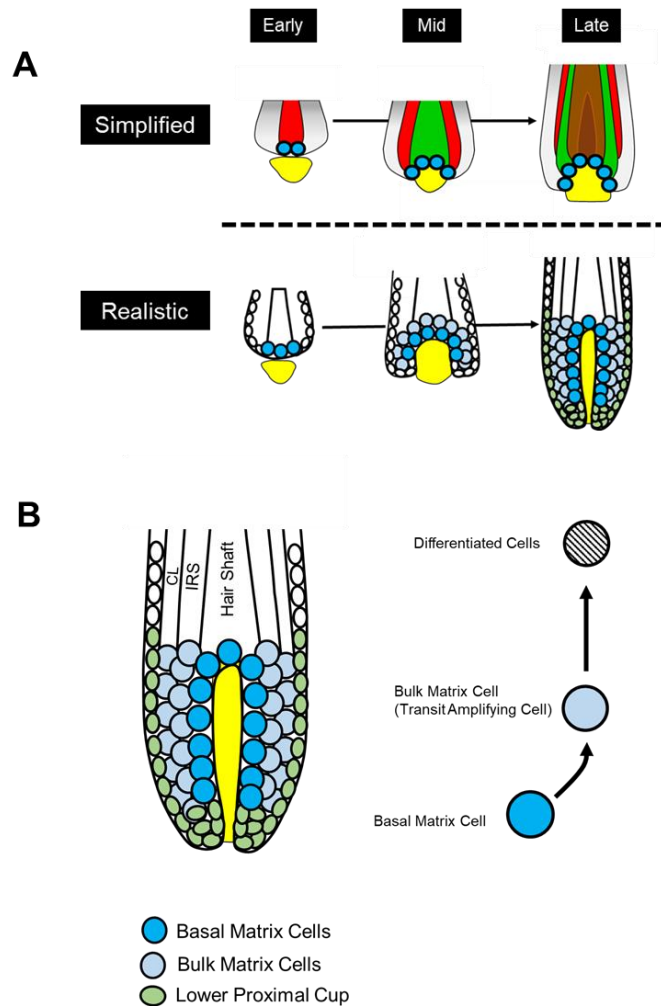
5.5 Figures

Figure 5.1. The Matrix Progenitor Population. **A. Matrix Progenitor Population Throughout Anagen**. The top represents a simplified view of matrix progenitor expansion throughout anagen, while the bottom depiction is more reflective of the actual process. In early regeneration, a small number of matrix cells (blue) sits at the bottom of the follicle. These early matrix cells can differentiate into the companion layer lineage (top, red). As regeneration continues the matrix undergoes a massive expansion, while the hair follicle wraps around the dermal papilla (yellow). Differentiation into the inner root sheath (green) and hair shaft (brown) lineages occurs after the follicle has engulfed the dermal papilla. In the bottom, basal matrix cells (dark blue) directly abut the DP and give rise to bulk matrix cells (light blue) which fill the remaining space in the anagen bulb. **B. Close-up View of the Anagen Bulb**. In late anagen, the follicle has wrapped around the dermal papilla (yellow). Basal matrix progenitors (dark blue) directly touch the basement membrane, while bulk matrix cells (light blue) do not. Right, basal matrix cells divide to give rise to the bulk matrix population which will ultimately go onto differentiate. The lower proximal cup (green) is a distinct population found at the bottom of the anagen bulb. The function of this cellular population is unknown. Abbreviations: CL: companion layer, IRS: inner root sheath. Aspects of **B** are adapted from [5].

5.6 Reference List

1.   Paus, R., et al., *A comprehensive guide for the recognition and classification of distinct stages of hair follicle morphogenesis.* J Invest Dermatol, 1999. **113**: p. 523-32.
2.   Muller-Rover, S., et al., *A comprehensive guide for accurate classification of murine hair follicles in distinct hair cycle stages.* J Invest Dermatol, 2001. **117**(1): p. 3-15.
3.   Yang, H., et al., *Epithelial-mesenchymal micro-niches govern stem cell lineage choices.* Cell, 2017. **169**(3): p. 483-496 e13.
4.   Mesler, A.L., et al., *Hair follicle terminal differentiation is orchestrated by distinct early and late matrix progenitors.* Cell Rep, 2017. **19**(4): p. 809-821.
5.   Sequeira, I. and J.F. Nicolas, *Redefining the structure of the hair follicle by 3d clonal analysis.* Development, 2012. **139**(20): p. 3741-51.
6.   Botchkarev, V.A., et al., *Noggin is required for induction of the hair follicle growth phase in postnatal skin.* FASEB, 2001. **15**: p. 2205-2214.
7.   Woo, W.M., H.H. Zhen, and A.E. Oro, *Shh maintains dermal papilla identity and hair morphogenesis via a noggin-shh regulatory loop.* Genes Dev, 2012. **26**(11): p. 1235-46.
8.   Ouspenskaia, T., et al., *Wnt-shh antagonism specifies and expands stem cells prior to niche formation.* Cell, 2016. **164**(1-2): p. 156-169.
9.   Gat, U., et al., *De novo hair follicle morphogenesis and hair tumors in mice expressing a truncated β-catenin in skin.* Cell, 1998. **95**(5): p. 605-614.
10.   Legue, E. and J.F. Nicolas, *Hair follicle renewal: Organization of stem cells in the matrix and the role of stereotyped lineages and behaviors.* Development, 2005. **132**(18): p. 4143-54.
11.   Huang, W., et al., *1393 lower proximal cup cells but not bulge stem cells regenerate hair follicles after chemotherapy injury.* Journal of Investigative Dermatology, 2018. **138**(5): p. S236.
12.   Barker, N., et al., *Identification of stem cells in small intestine and colon by marker gene lgr5.* Nature, 2007. **449**: p. 1003.
13.   Takeda, N., et al., *Hopx expression defines a subset of multipotent hair follicle stem cells and a progenitor population primed to give rise to k6+ niche cells.* Development, 2013. **140**(8): p. 1655-64.
14.   Jaks, V., et al., *Lgr5 marks cycling, yet long-lived, hair follicle stem cells.* Nat Genet, 2008. **40**(11): p. 1291-9.
15.   Veniaminova, N.A., et al., *Keratin 79 identifies a novel population of migratory epithelial cells that initiates hair canal morphogenesis and regeneration.* Development, 2013. **140**(24): p. 4870-80.
16.   Andl, T., et al., *Wnt signals are required for the initiation of hair follicle development.* Developmental Cell, 2002. **2**(5): p. 643-653.
17.   Huelsken, J., et al., *B-catenin controls hair follicle morphogenesis and stem cell differentiation in the skin.* Cell, 2001. **105**(4): p. 533-545.
18.   DasGupta, R. and E. Fuchs, *Multiple roles for activated lef/tcf transcription complexes during hair follicle development and differentiation.* Development, 1999. **126**: p. 4557-4568.

19. Kandyba, E., et al., *Competitive balance of intrabulge bmp/wnt signaling reveals a robust gene network ruling stem cell homeostasis and cyclic activation.* Proc Natl Acad Sci U S A, 2013. **110**(4): p. 1351-6.

20. Greco, V., et al., *A two-step mechanism for stem cell activation during hair regeneration.* Cell Stem Cell, 2009. **4**: p. 155-169.

21. Mithwani, A.A., et al., *Harlequin ichthyosis: A case report of prolonged survival.* BMJ Case Rep, 2014. **2014**.

22. Rajpopat, S., et al., *Harlequin ichthyosis: A review of clinical and molecular findings in 45 cases.* Arch Dermatol, 2011. **147**(6): p. 681-6.

23. Roberts, L.J., *Long-term survival of a harlequin fetus* J Am Acad Dermatol, 1989. **21**(2): p. 335-339.

24. Sakai K Fau - Akiyama, M., et al., *Abca12 is a major causative gene for non-bullous congenital ichthyosiform erythroderma.* 2009(1523-1747 (Electronic)).

25. Richard, G. *Autosomal recessive congenital ichthyosis* Gene Reviews [Internet] 2001 May 18, 2017; Available from: https://www.ncbi.nlm.nih.gov/books/NBK1420/.

26. Yanagi, T., et al., *Self-improvement of keratinocyte differentiation defects during skin maturation in abca12-deficient harlequin ichthyosis model mice.* Am J Pathol, 2010. **177**(1): p. 106-18.

27. Lefevre, C., et al., *Mutations in the transporter abca12 are associated with lamellar ichthyosis type 2.* Hum Mol Genet, 2003. **12**(18): p. 2369-78.

28. Thomas, A.C., et al., *Abca12 is the major harlequin ichthyosis gene.* J Invest Dermatol, 2006. **126**(11): p. 2408-13.

29. Kelsell, D.P., et al., *Mutations in abca12 underlie the severe congenital skin disease harlequin ichthyosis.* Am J Hum Genet, 2005. **76**(5): p. 794-803.

30. Walsh, D.M., et al., *A novel abca12 mutation in two families with congenital ichthyosis.* Scientifica, 2012. **2012**: p. 6.

31. Borst, P. and R.O. Elferink, *Mammalian abc transporters in health and disease.* Annu Rev Biochem, 2002. **71**: p. 537-92.

32. Akiyama, M., et al., *Mutations in lipid transporter abca12 in harlequin ichthyosis and functional recovery by corrective gene transfer.* J Clin Invest, 2005. **115**(7): p. 1777-84.

33. Dale, B.A., et al., *Heterogeneity in harlequin ichthyosis, an inborn error of epidermal keratinization: Variable morphology and structural protein expression and a defect in lamellar granules.* Journal of Investigative Dermatology, 1990. **94**(1): p. 6-18.

34. Smyth, I., et al., *A mouse model of harlequin ichthyosis delineates a key role for abca12 in lipid homeostasis.* PLoS Genet, 2008. **4**(9): p. e1000192.

35. Zuo, Y., et al., *Abca12 maintains the epidermal lipid permeability barrier by facilitating formation of ceramide linoleic esters.* J Biol Chem, 2008. **283**(52): p. 36624-35.

36. Zhang, L., et al., *Defects in stratum corneum desquamation are the predominant effect of impaired abca12 function in a novel mouse model of harlequin ichthyosis.* PLoS One, 2016. **11**(8): p. e0161465.

37. Akiyama, M., Dale, B. A., Smith, L. T. , Shimuzu, S., and Holbrook, K. A. , *Regional difference in expression of characterstic abnormality of harlequin ichthyosis in affected fetuses* Prenatal Diagnosis 1998. **18**: p. 425-436.

38. Rock, J.R., et al., *Basal cells as stem cells of the mouse trachea and human airway epithelium.* Proceedings of the National Academy of Sciences, 2009. **106**(31): p. 12771.

39. Kugler, M.C., et al., *Sonic hedgehog signaling in the lung. From development to disease.* American Journal of Respiratory Cell and Molecular Biology, 2015. **52**(1): p. 1-13.

40. Shulenin, S., et al., *Abca3 gene mutations in newborns with fatal surfactant deficiency.* 2004(1533-4406 (Electronic)).

41. Fitzgerald, M.L., et al., *Abca3 inactivation in mice causes respiratory failure, loss of pulmonary surfactant, and depletion of lung phosphatidylglycerol.* Journal of Lipid Research, 2007. **48**(3): p. 621-632.

42. Rajpopat, S., et al., *Harlequin ichthyosis: A review of clinical and molecular findings in 45 cases.* Archives of Dermatology, 2011. **147**(6): p. 681-686.

43. *Unigene* 2018.